UNIVERSITY OF ALBERTA

DERIVATIVE CHEMISTRY OF

HYDROTRIS(PYRAZOLYL)BORATE URANIUM(III) COMPLEXES

by

YIMIN SUN   ©

A thesis submitted to the Faculty of Graduate Studies and Research in partial fulfillment of

the requirements for the Degree of Doctor of Philosophy.

DEPARTMENT OF CHEMISTRY

EDMONTON, ALBERTA

Fall 1995

Canada

UNIVERSITY OF ALBERTA

RELEASE FORM

NAME OF AUTHOR: YIMIN SUN

TITLE OF THESIS: DERIVATIVE CHEMISTRY OF HYDROTRIS(PYRAZOLYL)BORATE URANIUM(III) COMPLEXES

DEGREE: DOCTOR OF PHILOSOPHY

YEAR THIS DEGREE GRANTED: 1995

(Signed)

#309, 9710 - 82 Ave.

Edmonton, Alberta
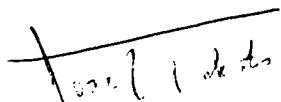
T6E 1Y5

Date: October 2 , 1995
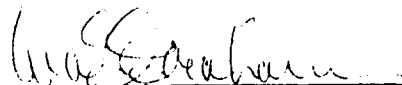
THE UNIVERSITY OF ALBERTA

FACULTY OF GRADUATE STUDIES AND RESEARCH
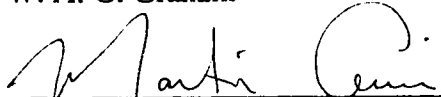
The undersigned certify that they have read, and recommend to the Faculty of Graduate Studies and Research for acceptance, a thesis entitled DERIVATIVE CHEMISTRY OF HYDROTRIS(PYRAZOLYL)BORATE URANIUM(III) COMPLEXES submitted by YIMIN SUN in partial fulfillment of the requirements for the degree of DOCTOR OF PHILOSOPHY.
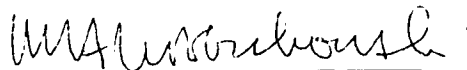
J. Takats (Supervisor)
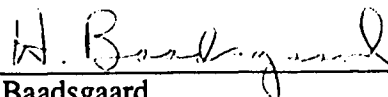
W. A. G. Graham
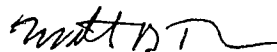
M. Cowie

M. Klobukowski

H. Baadsgaard

W. B. Tolman (External Examiner)

Date: September 25, 1995

To my wife Yichun and my lovely daughters Wenhui and Kim

Abstract

Reactions of $UI_3(THF)_4$ with $NaTp^{Me2}$ or KTp^{Me2} in 1:1 and 1:2 molar ratio gave $U(Tp^{Me2})I_2(THF)_2$ (1) and $U(Tp^{Me2})_2I$ (2), respectively, in 80% isolated yield. $U(Tp^{Me2})_2Br$ (3) was obtained in a similar way in 41% yield. The tridentate coordination mode of Tp^{Me2} in compound 1 was confirmed by crystal structure analysis. The structure of 2 shows that one ligand is tridentate and the other one is bidentate with the third pyrazolyl ring oriented toward the U(III) metal center in an unusual way. The orientation of this pyrazolyl ring represents the first example of side-on interaction of the pyrazolyl ring with a metal center. Complex 2 underwent ready iodide abstraction with $TlBPh_4$ to form the cationic complex, $[U(Tp^{Me2})_2THF][BPh_4]$ (4), which contains two η^3-Tp^{Me2} ligands and a coordinated THF molecule. The structural difference between complexes 2 and 4 is striking and indicates that the structure and bonding in these complexes are controlled by a subtle interplay of electronic and steric factors.

$U(Tp^{Me2})I_2(THF)_2$ proved to be a versatile starting material for the synthesis of $U(Tp^{Me2})[N(SiMe_3)_2]_2$ (5), $U(Tp^{Me2})[CH(SiMe_3)_2]_2(THF)$ (6), and $U(Tp^{Me2})[N(SiMe_3)_2]I$ (7). Even the mixed amido-hydrocarbyl complex, $U(Tp^{Me2})[N(SiMe_3)_2][CH(SiMe_3)_2]$ (8), could be prepared. The solid-state structures of 5, 6, and 8 were determined, all three compounds contain the Tp^{Me2} ligand bonded *via* the classical η^3-fashion. Coordination congestion, due to short contacts between the 3-methyl groups of the Tp^{Me2} ligand and the silyl methyl groups, is a common structural feature in these complexes. In solution, complexes 5, 6, and 8 are fluxional. Complex 5 rearranges much faster than 8, and it is argued that the reason for this is the strong preference of the hydrocarbyl ligand in 8 to occupy one of the apical sites of the trigonal bipyramid. Compounds 5 and 6 are thermally unstable in solution. The decomposition is solvent dependent. Unfortunately the reaction is dominated by B-N bond cleavage. Extension of the derivative chemistry of $U(Tp^{Me2})I_2(THF)_2$ (1) to the oxygen donor ligands met with

difficulty. From the reactions with two equiv of KOR (R=Et, ^{t}Bu, $C_6H_2Me_3$-2,4,6, and $C_6H_3{}^iPr_2$-2,6) only the U(IV) complexes, $U(Tp^{Me2})(OR)_3$, could be isolated. Bidentate ligands such as $^tBuC(O)CHC(O)^tBu^-$ (dpm$^-$), $^tBuCO_2^-$, and $H_2B(pz)_2^-$ did not cause redox reactions, but dpm$^-$ displaced the Tp^{Me2} ligand as well and gave U(III)(dpm)$_3$; the nature of the compound isolated from the $^tBuCO_2^-$ reaction is still not clear; only $U(Tp^{Me2})[(pz)_2BH_2]_2$ proved to be the expected product.

Reaction of $UI_3(THF)_4$ with three equivalents of $KH_2B(pz)_2$ gave the complex $U[H(\mu$-H$)B(pz)_2]_3(THF)$ (14), which contains an interesting example of agostic U$\cdots$H-B interaction in the presence of the oxygen donor THF ligand. The three-center two-electron B-H$\cdots$U bridge bonds were established by X-ray analysis. The THF in 14 is labile and can be removed by repeated cycles of dissolution of 14 in toluene and solvent removal. In solution, the molecules of both complexes are fluxional, but only for $U[H(\mu$-H$)B(pz)_2]_3$ (15) could a low temperature limiting ^1H NMR spectrum be obtained. The activation energy for equilibration of the BH_2 hydrogens is 51 kJ/mol.

The Klaui ligands, $[(\eta^5$-Cp$)Co\{P(=O)(OR)_2\}_3]^-$, designated as L_{OR}, are geometrically and electronically analogous to the $Tp^{R,R'}$ ligands. Attempts to synthesize Klaui analogues of the $U(Tp^{Me2})_nI_{3-n}$ complexes failed, however, redox reactions resulted in the formation of U(IV) complexes. Thus, the reaction of $UI_3(THF)_4$ with NaL_{OEt} in a 1:2 molar ratio gave a mixture of $U(L_{OEt})_2I_2/U(L_{OEt})_2(OEt)I$ (17) in an approximate 1:2 molar ratio. Iodide abstraction with TlBPh$_4$ from the *in situ* generated product of $UI_3(THF)_4$ with two equiv of NaL_{OEt} in toluene gave $[U(L_{OEt})_2(THF)_2][BPh_4]_2$ (18). Surprisingly, from the reaction of $UI_3(THF)_4$ with two equivalents of hydrated NaL_{OEt} a dimeric complex, $[(L_{OEt})U(CpCo\{P(=O)(OEt)_2\}_2\{P(=O)(OEt)(O)\})(H_2O)]_2I_2$ (22), was isolated.

Due to the high temperature required for the synthesis of Tp ligands, hetero ligands such as $HB(pz)_2(pz')$ or chiral $HB(pz)(pz')(pz'')$ ligands are not accessible *via* the classical synthesis. To circumvent this difficulty, ring splitting of the readily available pyrazobole,

[HB(pz)$_2$]$_2$, with various Lewis bases was attempted; only HNMe$_2$ and pyrrolidine gave the desired adducts, HB(pz)$_2$(L) (L=HNMe$_2$ (23), pyrrolidine (24)). Displacement of HNMe$_2$ from 23 by (3,5-Me$_2$pz)$^-$ did not proceed cleanly, but gave a 2:1 mixture of HB(pz)$_2$(3,5-Me$_2$pz) and HB(pz)(3,5-Me$_2$pz)$_2$. Deprotonation of the pyrrolidine adduct of HB(pz)$_2$(N-pyrrolidine) with Li^{t}Bu or NaH in THF resulted in MHB(pz)$_2$(N-pyrrolidinyl)borate (M=Li (25), Na (26)), which reacted with CoCl$_2$ and NiCl$_2$ to give the respective M[HB(pz)$_2$(N-pyrrolidinyl)]$_2$ (M=Co (27), Ni (28)) complexes. Single-crystal X-ray structure analysis of complexes 27 and 28 revealed that the ligand is coordinated to the metal ions in an η^3-fashion and the geometry about the metal ions is distorted tetragonal bipyramidal, consistent with the spectroscopic data.

Acknowledgements

I would like to thank Professor Josef Takats for his guidance and encouragement, for his sincere friendship and understanding, and for his assistance in the writing of this thesis.

I thank my friends and colleagues, especially Xingwang Zhang, Wenyi Fu, Tianfu Mao, John Washington, Ken Hoffmann, and Jason Cooke for support and providing a pleasant atmosphere for research. I would also like to thank Jackie Jorgensen for her assistance in typing the thesis.

I would like to thank Glen Bigam, Tom Nakashima, Tom Brisbane, Gerdy Aarts and Lai Kong for performing numerous experiments for me: their enthusiasm and professionalism is appreciated. The X-ray determinations provided by Bob McDonald, Victor W. Day, Andrew Bond and Robin Rogers are gratefully acknowledged.

I would like to thank other technical support staff of the Department of Chemistry for all their assistance, and practical help.

Finally, I would also like to thank my family for their support and patience during my studies.

Table of Contents

Chapter 1

Introduction

Chapter 2

Synthesis and Characterization of
Hydrotris(3,5-dimethylpyrazolyl)borate
U(III) Complexes

Chapter 3
Derivative Chemistry of U(Tp^{Me2})I$_2$(THF)$_2$ with Carbon, Nitrogen, and Oxygen Donor Ligands

Chapter 4
Synthesis and Structure of Uranium(III) Complexes
Containing Dihydrobis(pyrazolyl)borate Ligand

Chapter 5
Chemical Behavior of a Klaui Ligand towards a
U(III) Metal Center

Chapter 6

A New Approach to an Asymmetric
Hydrotris(pyrazolyl)borate: Synthesis and Characterization of
[HB(pz)₂(*N*-pyrrolidinyl)]⁻ and Its Transition Metal
Complexes, M[HB(pz)₂(*N*-pyrrolidinyl)]₂ (M=Co(II), Ni(II))

Chapter 7

Conclusions

List of Figures

Chapter 1

Chapter 2

Chapter 3

Chapter 4

Chapter 5

Chapter 6

List of Tables

Chapter 2

Chapter 3

Chapter 4

Chapter 5

Chapter 6

List of Compounds

Chapter 6

List of Abbreviations and Symbols

Å	Angstrom(s)
Anal.	analytical
atm	atmosphere(s)
ave	average
br	broad
ca.	circa (approximately)
Calc.	calculated
Cp	cyclopentadienyl
Cp*	pentamethylcyclopentadienyl
CTP	capped trigonal prism
CO	capped octahedron
δ	chemical shift in ppm
Δ	heating
deg	degree(s)
DME	dimethoxyethane
dmpe	bis(dimethylphosphino)ethane
dpm	$^tBuC(O)CHC(O)^tBu$
E.A.	elemental analysis
E.I.	electron ionization
eV	electron volts
FAB	fast atom bombardment
FT-IR	Fourier Transform Infrared
h	hour(s)
Hz	Hertz
^iPr	iso-propyl, $HC(CH_3)_2$-

IR	Infrared
J	coupling constant (NMR) or Joules($\Delta G^{\ddagger}$)
K	Kelvin
L_{OR}	$[(\eta^5\text{-Cp})Co\{(OR)_2P=O\}_3]^-$
LT	low temperature
LUMO	lowest unoccupied molecular orbital
λ	wavelength
Me	methyl, CH_3-
mg	milligram(s)
MHz	megahertz
mL	milliliters
mmol	millimoles
M.S.	mass spectrometry
NMR	nuclear magnetic resonance
ν	stretching frequency
PB	pentagonal bipyramid
Ph	phenyl, C_6H_5-
ppm	parts per million
pz	pyrazolyl
pz'	substituted pyrazolyl
s	singlet (NMR); strong (IR)
tr	triplet
m	meta-
o	ortho-
p	para-
^tBu	tertiary-butyl, $C(CH_3)_3$-
Tp	hydrotris(pyrazolyl)borate, $HB(pz)_3^-$

$\text{Tp}^{\text{R,R'}}$	hydrotris(3-R-5-R'pyrazolyl)borate, $\text{HB(3-R-5-R'pz)}_3^-$
THF	tetrahydrofuran
TMEDA	tetramethylethanediamine
V	Volt(s)
VSEPR	valence-shell electron-pair repulsion
VT	variable temperature

Chapter 1

Introduction

1.1. General Features of Uranium and Uranium Coordination Chemistry

There are only four elements in the actinide series, Ac, Th, Pa, and U, which occur in Nature in amounts sufficient for practical extraction.[1] Among the four elements uranium is the most important economically because it is used as fuel in nuclear reactors. The principal uranium isotope is ^{238}U in 99.2739% natural abundance, with minor ^{235}U in 0.7204% natural abundance. Both isotopes are radioactive with a half-life of 7.13×10^8yr and 4.50×10^9yr, respectively.

The electronic configuration of uranium is $5f^36d^17s^2$, with six electrons in the valence shell. Therefore, uranium can have multiple oxidation states. The most stable oxidation states for uranium are +4 and +6. Although the trivalent state, U(III), is readily obtained it is easily oxidized, $E°(U^{+4}/U^{+3}) = -0.631$V. Both U(IV) and U(III) are paramagnetic. The relatively large size of the ions, the availability of a large number of valence shell orbitals for bonding, and the high electrostatic attraction due to formal +3 to +6 charges result in high coordination numbers; 8 coordination is very common. Although the bonding in uranium complexes is predominantly ionic, the greater spatial extension of the 5f orbitals compared to the 4f orbitals results in some covalent contribution to the bonding, certainly more than in lanthanide complexes.

Investigation of organoactinide chemistry began around 1940 with the establishment of the Manhattan Project, although the main goal of the project was to find the most efficient way to enrich uranium in ^{235}U for the production of atomic bombs.[2] Today, five decades later, as the nuclear superpower, the Soviet Union, had collapsed, the Cold War is over. The problem we are facing now is what to do with the nuclear warheads, how to safely dispose the nuclear wastes generated from the production of

nuclear warheads, and how to protect our environment from the nuclear pollution. The solution to these problems will rely heavily on how well we understand the fundamental chemistry of the actinide elements, including that of uranium.

1.2. Organouranium Chemistry

The synthesis of UCp_3Cl by Reynolds and Wilkinson[3] in 1956 marked the beginning of organouranium chemistry. Since then, this research area has continued to attract the attention of numerous chemists. The chemistry of UCp_3Cl has been extensively studied and a great variety of derivatives have been synthesized and characterized[4-6] (eq. 1.1).

$$UCp_3Cl \ + \ Y^- \ \longrightarrow \ UCp_3Y \ + \ Cl^- \qquad 1.1$$

$$Y = F^-, SCN^-, OCN^-, BH_4^-, OR^-, C(CN)_3^-, R_2N^-$$
$$R^- (various \ alkyl, \ aryl, \ and \ alkenyl \ groups)$$
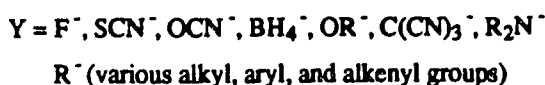
Although "UCp_2Cl_2" was reported to form from the stoichiometric reaction of UCl_4 and TlCp in DME,[7] it was soon discovered that the reaction product was in fact a mixture of $UC_{r-x}Cl/UCpCl_3(DME)$ or UCp_3Cl/UCl_4. Thus, UCp_2Cl_2 appears not to be stable and it is susceptible to the facile ligand redistribution reactions depicted in eq. 1.2. Efforts have

$$2UCp_2Cl_2 \ \xrightarrow{\ L\ } \ UCp_3Cl \ + \ UCpCl_3L$$
$$3UCp_2Cl_2 \ \xrightarrow{\ L\ } \ 2UCp_3Cl \ + \ UCl_4(L)_x \qquad 1.2$$
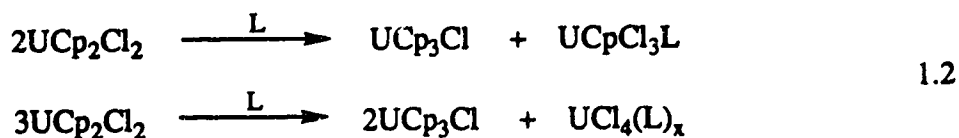
been made to stabilize UCp_2Cl_2 against disproportionation by complexing the molecule with the bulky bidentate ligand $Ph_2P(O)CH_2CH_2P(O)Ph_2$,[8] by tying the two Cp rings together,[9] and by using bulky, substituted Cp moieties. The most successful method by far was the use of the bulky pentamethylcyclopentadienyl (Cp*) ligand (eq. 1.3).[10] This is

$$UCl_4 + excessCp^*MgX \longrightarrow UCp^*_2Cl_2 + MgXCl \qquad 1.3$$

not surprising in view of the dominant role steric effects play in the stability of f-element complexes, since, as mentioned before, the bonding in these complexes is predominantly ionic. As shown in Scheme 1.1, $UCp^*_2Cl_2$ is a very useful starting material for the preparation of many organouranium complexes.

Scheme 1.1 Reactions of $UCp^*_2Cl_2$
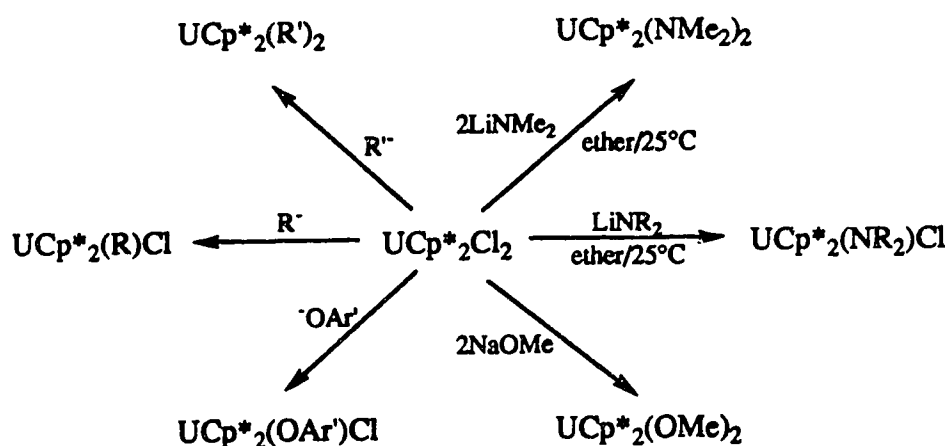
$R=Me, CH_2SiMe_3, CH_2CMe_3, CH(SiMe_3)_2, C_6H_5, CH_2C_6H_5$

$R'=Me, CH_2SiMe_3, CH_2C_6H_5, 1/2(CH_2CH=CHCH_2)$

Compared to uranium(IV) the organic chemistry of U(III) is very limited. The first organouranium(III) complex, UCp_3, was prepared by Kanellakopulos[11] in two different ways (eq. 1.4 and 1.5). Since then a number of different ways have been found to prepare

$$U^0 + 3UCp_4 \xrightarrow{\text{benzene}} 4UCp_3 \qquad 1.4$$
$$42\%$$

$$UCl_3 + 3KCp \xrightarrow{\text{THF}} UCp_3THF + 3KCl \qquad 1.5$$
$$95\%$$
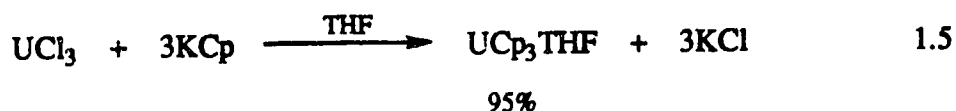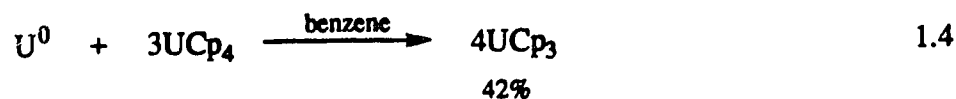
UCp₃. Nevertheless, the most convenient method remains the reaction UCl$_3$ with 3 equiv of KCp in THF as shown in eq. 1.5. The method is straightforward and proceeds in 95% yield. Unfortunately, when this method was extended to the preparation of UCp$_2$Cl or UCpCl$_2$, difficulties were encountered.[12] Elemental analysis suggested that UCp$_2$Cl may have been formed from the reaction of UCl$_3$ with TlCp, but X-ray powder diffraction showed that a major constituent of the crude reaction product was in fact UCp$_3$Cl, a U(IV) complex. Indeed, sublimation gave UCp$_3$Cl in approximately 50% yield. The difficulties encountered in the preparation of UCp$_2$Cl and UCpCl$_2$ directly from uranium trichloride, to a large extent, may relate to the starting material, UCl$_3$, which has been shown to possess a polymeric structure in which each uranium atom is surrounded by nine chlorine atoms.[13] Because of this polymeric nature and the high lattice energy associated with this structure, UCl$_3$ has low solubility in most common organic solvents.[14] Although solvated UCl$_3$(THF)$_x$ can be prepared readily, its composition appears to depend on its method of preparation. The ill defined nature of UCl$_3$(THF)$_x$ still complicates reactions and renders isolation of pure products difficult.[12] Most of the UCp'$_2$Cl type complexes were prepared by reduction of U(IV) complexes with a variety of reducing agents.[15-18] So far there are only two reports, the successful synthesis of [U(^{t}Bu$_2$C$_5$H$_3$)$_2$Cl]$_2$[19] and UCp*I$_2$(THF)$_3$,[20] by direct reaction of U(III) halides with substituted cyclopentadienyl ligands.

1.3. Poly(pyrazolyl)borate Chemistry of Uranium

The poly(pyrazolyl)borate ligands, (KH$_n$B(pz)$_{4-n}$, n=1,2; pz=pyrazolyl), were first synthesized by Trofimenko in 1966.[21] Since then this ligand system has been widely used in inorganic, organometallic, and bioinorganic chemistry.[22-25] A perspective view of the hydrotris(pyrazolyl)borate ligand system, designated as Tp$^{R,R'}$, is shown in Fig. 1.1. The Tp$^{R,R'}$ ligand is monoanionic and a six-electron donor, and in this sense it is electronically analogous to the Cp/Cp* ligands. However, the two ligand systems are sterically quite
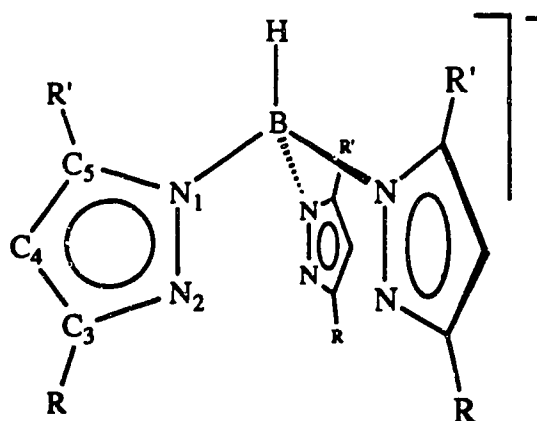
Fig. 1.1 Hydrotris(pyrazolyl)borate Ligand

different. The free $Tp^{R,R'}$ ligand possesses C_{3v} symmetry, and usually interacts with metal ions in a tridentate mode acting as a six-electron donor. However, in some cases, depending on the coordination environment of the metal ion, it can bind in a bidentate fashion acting as a four-electron donor with one pyrazolyl ring not interacting with the metal ion. The effective size of this ligand system can be greatly influenced by the substituents on the 3-position of the pyrazolyl rings, and the availability of a variety of substituents allows for fine tuning of the steric properties of the ligand. The cone angle of $Tp^{R,R'}$ is usually greater than 180° (Tp is 180°), and this provides a protective pocket for the ancillary ligands coordinated to metal center. Since the bonding in uranium complexes is mostly ionic, steric factors play a very important role in the stabilization of the complexes, thus the bulky $Tp^{R,R'}$ ligands may allow the preparation of some complexes which could not be obtained by using the Cp/Cp* ligands.

Bagnall et al.[26-28] were the first to introduce the poly(pyrazolyl)borate ligands to uranium chemistry. A series of poly(pyrazolyl)borate complexes of uranium, including $U(Tp)_2Cl_2$ and $U(Tp^{Me_2})_2Cl_2$,[26,28] were prepared, as shown in eq. 1.6 and 1.7. However, ^{11}B NMR studies[29] indicated that the reaction of UCl_4 with 2 equiv of KTp^{Me_2} was not a simple metathesis. The ^{11}B NMR spectrum of the reaction mixture displayed

$$UX_4 + 2KTp \xrightarrow{\text{THF}} U(Tp)_2X_2L + 2KX \qquad 1.6$$

X=Cl; L=THF, DMA

X=Br; L=THF

$$UCl_4 + 2KTp^{Me_2} \xrightarrow{\text{THF}} U(Tp^{Me_2})_2Cl_2 + 2KCl \qquad 1.7$$
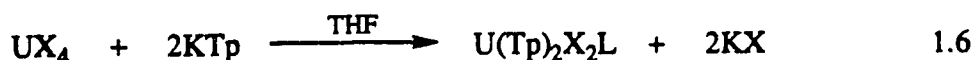
three resonances and suggested that ligand redistribution and formation of mixtures possibly complicated the reaction. Reaction of UCl_4 with one equiv of KTp^{Me_2} cleanly gave $U(Tp^{Me_2})Cl_3(THF)$.[30] The complex has been structurally characterized and represents the first X-ray determination of an actinide $Tp^{R,R'}$ complex. The structure (Fig. 1.2) consists of a seven coordinate uranium with a capped octahedral geometry, the Tp^{Me_2} ligand being bonded to uranium in an η^3-fashion. After these initial studies the chemistry of U(IV) $Tp^{R,R'}$ complexes was mainly developed by Pires de Matos, Santos, Marques et $al.$ and numerous derivatives have been reported, such as $U(Tp)_2(OR)_xCl_{2-x}$ (x = 1,2; R = ^iPr, ^tBu, $C_6H_2Me_3$-2,4,6)[31]; $U(Tp)_2(SR)_2$ (R = ^iPr, ^tBu)[32,33]; $U(Tp^{Me_2})(OR)_xCl_{3-x}$ (R = ^iPr, ^tBu, $C_6H_2Me_3$-2,4,6)[34]; $U(Tp^{Me_2})(OPh)_2Cl(THF)$[35,36]; $U(Tp^{Me_2})(Cp)R_xCl_{2-x}$ (R = Me, X = 0-2)[37]; $U(Tp^{Me_2})(R)Cl_2$ (R = CH_2-$C_6H_4NMe_2$-2, $C_6H_4CH_2NMe_2$-2)[37b]; $U(Tp^{Me_2})(NR_2)Cl_2$ (R = Ph, $SiMe_3$)[38]; $U(Tp^{Me_2})(O_2CMe)_3$[39]; $U(Tp^{Me_2})(CH(SiMe_3)_2)Cl_2$ and $U(Tp^{Me_2})(CH_2(SiMe_3))_xCl_{3-x}$[40].

Studies of the poly(pyrazolyl)borate chemistry of uranium(III) began only a decade ago. Santos et $al.$[41-43] studied the reaction of $UCl_3(THF)_x$ with $KH_nB(pz)_{4-n}$ (n = 1,2; pz = pyrazolyl, 3,5-Me_2pz) and the complexes $U[H_2B(pz)_2]Cl_2$, $U(Tp)Cl_2$, $U[H_2B(3,5-Me_2pz)_2]_3$, and $U(Tp^{Me_2})Cl_2$ were prepared and characterized by elemental analysis, ^1H, ^{11}B NMR, and IR spectroscopies. Among these U(III) poly(pyrazolyl)borate complexes only $U[H_2B(3,5-Me_2pz)_2]_3$ was structurally characterized. Reduction of preformed U(IV) complexes was also utilized to synthesize U(III) poly(pyrazolyl)borate derivatives. Isabel Santos[44] has demonstrated that reduction of $U(Tp^{Me_2})Cl_3(THF)$ with $NaC_{10}H_8$ in THF
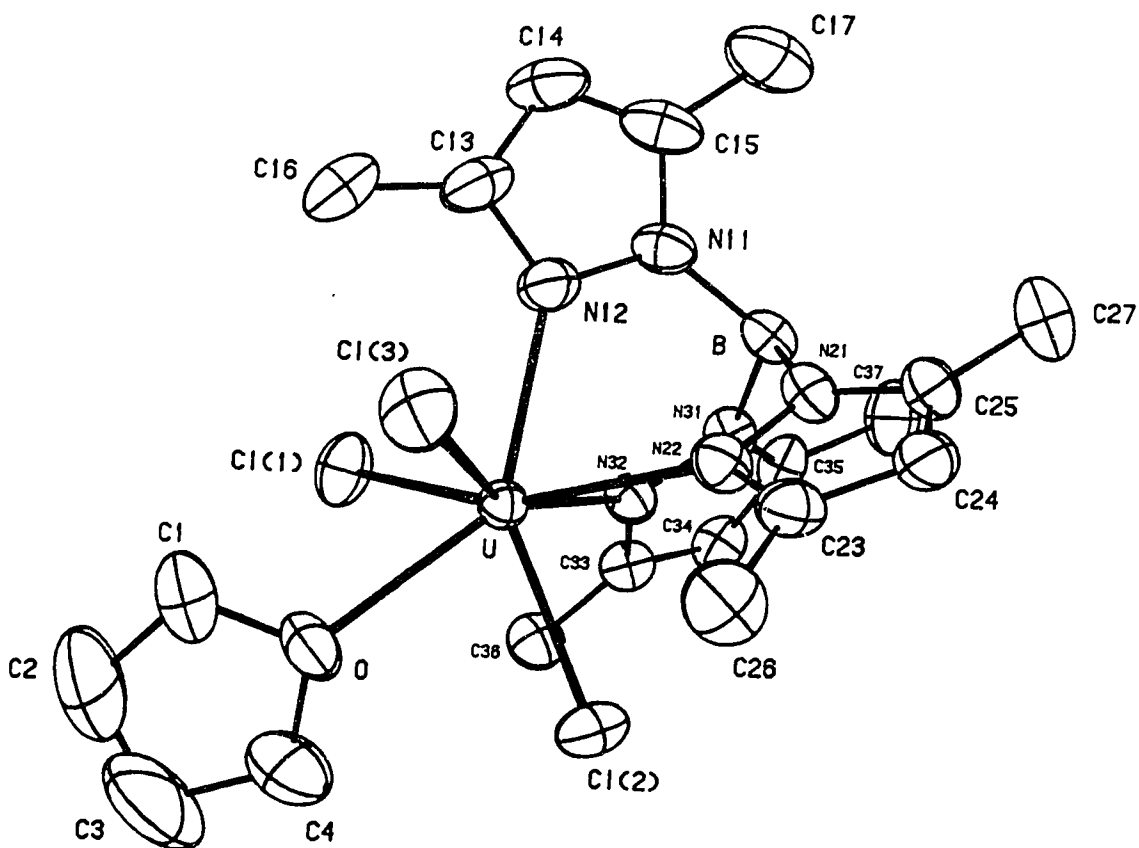
Fig. 1.2 Molecular Structure of U(Tp^{Me_2})Cl$_3$(THF)

gave the same dark blue solid as the one isolated from the reaction of UCl$_3$(THF)$_x$ with KTp^{Me_2}. Reduction of U(Tp^{Me_2})[N(SiMe$_3$)$_2$]Cl$_2$ in a similar fashion gave a red solid formulated as U(Tp^{Me_2})[N(SiMe$_3$)$_2$]Cl.[44] Unfortunately, the yields of many of the reactions were not reported, and no further reports on the derivative chemistry have appeared.

It is clear that the poly(pyrazolyl)borate chemistry of U(III) is comparatively much less developed than that of U(IV). A major reason may be the lack of a suitable starting material. As mentioned before, UCl$_3$(THF)$_x$, the commonly used precursor, is obtained by reduction of UCl$_4$ with a variety of reducing agents such as NaH,[12] Na$_2$C$_2$,[45] and sodium naphthalide.[46] Its composition depends on its method of preparation and its

structure is ill defined, resulting in complicated reactions and difficulties in isolating pure products. This situation changed dramatically when Sattleberger *et al.*[20,47] reported the successful and convenient synthesis of $UI_3(THF)_4$ on a 50g scale by reaction of clean uranium turnings with iodine in THF (eq. 1.8). Preliminary studies

$$U^0 \; + \; 1.5 \, I_2 \quad \xrightarrow[\text{0°C}]{\text{THF}} \quad UI_3(THF)_4 \qquad\qquad 1.8$$

$$65\%$$
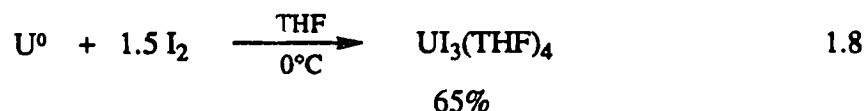
showed that $UI_3(THF)_4$ was indeed a very useful starting material. Syntheses of known compounds proceeded in a simpler and cleaner fashion and gave higher isolated yields (Scheme 1.2); preparation of new complexes was also possible.[20]

Scheme 1.2[a]

$$U[N(SiMe_3)_2]_3$$

(i)

$$UI_3(THF)_4$$

(iii)   (ii)

$$U(OC_6H_3Me_2\text{-}2,6)_3THF \qquad\qquad UCp^*I_2(THF)_3$$
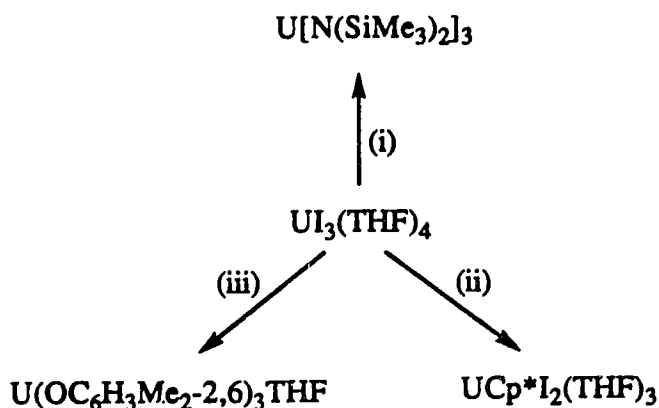
[a]Conditions: (i) 3 equiv of $NaN(SiMe_3)_2$ in THF at 23°C for 24 h, >90%;

(ii) 1 equiv of KCp^* in THF 23°C for 24 h, 80%;

(iii) 3 equiv of $KOC_6H_3Me_2\text{-}2,6$ in THF at 23°C for 24 h, >90%

1.4. Chemistry of Uranium with a Tripodal Oxygen Donor Ligand; the Klaui Ligand System

Another class of tripodal ligands which have been widely utilized for the synthesis of a great number of transition metal complexes in various oxidation states[48] was

synthesized by Klaui.[49] The ligand, designated as L_{OR}, is shown in Fig. 1.3, and is constructed by attaching three $[(P=O)(OR)_2]^-$ arms to a $CpCo^{2+}$ moiety. Although both
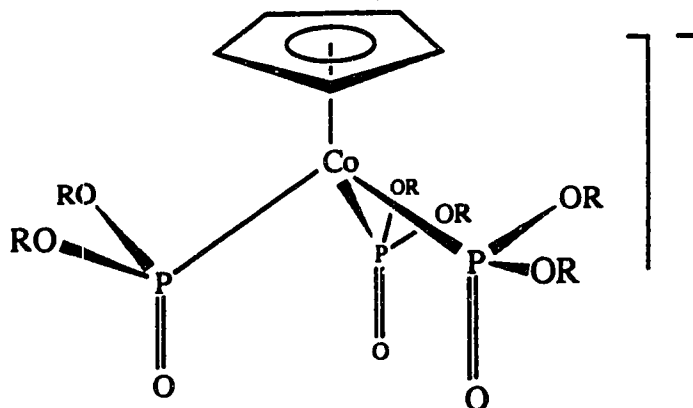
Fig. 1.3 Klaui Ligand

Trofimenko and Klaui ligands are tripodal they are different sterically and chemically. The cone angle of L_{OEt} (160°) is smaller than that of Tp (180°). The low position of L_{OEt} in the spectrochemical series, near the hydroxide and fluoride ions, makes it distinctly different from Tp. An advantage of the Klaui ligand is that it provides a convenient ^{31}P NMR handle which facilitates elucidation of the molecular structure. So far there are only two reports on the application of the Klaui ligand to the chemistry of uranium(IV) and no report on uranium(III). Reactions of UCl_4 with NaL_{OEt} were studied by two research groups[50,51] independently and $U(L_{OEt})Cl_3(THF)$, $U(L_{OEt})_2Cl_2$, and $U(L_{OEt})CpCl_2$ were synthesized with yields ranging from 30 to 72%.

1.5. Scope of the Thesis

As indicated in the introduction, at the start of this thesis there were very few reports on the synthesis of organo derivatives of U(III), because of this the thesis work focused on developing this area. The initial research target was the synthesis of $U(Tp^{R,R'})_nI_{3-n}$ (n=1,2) type complexes by using $UI_3(THF)_4$. Following this, it was of

interest to develop the derivative chemistry of $U(Tp^{R,R'})_n I_{3-n}$ (n=1, 2) with a variety of nucleophilic ligands, such as alkoxide, aryloxide, hydride, amide, hydrocarbyl, etc. and to study the structure and reactivity of these derivatives. As mentioned, the chemistry of U(III) complexes with Klaui ligan has not been explored. Attempts were made to prepare such uranium(III) complexes with the intention of comparing their structure and reactivity with those of the analogous $Tp^{R,R'}$ complexes.

1.6. References

(1) Cotton, F. A.; Wilkinson, G. *Advanced Inorganic Chemistry;* Fifth ed.; John Wiley & Sons, Inc.: New York, 1988, pp 980.

(2) Schlesinger, H. I.; Brown, H. C.; Katz, J. J.; Archer, S.; Lad, R. A. *J. Am. Chem. Soc.* **1953,** *75,* 2446.

(3) Reynolds, L. T.; Wilkinson, G. *J. Inorg. Nucl. Chem.* **1956,** *2,* 246.

(4) Gebala, A. E.; Tsutsui, M. *J. Am. Chem. Soc.* **1973,** *95,* 91.

(5) Marks, T. J.; Seyam, A. M.; Kolb, J. R. *J. Am. Chem. Soc.* **1973,** *95,* 5529.

(6) Brandi, G.; Brunelli, M.; Lugli, G.; Mazzei, A. *Inorg. Chim. Acta* **1973,** *7,* 319.

(7) Zanella, P.; Faleschini, S.; Doretti, L.; Faraglia, G. *J. Organomet. Chem.* **1971,** *26,* 353.

(8) Bagnall, K. W.; Edwards, J.; Tempest, A. C. *J. Chem. Soc., Dalton Trans.* **1979,** 1321.

(9) Secaur, C. A.; Day, V. W.; Ernst, R. D.; Kennelley, W. J.; Marks, T. J. *J. Am. Chem. Soc.* **1976,** *98,* 3713.

(10) Fagan, P. J.; Manriguez, J. M.; Maatta, E. A.; Seyam, A. M.; Marks, T. J. *J. Am. Chem. Soc.* **1981,** *103,* 6650 and references therein.

(11) Kanellakopulos, B.; Fischer, E. O.; Dornberger, E.; Baumgartner, F. *J. Organomet. Chem.* **1970,** *24,* 507-514.

(12) Moody, D. C.; Odom, J. D. *J. Inorg. Nucl. Chem.* **1979,** *41,* 533.

(13) Zachariasen, W. H. *J. Chem. Phys.* **1948,** *16,* 254.

(14) Barnard, R.; Bullock, J. I.; Gellatly, B. J.; Larkworthy, L. F. *J. Chem. Soc., Dalton Trans.* **1973,** 604.

(15) Manriguez, J. M.; Fagan, P. J.; Marks, T. J.; Vollmer, S. H.; Day, C. H.; Day, V. W. *J. Am. Chem. Soc.* **1979,** *101,* 5075-5078.

(16) Fagan, P. J.; Manriguez, J. M.; Marks, T. J.; Day, C. S.; Vollmer, S. H.; Day, V. W. *Organometallics* **1982,** *1,* 170-180.

(17) Blake, P. C.; Lappert, M. F.; Taylor, R. G.; Atwood, J. L.; Hunter, W. E.; Zhang, H. *J. Chem. Soc., Chem. Commun.* **1986**, 1394-1395.

(18) Blake, P. C.; Lappert, M. F.; Taylor, R. G.; Atwood, J. L.; Zhang, H. *Inorg. Chim. Acta* **1987**, *139*, 13.

(19) Zalkin, A.; Stuart, A. L.; Andersen, R. A. *Acta. Cryst.* **1988**, *41*, 2106-2108.

(20) Clark, D. L.; Sattelberger, A. P.; Bott, S. G.; Vrtis, R. N. *Inorg. Chem.* **1989**, *28*, 1771-1773.

(21) Trofimenko, S. *J. Am. Chem. Soc.* **1966**, *88*, 1842.

(22) Niedenzu, K.; Trofimenko, S. *Top. Curr. Chem.* **1986**, *131*, 1-37.

(23) Trofimenko, S. *Prog. Inorg. Chem.* **1986**, *34*, 115-209.

(24) Trofimenko, S. *Chem. Rev.* **1993**, *93*, 943-980.

(25) Kitajima, N.; Tolman, W. B. *Prog. Inorg. Chem.* **1995**, in press.

(26) Bagnall, K. W.; Edwards, J.; duPreez, L. G. H.; Warren, R. F. *J. Chem. Soc., Dalton Trans.* **1975**, 140.

(27) Bagnall, K. W.; Beleshti, A.; Heatley, F. *J. Less-Common Met.* **1978**, *61*, 171.

(28) Bagnall, K. W.; Edwards, J. *J. Less-Common Met.* **1976**, *48*, 159.

(29) Marques, N.; Pires de Matos, A. *Inorg. Chim. Acta* **1984**, *95*, 75-77.

(30) Ball, R. G.; Edelmann, F.; Matisons, J. G.; Takats, J.; Marques, N.; Marcalo, J.; Matos, A. P. D.; Bagnall, K. W. *Inorg. Chim. Acta* **1987**, *132*, 137-143.

(31) Santos, I.; Marcalo, J.; Marques, N.; Pires de Matos, A. *Inorg. Chim. Acta* **1987**, *134*, 315.

(32) Santos, I.; Marques, N.; Pires de Matos, A. *Inorg. Chim. Acta* **1987**, *139*, 89.

(33) Domingos, A.; Pires de Matos, A.; Santos, I. *Polyhedron* **1992**, *11*, 1601.

(34) Marques, N.; Marcalo, J.; Pires de Matos, A.; Bagnall, K. W. *Inorg. Chim. Acta* **1987**, *134*, 309.

(35) Domingos, A.; Marcalo, J.; Marques, N.; Pires de Matos, A.; Takats, J.; Bagnall, K. W. *J. Less-Common. Met.* **1989**, *149*, 271.

(36) Domingos, A.; Pires de Matos, A.; Santos, I. *J. Less-Common. Met.* **1989**, *149*, 279.

(37) (a) Domingos, A.; Marques, N.; Pires de Matos, A. *Polyhedron* **1990**, *9*, 69;

(b) Silva, M.; Marques, N.; Pires de Matos, A. *J. Organomet. Chem.* **1995**, *493*, 129-132.

(38) Marcalo, J.; Marques, N.; Pires de Matos, A.; Bagnall, K. W. *J. Less-Common Met.* **1986**, *122*, 219.

(39) Domingos, A.; Marcalo, J.; Marques, N.; Pires de Matos, A. *Polyhedron* **1992**, *11*, 501.

(40) Domingos, A.; Marques, N.; Pires de Matos, A.; Santos, I.; Silva, M. *Organometallics* **1994**, *13*, 654-662.

(41) Santos, I.; Marques, N.; De Matos, A. P. *Inorg. Chim. Acta* **1985**, *110*, 149-151.

(42) Santos, I.; Marques, N.; De Matos, A. P. *J. Less-Common Met.* **1986**, *122*, 215-218.

(43) Carvalho, A.; Domingos, A.; Gaspar, P.; Marques, N.; Pires de Matos, A.; Santos, I. *Polyhedron* **1992**, *11*, 1481-1488.

(44) Santos, I.; Marques, N.; Pires de Matos, A. *Inorg. Chim. Acta* **1987**, *139*, 87-88.

(45) Moody, D. C.; Zozulin, A. J.; Salazar, K. V. *Inorg. Chem.* **1982**, *21*, 3856.

(46) Andersen, R. A. *Inorg. Chem.* **1979**, *18*, 1507-1509.

(47) Avens, L. R.; Bott, S. G.; Clark, D. L.; Sattelberger, A. P.; Watkin, J. G.; Zwick, B. D. *Inorg. Chem.* **1994**, *33*, 2248-2256.

(48) Klaui, W. *Angew. Chem., Int. Ed. Engl.* **1990**, *29*, 627.

(49) Klaui, W. *Naturforsch.* **1979**, *B34*, 1403.

(50) Baudry, D.; Ephritikhine, M.; Klaui, W.; Lance, M.; Nierlich, M.; Vinger, J. *Inorg. Chem.* **1991**, *30*, 2333-2336.

(51) Wedler, M.; Gilje, J. W.; Noltemeyer, M.; Edelmann, F. T. *J. Organomet. Chem.* **1991**, *411*, 271-280.

Chapter 2

Synthesis and Characterization of
Hydrotris(3,5-dimethylpyrazolyl)borate U(III) Complexes.

2.1. Introduction

Since the first preparation,[1-3] and especially with the introduction of the so-called coordination-controlling "second generation" of hydrotris(pyrazolyl)borate ligands, $(HB(3-R-5-R'pz)_3 \equiv Tp^{R,R'})$, this ligand system has been widely used in inorganic, bioinorganic and organometallic chemistry.[4-7] The main reason for the popularity is the facility by which various substituents can be introduced into the 3- and 5- positions of the pyrazolyl ring. Due to their closeness to and orientation toward the metal center, the substituents at the 3-position have a profound steric effect on the metal ions and the availability of a variety of substituents allows for fine tuning the steric size of the ligand and thereby the coordination environment of the metal center. In addition, the ligands exhibit variable bonding modes from classical tridentate to bidentate;[5,6,8] and even monodentate behavior has been observed.[9]

However, application of hydrotris(pyrazolyl)borates as stabilizing ligands has been mainly confined to transition metal chemistry.[10,11] With the actinide metals, reports have appeared on U(IV) and Th(IV) complexes,[12-15] but complexes of U(III) have been very little studied.[16,17] In general, the coordination and organometallic chemistries of U(III) are not well developed due in part to the ease of oxidation to the +4 state, $(E°(U^{+4}/U^{+3}) = -0.631V)$ and the lack of suitable starting materials. $UCl_3(THF)_x$, a commonly used precursor, apparently suffers from variable composition that leads to synthetic difficulties.[18] This latter obstacle has been eliminated by the convenient and high yield synthesis of $UI_3(THF)_4$ by Sattelberger.[19] We decided to take advantage of this development and use $UI_3(THF)_4$ as an entry into U(III) poly(pyrazolyl)borate chemistry.

In this chapter the successful synthesis and X-ray structures of U(III) hydrotris(3,5-dimethylpyrazolyl)borate compounds, $U(Tp^{Me2})I_2(THF)_2$ (1), $U(Tp^{Me2})_2I$ (2), $U(Tp^{Me2})_2Br$ (3), and $[U(Tp^{Me2})_2THF][BPh_4]$ (4) are reported.

2.2. Results and Discussion

2.2.1. Synthesis of the Complexes

The reaction between $UI_3(THF)_4$ and one equiv of KTp^{Me2} proceeds readily and gives, after simple work-up, $U(Tp^{Me2})I_2(THF)_2$ (1) in 82% isolated yield (eq. 2.1). Compound 1 is sparingly soluble in toluene, benzene, and THF. Because of the low

$$UI_3(THF)_4 \; + \; KTp^{Me}{}_2 \quad \xrightarrow{\;THF/r.t.\;} \quad U(Tp^{Me}{}_2)I_2(THF)_2 \; + \; KI \downarrow \qquad 2.1$$

<div align="center">1 (black crystals)</div>
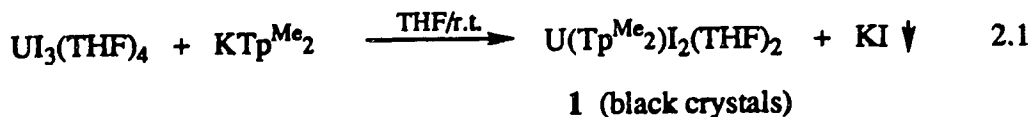
solubility of $U(Tp^{Me2})I_2(THF)_2$ in THF, prolonged stirring of the reaction mixture sometimes resulted in precipitation and contamination of the product with KI. In an attempt to overcome this problem, advantage was taken of the good solubility of NaI in THF. As shown in eq. 2.2, using $NaTp^{Me2}$, $U(Tp^{Me2})I_2(THF)_2$ precipitates from solution while

$$UI_3(THF)_4 \; + \; NaTp^{Me}{}_2 \quad \xrightarrow{\;THF/r.t.\;} \quad U(Tp^{Me}{}_2)I_2(THF)_2 \downarrow \; + \; NaI \qquad 2.2$$

<div align="center">1 (black crystalline powder)</div>
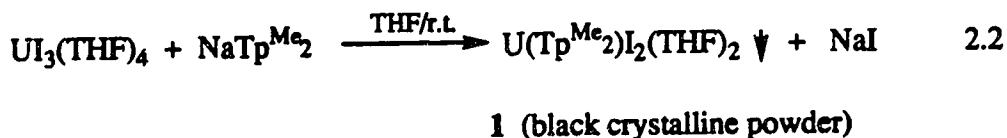
NaI remains dissolved. The yields for these two preparations are very similar. Although the latter method seemingly has an obvious advantage over the former, we found that the precipitation of $U(Tp^{Me2})I_2(THF)_2$ sometimes did not occur even after the reaction mixture was stirred for several hours. Cooling concentrated solutions of such reactions did produce a crystalline product. However, on warming the crystals to room temperature, they melted. It is possible that an anionic ate-type complex, $[U(Tp^{Me2})I_3][Na(THF)_x]$,

was formed, (eq. 2.3). Formation of such compounds often complicates the preparation

$$UI_3(THF)_4 + NaTp^{Me}2 \xrightarrow{THF/r.t.} [U(Tp^{Me}2)I_3][Na(THF)_x] \qquad 2.3$$
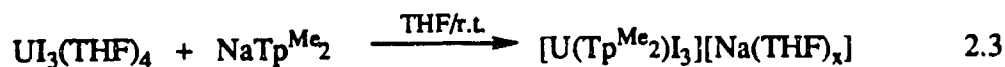
of MCp_nX_{3-n} complexes.[20-23] In an effort to discover a reliable and reproducible preparation of 1, the preparation using KTp^{Me2} was repeated several times. It was observed that precipitation often occurred when older, scratched vessels were used. Thus, use of new glassware is strongly recommended. Alternatively, deliberately scratched vessels will induce precipitation of 1 and are thus convenient when using $NaTp^{Me2}$. Attempts to remove coordinated THF ligands from compound 1 met with failure.

The preparation of $U(Tp^{Me2})_2I$ (2) did not present similar problems, since the solubility of $U(Tp^{Me2})_2I$ in THF is much greater than that of $U(Tp^{Me2})I_2(THF)_2$. A solution of KTp^{Me2} can be added in one portion to a slurry of $UI_3(THF)_4$ in THF. After stirring for about three hours, filtration gives a clear, dark blue solution and almost quantitative precipitation of KI. Analytically pure $U(Tp^{Me2})_2I$ (2) is obtained in good yield either by stripping off all solvent and triturating the residue with hexane or pentane, or by cooling concentrated solutions at -40°C. The analogous bromide, $U(Tp^{Me2})_2Br$ (3), is obtained in a similar way.

Although compounds 1 and 2 can be prepared readily and in good yields, prolonged stirring of the reaction mixtures or storing the solutions at room temperature for long periods of time resulted in cleavage of the B-N bond of the Tp^{Me2} ligand and formation of pyrazobole, $[HB(3,5-Me_2pz)_2]_2$; the nature of the uranium by-product complex is not known. Therefore, such treatment must be avoided. B-N bond cleavage is a commonly observed complication in poly(pyrazolyl)borate chemistry, and often occurs with a strong Lewis acidic metal center.[24,25] In our laboratory the pyrazobole, $[HB(3,5-Me_2pz)_2]_2$, was isolated and characterized previously from the reaction of $ScCl_3$ with KTp^{Me2}.[26]

As a first step in studying the reactivity of compounds 1 and 2, iodide abstraction with TlBPh$_4$ was attempted. It is interesting that compound 2 reacts immediately with TlBPh$_4$ to form [U(Tp^{Me2})$_2$THF][BPh$_4$] (4), eq. 2.4, while there is no reaction with

$$U(Tp^{Me2})_2I + TlBPh_4 \xrightarrow{\text{THF/r.t.}} [U(Tp^{Me2})_2THF][BPh_4] + TlI \downarrow \qquad 2.4$$
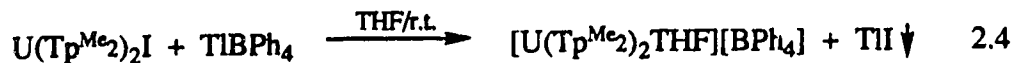
4 (black crystals)

compound 1. Compound 4 is insoluble in toluene, benzene and hexane, but it is soluble in THF. The coordinated THF could not be removed by heating the sample at 80°C for a few hours under high vacuum. Although compound 4 is stable in the solid state, it is not stable in THF. The compound decomposed in a few weeks in a flame-sealed NMR tube kept at room temperature and deposited a black solid. The nature of the decomposition product is unknown.

The formulations of the complexes 1-4 are based on elemental analyses and spectroscopic characterization. Mass spectrometry was successful only for compound 2. The IR spectra in each case showed the characteristic B-H stretch in the 2500 cm^{-1} region.

The ^{1}H NMR spectra for all four compounds are deceptively simple, displaying only a single set of signals (ratio 3:3:1) for the pyrazolyl groups. The spectra of complexes 1, 2, and 4 are shown in Fig. 2.1, 2.2, and 2.3. In particular, the shape of the resonances of 2 remains unchanged down to -100°C, while those for 3 broadens only. There is virtually no change in the line width at half-height of the methyl resonance at -11.71 ppm for compound 2 (from 49Hz to 52Hz) while there is a dramatic change from 18Hz to 640Hz for the same resonance of compound 3. The simple spectra indicate that the molecules are fluxional in solution, but because the low temperature limiting spectra could not be obtained, the coordination mode of the Tp^{Me2} ligands and the structure of the
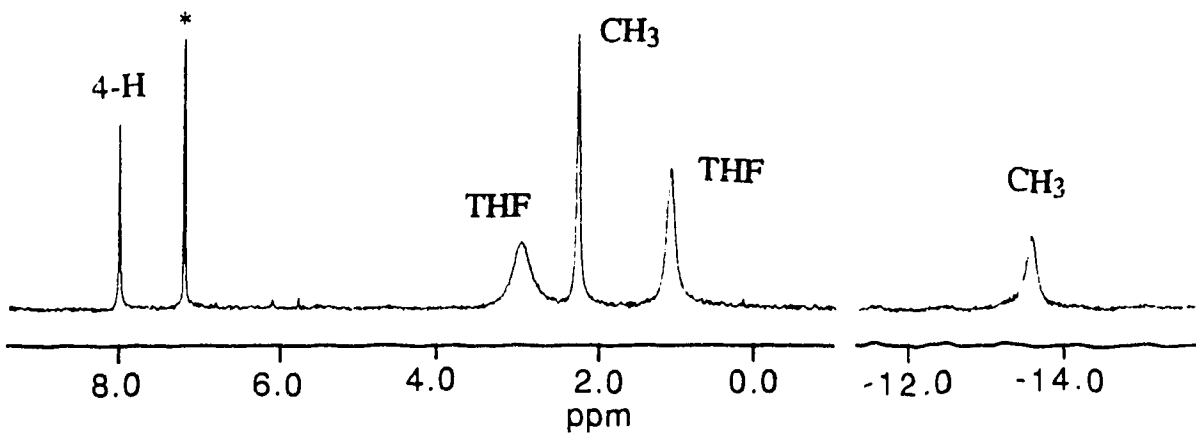
Fig. 2.1 ¹H NMR Spectrum of U(Tp^{Me2})I_2(THF)_2 (1) (C_6D_6, 24°C)
Throughout this thesis, the residual proton resonance(s) of deuterated solvents is(are) marked with *.
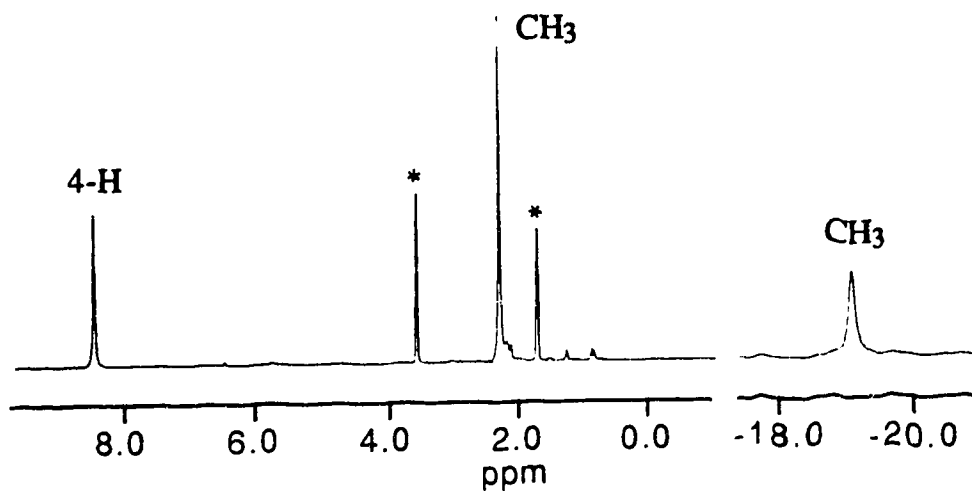
Fig. 2.2 ¹H NMR Spectrum of U(Tp^{Me2})_2I (2) (THF-d_8, -40°C)
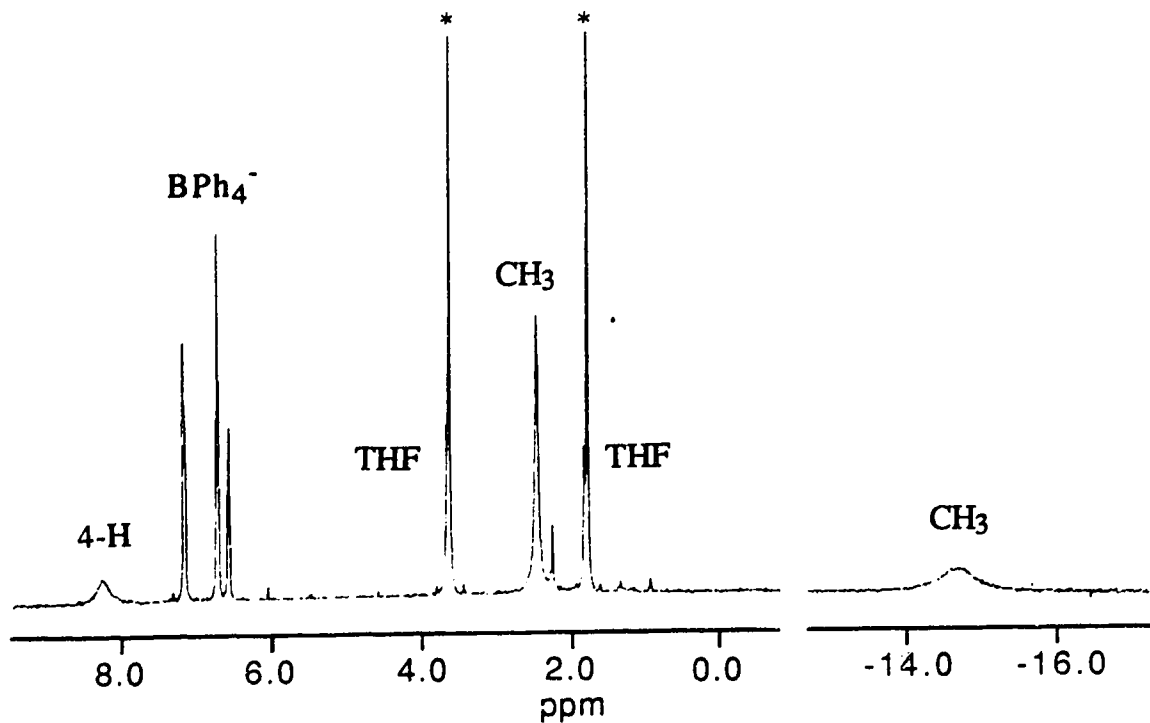
Fig. 2.3 ^{1}H NMR Spectrum of [U(Tp^{Me_2})$_2$THF][BPh$_4$] (4) (THF-d$_8$, 24°C)

complexes could not be deduced. Due to the paramagnetic nature of U(III) and the attendant broad signals, the assignment of the ^{1}H NMR spectra is solely based on integration. Thus, for compound 1, U(Tp^{Me_2})I$_2$(THF)$_2$, the assignment of the Tp^{Me_2} methyl protons and the THF α- or β-protons may not be reliable as a result of the closeness of their integration. The resonances due to coordinated THF were confirmed by deliberate addition of free THF which caused the peaks at 2.60 and 0.86 ppm to move toward free THF. This also revealed the occurrence of facile THF dissociation from U(Tp^{Me_2})I$_2$(THF)$_2$ in solution.

2.2.2. Crystal Structures of the Complexes

To establish the solid-state structures, single-crystal X-ray diffraction analyses of complexes 1, 2, and 4 were carried out. Perspective views of the molecules are shown in

Fig. 2.4, 2.5, and 2.6, respectively and selected bond distances and angles are given in Table 2.1.

U(Tp^{Me2})I$_2$(THF)$_2$ (1)

The structure of complex 1 is shown in Fig. 2.4. The Tp^{Me2} ligand coordinates to U(III) in an η^3-fashion and two iodide ions and two THF complete the coordination sphere to give a seven coordinate U(III) metal center. The geometry around uranium is best described as a capped octahedron (CO, 3:3:1 structure) which represents one of the basic polytopal forms for seven-coordination, the other two being the capped trigonal prism (CTP) and pentagonal bipyramid (PB).[27,28] The capped site is occupied by I1. One triangular face is formed by I2, O41, and O51, while N12, N22, and N32 span the other triangular face which is opposite to the capped site. The U-O bond lengths are 2.65(1) and 2.58(1)Å, and U-N bond distances are almost the same 2.56(1), 2.53(1), and 2.51(1)Å.

U(Tp^{Me2})$_2$I (2)

The molecular structure is shown in Fig. 2.5. The most interesting feature is that the coordination modes of the two Tp^{Me2} ligands are very different. One of the Tp^{Me2} ligands coordinates to the U(III) metal center in a typical tridentate mode, via N41, N51, and N61. However, the other ligand is unusual. Two of the pyrazolyl nitrogens, N11 and N21, are bonded to uranium metal center at normal U-N separations, 2.559(6) and 2.591(5)Å, respectively. The orientation of the third pyrazolyl ring of this ligand is such that the lone pair electrons of the potential donor atom, N31, are not pointing at the metal. Instead, the N-N bond of the pyrazolyl ring interacts with the U(III) in a side-on bonding mode. Indeed, the U-N31 (2.807(5)Å) and U-N32 (2.833(5)Å) distances are closely comparable and are only 0.2-0.3Å longer than the average of the remaining U-N bond lengths (2.57(6) Å). This is an example of a secondary, π-interaction, although the bonding in f-element complexes is commonly thought of as being largely ionic.[29]
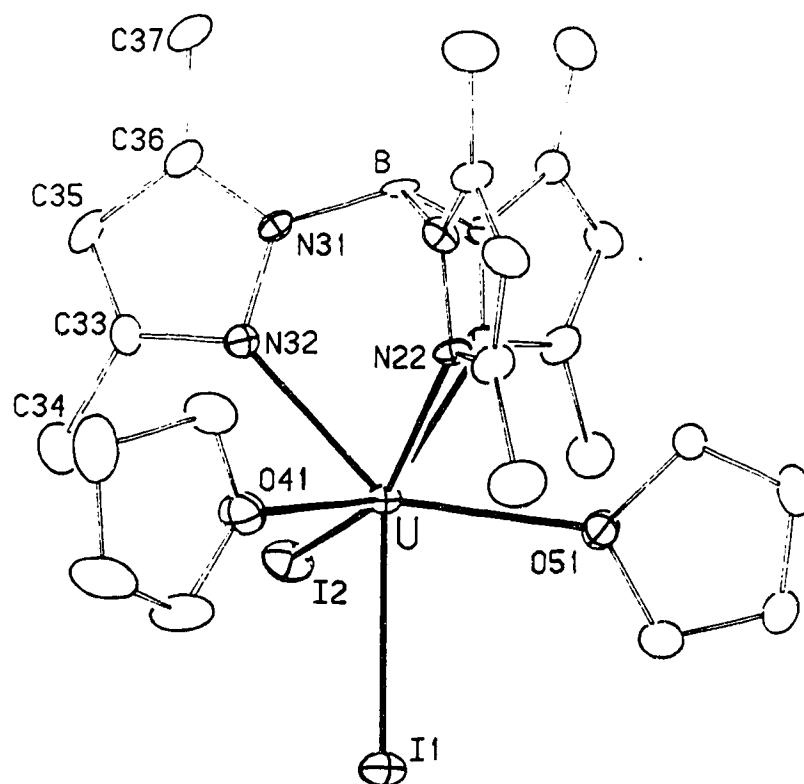
Fig. 2.4 Molecular Structure of U(Tp^{Me_2})I$_2$(THF)$_2$ (1)
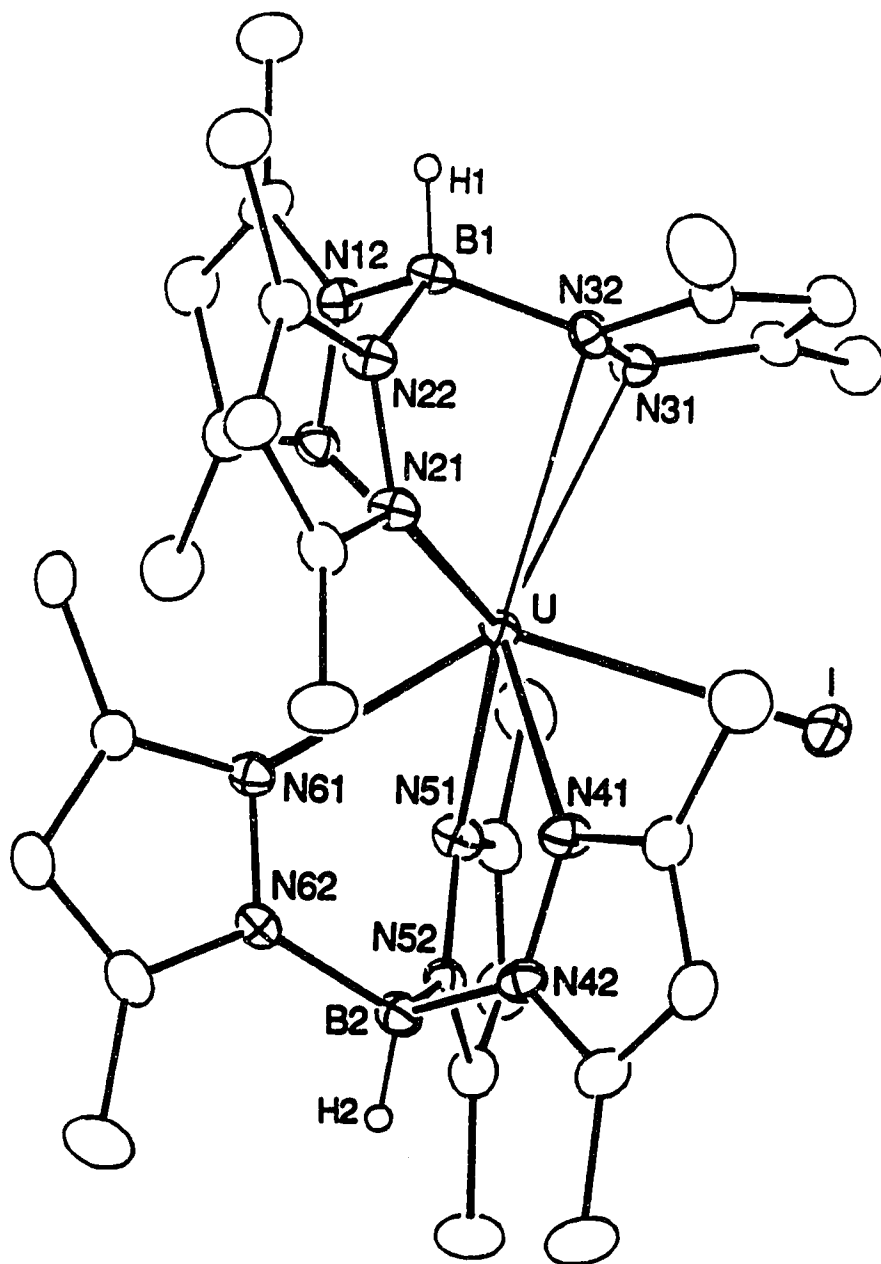
Fig. 2.5 Molecular Structure of U(Tp^{Me2})$_2$I (2)

However, Andersen[30] has shown that the U(III) compounds, $U(C_5H_4R)_3$ (R= Me, SiMe$_3$), prefer soft donor ligands and form complexes with classical π-acceptor ligands such as CNR' and CO. In fact the first stable CO uranium(III) complex has been prepared and structurally characterized recently.[31] That is, U(III) is capable of displaying characteristic covalent and π-type bonding interactions. The strength of the interaction between U(III) and N31-N32 in compound **2** does not rival that observed with $U(C_5H_4R)_3(L)$, L = CNR' and CO.[30] The N31-N32 distance is not different from the other N-N bond distances; however, a slight increase in the B-N bond length to the "dangling" pyrazolyl ring (1.561(7)Å) and, more significantly, the "pyramidalization" of N32 (sum of angles of N31-N32-C34, N31-N32-B1, and C34-N32-B1 (352.4(6)°) is less than 360°) in the complex **2** further corroborates the presence of an attractive interaction between uranium and pyrazolyl ring. Changes in hybridization and the attendant out-of-plane bending of the substituents is one of the typical consequences of metal coordination to unsaturated ligands.[32] It is interesting to note that, in the 16-electron complex $Rh(\eta^2\text{-}Tp^{Me2})(CNCH_2CMe_3)_2$,[33] the orientation of the third pyrazolyl group is similar to that in compound **2**. However, in that case no secondary interaction between Rh and the pyrazolyl ligand was detected, the calculated Rh-N distances being 3.92 Å and 3.30 Å, more than 1.2 Å longer than the normal Rh-N σ bonds.

The geometry around the U(III) center in **2** is best described as a capped octahedron. One triangular face is formed by N11, N21, and N61 while the other comprises N41, N51, and the midpoint of N31-N32, with the iodide capping the latter face of the octahedron. Another noteworthy feature of this structure is the U-N61 bond distance (2.657(5)Å), trans to the weakly interacting pyrazolyl ring, which is significantly longer than the other two U-N bond lengths of the η^3-Tp^{Me2} ligand (U-N41, 2.509(5) and U-N51, 2.510(5)Å, respectively). It is as if the solid state structure represents a snapshot in the trajectory of the fluxional process in solution. As one pyrazolyl group becomes fully coordinated, another changes its bonding mode and the exchange process initiates. The

Table 2.1 Selected Bond Distances (Å) and Angles (°) for Complexes 1, 2, and 4

1		2		4	
Bond Distances					
U-N12	2.56(1)	U-N11	2.559(6)	U-N11	2.552(5)
U-N22	2.53(1)	U-N21	2.591(5)	U-N21	2.512(5)
U-N32	2.51(1)	U-N41	2.509(5)	U-N31	2.621(5)
		U-N51	2.510(6)	U-N41	2.641(5)
		U-N61	2.657(5)	U-N51	2.555(5)
		U-N31	2.807(5)@	U-N61	2.490(5)
		U-N32	2.833(5)@		
U-N$_{ave}$	2.53(3)	U-N$_{ave}$	2.57(6)#	U-N$_{ave}$	2.54(4)
U-I1	3.198(2)	U-I	3.2196(8)		
U-I2	3.145(2)				
U-I$_{ave}$	3.172(37)				
U-O41	2.65(1)			U-O1	2.564(4)
U-O51	2.58(1)				
U-O$_{ave}$	2.62(5)				
Bond Angles					
I1-U-I2	85.70(5)	I-U-N*	85.1	O1-U-N31	74.8(2)
I1-U-O41	79.0(3)	I-U-N41	74.8(1)	O1-U-N51	70.7(1)
I1-U-O51	81.6(2)	I-U-N51	76.1(1)	O1-U-N61	83.4(2)
I1-U-N12	143.0(3)	I-U-N11	135.0(1)	O1-U-N11	135.0(1)
I1-U-N22	123.6(2)	I-U-N22	132.5(1)	O1-U-N21	132.5(1)
I1-U-N32	137.8(2)	I-U-N61	133.9(1)	O1-U-N41	134.5(2)

@ The side-on U-N bonds; # The side-on U-N bonds are not included;
N* is the center of N31-N32.

presence of subtly different U-pyrazolyl interactions is consistent with the highly fluxional structure of complex 2.

It was not clear whether the unusual structure is due to steric or electronic factors. To gain better understanding the bromide analogue was prepared. Preliminary results from Prof. V. Day show that this complex is seven coordinate and both Tp^{Me2} ligands are coordinated to U(III) metal center in an η^3-fashion. Thus, a relatively small change in the size of the halide (I⁻, 2.06Å; Br⁻, 1.82Å) results in a major structural change. This suggests that the unusual bonding observed in $U(Tp^{Me2})_2I$ (2) is steric in origin.

$[U(Tp^{Me2})_2THF][BPh_4]$ (4)

The molecular structure is shown in Fig. 2.6. It is immediately evident that the U(III) metal center is coordinated by two η^3-Tp^{Me2} ligands as well as a THF molecule to give a seven-coordinate U(III) ion. Just like compounds 1 and 2 the geometry around the U(III) center for 4 is best described as a capped octahedron. One triangular face is formed by N11, N21, and N41, while the other comprises N31, N51, and N61 with the oxygen atom of coordinated THF capping the latter face of the octahedron. Removal of iodide from $U(Tp^{Me2})_2I$ (2) resulted in a decrease in the coordination congestion about the U(III) center, and thus the disappearance of the unusual side-on bonded interaction. However, coordination of THF and formation of seven coordinate U(III) was somewhat surprising. Since $M(Tp^{Me2})_2$ (M=Sm, Yb)[34] have no coordinated THF, this is most reasonably attributed to the enhanced Lewis acidity of U(III) compared to the divalent complexes. Although the THF ligand is smaller than iodide, its steric effect can still be seen. The distance from U(III) to N31 (2.621(5)Å), the nitrogen which now occupies the site of the side-on interaction in compound 2, is slightly longer than the other two U-N bond lengths of the same Tp^{Me2} ligand (U-N11, 2.552(5) and U-N21, 2.512(5)Å, respectively). Also the U-N41 bond distance (2.641(5)Å), the one trans to U-N31, is slightly longer than the other two U-N bond lengths (U-N51, 2.555(5) and U-N61, 2.490(5)Å, respectively).
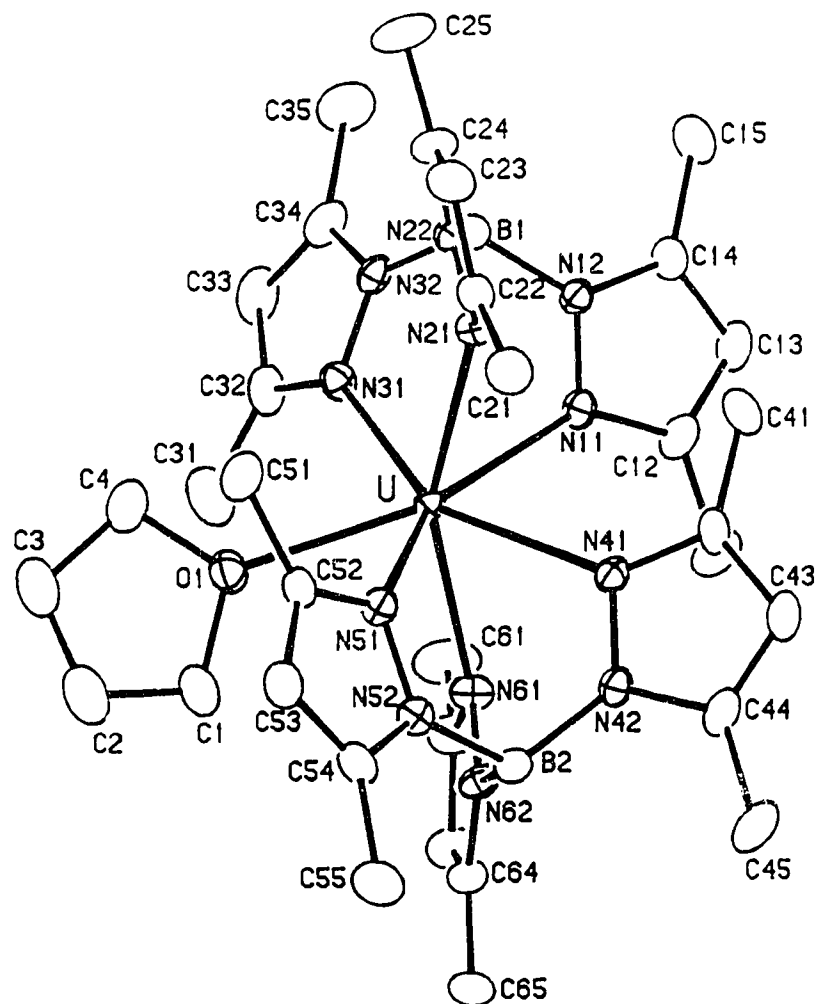
Fig. 2.6 Molecular Structure of $[U(Tp^{Me2})_2THF]^+$ (4)

As in compound **2**, the symmetry about U(III) is C_1, so the simple ^{1}H NMR spectrum of **4** must be due to facile interchange between the two pyrazolylborate ligands.

2.2.3. Structural Comparison

The stereochemistry of a homoleptic ML_7 complex with capped octahedral geometry can be defined by the angular parameters Φ_B and Φ_E, the angles the M-B and M-E bonds make with the threefold axis.[27] The capping atom is associated with the greatest repulsion energy. The calculated parameters are: $\Phi_B=74.6°$; $\Phi_E=130.3°$.
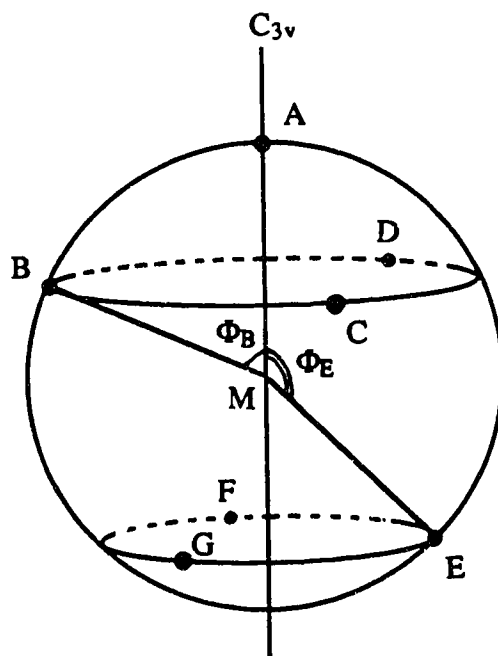
Fig. 2.7 The Stereochemistry of the Capped Octahedron

The averaged structural parameters , assuming full C_{3v} symmetry, for complexes **1**, **2**, and **4** are calculated to be: $\Phi_B=82.1°$; $\Phi_E=134.8°$ for **1**, $\Phi_B=78.7°$; $\Phi_E=133.8°$ for **2**, and $\Phi_B=76.3°$; $\Phi_E=131.9°$ for **4**, respectively. A clear trend can be readily seen.

Compound 1 experiences the greatest distortion from regular capped octahedral geometry, followed by compound 2, while compound 4 is the least distorted. The logical reasons for this is the large size of iodide and the rigidity of the Tp^{Me2} ligand. Also the "low coordination environment of compound 4, UN_6O, approximates C_{3v} symmetry the best. The structural similarity between compound 1, $U(Tp^{Me2})Cl_3(THF)$,[14] and $U(Tp^{Me2})Cl_3OP(OEt)_3$[35] provides a very interesting comparison. In the three structures the Tp^{Me2} ligand occupies the triangular face which is trans to the capped site. Because of the rigidity of the Tp^{Me2} ligand the Φ_E angles are virtually the same (134.8° for 1, 134.9° for $U(Tp^{Me2})Cl_3(THF)$, and 135.4° for $U(Tp^{Me2})Cl_3OP(OEt)_3$). The steric repulsion in complex 1 between the I1 and I2, O41, and O51 causes the triangular face to open up to release the steric repulsion and results in a Φ_B of 82.1°, which is 6.3° and 7.5° greater than in $U(Tp^{Me2})Cl_3OP(OEt)_3$ (75.8°) and $U(Tp^{Me2})Cl_3(THF)$ (74.6°), respectively. The length of the U-I1 bond, 3.198(2)Å, is 0.053Å longer than the U-I2 bond length and is another indication of this steric repulsion. It is not difficult to see that, for compounds 1, 2, and 4, as the number of iodide ligands increases the complex experiences a greater distortion.

A comparison between U-L bond distances is rendered difficult by the large spread between what often are chemically non-equivalent sites. Some trend in U-I distances can be detected, the average U-I bond lengths being: 3.13(3)Å $(UI_3(THF)_4) \leq 3.172(37)$Å (1) < 3.2196(8)Å (2) (although the large difference between the U-I distances in 1 makes the averaging somewhat artificial). This can be interpreted as showing that a Tp^{Me2} ligand occupies somewhat more space than two coordinated THF and one iodide. The presence of more Tp^{Me2} ligands will cause more congestion around U(III) resulting in a longer U-I bond length to release the strain; the congestion appears to be: $2>1\geq UI_3(THF)_4$. This sequence can explain why compound 2 can undergo iodide abstraction readily, but not compound 1 and $UI_3(THF)_4$, although the "chelate effect", in the formation of two η^3-Tp^{Me2} ligand in 2, cannot be discounted as contributing to the ease of iodide abstraction in

this complex. The average U-N bond lengths for compounds 1, 2, and 4 are 2.53(3), 2.54(4), and 2.56(6)Å, respectively, but due to the large average deviation a meaningful comparison is not warranted. However, the U-O$_{THF}$ seems follow the U-I bond length trend: 2.62(5)Å (1)>2.564(4)Å (4)>2.52(4)Å UI$_3$(THF)$_4$.

2.3. Conclusions

Straightforward synthesis affords the complexes U(Tp^{Me2})I$_2$(THF)$_2$, U(Tp^{Me2})$_2$I, and U(Tp^{Me2})$_2$Br in good yields; U(Tp^{Me2})$_2$I readily undergoes iodide abstraction with TlBPh$_4$ to form the cationic compound, [U(Tp^{Me2})$_2$THF][BPh$_4$]. X-ray structural analyses revealed that the mode of coordination of the hydrotris(pyrazolyl)borate ligand, Tp^{Me2}, depends on the nature of the ancillary ligand(s) on the U(III) metal center.

2.4. Experimental Section

2.4.1. General Procedures

The preparation and handling of the compounds were carried out under an atmosphere of purified argon or nitrogen using either standard Schlenk techniques in conjunction with a double vacuum manifold or in a nitrogen-filled Vacuum Atmospheres HE-553-2 DRILAB. Solvents were dried over potassium benzophenone ketyl (THF) or potassium metal (pentane and hexane), and were distilled and degassed prior to use.

Infrared spectra were recorded on a BOMEM MB-100 FT interferometer using samples pressed in KBr pellet form. NMR spectra were recorded on either Bruker WH-200 or AM-400 FT spectrometer using sample tubes flame sealed under vacuum. Mass spectra were recorded on an A.E.I. MS9 or A.E.I. MS12 mass-spectrometer. Elemental analyses were performed by the Microanalytical Laboratory, Department of Chemistry, University of Alberta.

2.4.2. Preparation of Starting Materials

The ligands, MTp^{Me2} (M=K, Na), were prepared according to published methods.[3] $TlBPh_4$ was synthesized by the reaction of Tl_2SO_4 with 2 equiv of $NaBPh_4$ in water followed by filtration, washing with Et_2O, and drying under vacuum. The preparation of $UI_3(THF)_4$ followed the published procedure[19] and is described below:

Uranium turnings (9.94 g, 4.2×10^{-2} mol) were treated with concentrated nitric acid, HNO_3, three times until the black oxide coating was completely removed. The oxide-free turnings were washed with plenty of H_2O (5x50mL), then with acetone (3x40mL); this was followed by drying under vacuum for 10 min and washing again with freshly distilled THF (2x30mL). To activate the turnings, HgI_2 (300 mg)were added and the mixture was stirred in 50mL of THF. Initially the color of the supernatant solution was light blue, but it then turned brown after about 10 min of stirring. The mixture was filtered and the residue was washed with THF until the filtrate was colorless. THF (130mL) was added to the turnings and the mixture was cooled in a -17°C ice-salt bath for 30 minutes. Sublimed I_2 (13.94g, 5.5×10^{-2}mol) was added in one portion. The flask was taken out of the ice-salt bath and gently shaken. After it became warm to the hand it was put back to the ice-salt bath and the mixture was stirred for about 20 minutes. This operation was repeated once more. The mixture was then allowed to warm for one hour. The color of the mixture changed from dark red (I_2) to intense green. At this stage the mixture was transferred to the dry box and was vigorously stirred for three days. Formation of a purple-blue microcrystalline powder was observed after stirring overnight. Filtration gave a very dark-colored supernatant solution and a mixture of $UI_3(THF)_4$ with excess uranium turnings. Crystalline $UI_3(THF)_4$ (11.13g) was obtained by extraction with THF followed by cooling the supernatant solution at -40°C to give a second crop of $UI_3(THF)_4$ (0.45g). The combined yield was 30%.

$UBr_3(THF)_4$ was prepared in a the same way as $UI_3(THF)_4$ by substituting I_2 with Br_2.

2.4.3. Synthetic Procedures

U(Tp^{Me2})I$_2$(THF)$_2$ (1)

(a). **Using KTp^{Me2}:** A solution of KTp^{Me2} (1.133g, 3.37x10^{-3}mol) in 15mL of THF was added dropwise to a slurry of UI$_3$(THF)$_4$ (3.055g, 3.37x10^{-3}mol) in the same solvent (150mL). After the addition was complete (ca. 30min) the mixture was stirred for one hour only. The mixture was filtered int > flasks which were kept at -40°C for several days. Compound 1 was isolated as dark-blue crystals (combined amount 2.27g, 73% isolated yield). IR (KBr, cm^{-1}): v(B-H) 2560. ^{1}H NMR (C$_6$D$_6$, 24°C, δ ppm): 2.2, -13.56 (s, s, 9H, 9H, 3,5-Me-pz); 7.95 (s, 3H, 4-H-pz); 2.60, 0.86 (m, m, 8H, 8H, CH_2, THF). ^{11}B NMR (C$_6$D$_6$, 24°C, δ ppm): 21.40. Anal. Calc. for C$_{23}$H$_{38}$BN$_6$O$_2$I$_2$U: C, 29.60; H, 4.10; N, 9.01. Found. C, 29.11; H, 4.15; N, 8.83%.

The preparation was repeated several times. It was noticed that scratched, old flasks appeared to stimulate premature crystallization of product and resulted in difficulty in separating KI from 1. It is highly recommended that a flask without scratches be used. Moreover, extended periods of stirring should be avoided because precipitation of product was observed even when a new flask was used.

(b). **Using NaTp^{Me2}:** A solution of NaTp^{Me2} (262mg, 8.20x10^{-4}mol) in THF (5mL) was added in one portion to a slurry of UI$_3$(THF)$_4$ (744mg, 8.20x10^{-4}mol) in THF (5mL). After stirring for three hours a dark-blue microcrystalline powder was formed. The solution was cooled at -40°C overnight and inverse filtration gave 488mg (63% yield) of analytically pure 1.

The preparation also met some difficulties. The product did not always precipitate. In order to ensure consistent precipitation of the product the surface of a flask was deliberately roughed up with Silicon Carbide Grain #150.

U(Tp^{Me2})$_2$I (2)

A solution of KTp^{Me2} (285mg, 8.46x10^{-4}mol) in THF (20mL) was added dropwise to a slurry of UI$_3$(THF)$_4$ (384mg, 4.23x10^{-4}mol) in the same solvent (15mL.). The reaction mixture was stirred at room temperature for three hours. Following inverse filtration, the solution was concentrated under vacuum to about 5mL. Cooling the solution at -40°C overnight gave 2 as dark-blue crystalline powder, 325mg, in 80% yield. IR (KBr, cm^{-1}): ν(B-H) 2484. ^{1}H NMR (C$_6$D$_6$, 24°C, δ ppm): 0.33, -11.71 (s, s, 18H, 18H, 3,5-Me-pz); 7.44 (s, 6H, 4-H-pz). ^{1}H NMR (THF-d$_8$, -100°C, δ ppm): 4.10, -24.94 (s, s, 18H, 18H, 3,5-Me-pz); 9.35 (s, 6H, 4-H-pz); 18.32 (br, 2H, H-B). ^{11}B NMR (C$_6$D$_6$, 24°C, δ ppm): 2.99. M.S.: 959(M)$^+$; 832(M-I)$^+$. Anal. Calc. for C$_{30}$H$_{44}$B$_2$N$_{12}$IU: C, 37.56; H, 4.62; N, 17.52; I, 13.29. Found: C, 37.40; H, 4.78; N, 16.66; I, 12.95%.

U(Tp^{Me2})$_2$Br (3)

A solution of KTp^{Me2} (291mg, 8.66x10^{-4}mol) in THF (5mL) was added in one portion to a slurry of UBr$_3$(THF)$_4$ (332mg, 4.33x10^{-4}mol) in THF (4mL). The reaction mixture was stirred at room temperature for three hours. An immediate color change from purple-red to purple-blue was observed. Following inverse filtration, the solution was concentrated under vacuum to about 4mL. Cooling the solution at -40°C gave 84mg of 3 as dark-blue crystalline powder. After concentrating the solution and cooling it at -40°C a second batch of crystalline powder (76mg) was obtained. The combined yield was 41%. IR (KBr, cm^{-1}): ν(B-H) 2555, 2485. ^{1}H NMR (toluene-d$_8$, 24°C, δ ppm): 1.04, -13.89 (s, s, 18H, 18H, 3,5-Me-pz); 7.65 (s, 6H, 4-H-pz); 9.20 (br, 2H, H-B). ^{11}B NMR (toluene-d$_8$, 24°C, δ ppm): 9.00. Anal. Calc. for C$_{30}$H$_{44}$B$_2$N$_{12}$BrU: C, 39.50; H, 4.86; N, 18.42; Br, 8.76. Found: C, 40.24; H, 4.83; N, 18.15; Br, 9.07%.

[U(Tp^{Me2})$_2$THF][BPh$_4$] (4)

Solid TlBPh$_4$ (128mg, 2.44x10^{-4}mol) was added to a solution of U(Tp^{Me2})$_2$I (234mg, 2.44x10^{-4}mol) in THF (15mL) in several portions. A yellow precipitate formed immediately and the color of solution turned from dark blue to turquoise. After stirring overnight and filtration, the solvent was stripped off under vacuum, and the residue was washed with hexane (10mL). The solid was redissolved in THF. Gas phase diffusion of hexane over a few days at room temperature resulted in the formation of big black crystals of 4 (191mg, 65% yield). IR (KBr, cm^{-1}): v(B-H) 2484. ^{1}H NMR (THF-d$_8$, 24°C, δ ppm): 2.38, -14.76 (s, s, 18H, 18H, 3,5-*Me*-pz); 8.22 (s, 6H, 4-*H*-pz); 7.10, 6.65, 6.50 (s, t, t, 8H, 8H, 4H, BPh$_4$$^-$). ^{11}B NMR (THF-d$_8$, 24°C, δ ppm): 14.64 (br, Tp^{Me2}), -6.19 (s, BPh$_4$$^-$). Anal. Calc. for C$_{58}H_{72}B_3N_{12}$OU: C, 56.93; H, 5.93; N, 13.73; Found: C, 57.01; H, 5.96; N, 13.66%.

2.4.4. X-ray Data Collection, Structure Solution and Refinement

Sample preparation, data collection, structure solution and refinement are very similar throughout the thesis. Therefore, a general description is given in this first experimental chapter, in the following Chapters only special features pertinent to the respective compounds will be listed.

A black crystal of U(Tp^{Me2})I$_2$(THF)$_2$ (1) suitable for X-ray analysis was obtained by slowly concentrating a saturated THF solution over a few hours. Liquid phase diffusion of hexane into a THF solution is recommended in order to grow X-ray quality single crystals of U(Tp^{Me2})$_2$I (2). For compound 4, gas phase diffusion of hexane into THF solution over a few weeks works very well.

Single crystals of the respective complexes were sealed in thin-wall glass capillaries under an inert atmosphere, mounted and optically centered in the X-ray beam of either an Enraf-Nonius CAD4 or a Siemens P1 automated diffractometer. All intensity measurements were performed using MoK$_\alpha$ radiation (λ=0.7107Å) with a graphite crystal,

incident beam monochromator. The automatic peak search and reflection indexing programs generated the cells. The proper choices of space groups were confirmed by the successfu' 'ution and refinement of the structures. The cell constants and orientation matries were obtained from a least-squares refinement of the setting angles of ca. 25 reflections in an approximate range $8° < 2\theta < 30°$. The intensity data were collected by either ω-2θ or θ-2θ scan techniques. After data collection, Lorenz and polarization corrections were applied. The position of the uranium atom was derived from a three-dimensional Patterson map. The remaining non-hydrogen atoms were located from a serie. of difference Fourier maps. Adjustment of atomic parameters was carried out by full-matrix least-squares refinement on F_o minimizing the function $\sum w(|F_o|-|F_c|)^2$, where $|F_o|$ and $|F_c|$ are the observed and calculated structure factor amplititudes and the weighting factor w is $4F_o^2/s^2(F_o^2)$. The neutral atom scattering factors and anomalous dispersion terms were taken from the usual sources.[36] Hydrogen atom positions were calculated by assuming a C-H bond length of 0.95Å and the appropriate sp^2 or sp^3 geometry. A summary of the crystallographic data, intensity data collection and refinement are presented in Table 2.3. Further details concerning the structures can be obtained from Dr. R. McDonald and Professor V. W. Day.

Table 2.2 Crystallographic Data for Complexes 1, 2, and 4

compounds	1	2	4
mol formula	$C_{23}H_{38}BI_2N_6O_2U$	$C_{30}H_{44}B_2IN_{12}$	$C_{58}H_{72}B_3N_{12}OU$
formula weight	925.19	959.32	1223.76
space group	$P2_1/c$	$P\bar{1}$	$P2_1/c$
a,Å	9.996(5)	11.866(2)	13.977(4)
b,Å	18.575(6)	15.062(2)	22.357(5)
c,Å	16.663(5)	11.423(2)	18.523(3)
α,deg	90	93.12(1)	90
β,deg	93.99(4)	115.32(1)	90.46(2)
γ,deg	90	82.84(1)	90
V,Å³	3086(4)	1831(1)	5788(4)
Z	4	2	4
crystal diemnsions (mm)	0.52x0.40x0.33	0.19x0.55x0.66	0.63x0.22x0.19
linear absorbance coefficient (cm⁻¹)	50.74	69.95	27.06
diffractometer		Enraf-Nonius CAD4	
radiation(Å)		MoKα(0.7107) from graphite monochromater	
scan mode	ω-2θ	θ-2θ	θ-2θ
2θ limits(deg)	3.0-56.0	2.0-50.0	2.0-50.0
temp, °C	23	23	23
no. of unique data (I>3σ(I))	3441	5068	5910
no. of variables	316	415	676
R	0.056	0.043	0.032
Rw	0.060	0.053	0.036

2.5. References

(1)   Trofimenko, S. *J. Am. Chem. Soc.* **1966**, *88*, 1842.

(2)   Trofimenko, S. *J. Am. Chem. Soc.* **1967**, *89*, 3170.

(3)   Trofimenko, S. *J. Am. Chem. Soc.* **1967**, *89*, 6288.

(4)   Niedenzu, K.; Trofimenko, S. *Top. Curr. Chem.* **1986**, *131*, 1-37.

(5)   Trofimenko, S. *Prog. Inorg. Chem.* **1986**, *34*, 115-209.

(6)   Trofimenko, S. *Chem. Rev.* **1993**, *93*, 943-980.

(7)   Kitajima, N.; Tolman, W. B. *Prog. Inorg. Chem.* **1995**, in press.

(8)   Krentz, R. Ph. D. Thesis, University of Alberta, 1989.

(9)   Gutierrez, E.; Hudson, S. A.; Monge, A.; Nicasio, M. C.; Paneque, M.; Carmona, E. *J. Chem. Soc., Dalton Trans.* **1992**, 2651.

(10) Trofimenko, S. *Acc. Chem. Res.* **1971**, *4*, 17-22.

(11) Trofimenko, S. *Chem. Rev.* **1972**, *72*, 497-509.

(12) Bagnall, K. W.; Edwards, J.; du Preez, J. G. H.; Warren, R. F. *J. Chem. Soc., Dalton Trans.* **1974**, 140-143.

(13) Bagnall, K. W.; Beheshti, A.; Heatley, F. *J. Less-Common Met.* **1978**, 171-176.

(14) Ball, R. G.; Edelmann, F.; Matisons, J. G.; Takats, J.; Marques, N.; Marcalo, J.; Matos, A. P. D.; Bagnall, K. W. *Inorg. Chim. Acta* **1987**, *132*, 137-143.

(15) Domingos, A.; Marcalo, J.; Marques, N.; De Matos, P. *J. Less-Common Met.* **1989**, *149*, 271-277.

(16) Santos, I.; Marques, N.; De Matos, A. P. *Inorg. Chim. Acta* **1985**, *110*, 149-151.

(17) Santos, I.; Marques, N.; De Matos, A. P. *J. Less-Common Met.* **1986**, *122*, 215-218.

(18) Moody, D. C.; Odom, J. D. *J. Inorg. Nucl. Chem.* **1979**, *41*, 533.

(19) Clark, D. L.; Sattelberger, A. P.; Bott, S. G.; Vrtis, R. N. *Inorg. Chem.* **1989,** *28,* 1771-1773.

(20) Fagan, P. J.; Manriguez, J. M.; Marks, T. J.; Day, C. S.; Vollmer, S. H.; Day, V. W. *Organometallics* **1982,** *1,* 170-180.

(21) Blake, P. C.; Lappert, M. F.; Taylor, R. G.; Atwood, J. L.; Zhang, H.-M. *Inorg. Chim. Acta* **1987,** *139,* 18.

(22) Watson, P. L. *J. Chem. Soc., Chem. Commun.* **1980,** 652-653.

(23) Wayda, A. L.; Evans, W. J. *Inorg. Chem.* **1980,** *19,* 2190-2192.

(24) Kime-Hunt, E.; Spartalian, K.; DeRusha, M.; Nunn, C. M.; Carrano, C. J. *Inorg. Chem.* **1989,** *28,* 4392-4399.

(25) Bradley, D. C.; Hursthouse, M. B.; Newton, J.; Walker, N. P. C. *J. Chem. Soc., Chem. Commun.* **1984,** 188.

(26) Matisons, J. G. unpublished results.

(27) Kepert, D. L. *Inorganic Stereochemistry*; Springer-Verlag/Berlin Heidelberg, **1982;** Vol. 6, pp 117.

(28) Hoffmann, R. H.; Beier, G. F.; Muetterties, E. L.; Rossi, A. R. *Inorg. Chem.* **1977,** *16,* 511-522.

(29) Raymond, K. N.; Eigenbrot, C. W. J. *Acc. Chem. Res.* **1980,** *13,* 276.

(30) Brennan, J. G.; Andersen, R. A.; Robbins, J. L. *J. Am. Chem. Soc.* **1986,** *108,* 335.

(31) Parry, J.; Carmona, E.; Coles, S.; Hursthouse, M. *J. Am. Chem. Soc.* **1995,** *117,* 2649-2650.

(32) Mingos, D. M. P. In *Comprehensive Organometallic Chemistry*; E. W. Abel, F. G. A. Stone and G. Wilkinson, Ed.; Pergamon Press: Oxford, **1982;** Vol. III; Chapter 1.

(33) Jones, W. D.; Hessell, E. T. *Inorg. Chem.* **1991,** *30,* 778.

(34) Zhang, X. Ph. D. Thesis, University of Alberta, **1995.**

(35) Maier, R.; Muller, J.; Kanellakopulos, B.; Apostolidis, C.; Domingos, A.; Marques, N.; Pires de Matos, A. *Polyhedron* **1993**, *12*, 2801-2808.

(36) Cromer, D. T.; Waber, J. T. *International Tables for X-ray Crystallography*; Kynoch Press: Birmingham, 1974; Vol. 4, pp Table 2.2B.

Chapter 3

Derivative Chemistry of $U(Tp^{Me_2})I_2(THF)_2$ with
Carbon, Nitrogen, and Oxygen Donor Ligands

3.1. Introduction

In Chapter 2 it was demonstrated that $U(Tp^{Me_2})I_2(THF)_2$ can be readily prepared *via* the simple metathesis reaction of $UI_3(THF)_4$ with one equiv of Tp^{Me_2} in high yield. The complex has been fully characterized and X-ray analysis has confirmed its monomeric nature which may be crucial to its derivative chemistry. The main goal of this thesis was the utilization of the bulky Tp^{Me_2} ligand as a means of stabilizing various U(III) derivatives. High on the list were hydrocarbyl complexes, since two-electron metal-carbon σ bonds represent one of the fundamental building blocks in organometallic chemistry. The creation and transformation of such bonds are crucial steps in many catalytic processes.

Since the early 1940's, all attempts to synthesize simple uranium tetraalkyls were unsuccessful.[1,2] The products of these reactions, eq. 3.1, presumed to be uranium

$$UCl_4 \ + \ 4RLi \ \longrightarrow \ [UR_4] \ + \ 4LiCl \qquad 3.1$$

tetraalkyls, were unstable at room temperature and could not be isolated for detailed characterization. It was argued that facile β-H elimination was responsible for the instability of the complexes.[3] The first isolable σ-bonded actinide organometallics were prepared in 1973 as shown in eq. 3.2.[4-6] The coordination saturation of the uranium metal

$$U(\eta^5\text{-Cp})_3Cl \ \xrightarrow{\text{RMgX or RLi}} \ U(\eta^5\text{-Cp})_3R \qquad 3.2$$

R=alkyl, aryl, alkenyl

center by three η^5-cyclopentadienyl groups is the key for the thermal stability of the

compounds. Therefore, by using excess RLi to saturate the coordination of the U(IV) ion, a number of anionic homoleptic uranium(IV) complexes, $[LiL_n]_2[UR_6]$ (L=THF, Et_2O, and TMEDA), have been prepared also[7] (eq. 3.3). Since then the chemistry of U(IV)

$$UCl_4 \quad + \quad excess\ RLi \quad \longrightarrow \quad Li_2UR_6(L)_n \quad + \quad 4LiCl \qquad 3.3$$

R=CH_3, CH_2SiMe_3, C_6H_5, o-C_6H_4NMe_2
L=THF, Et_2O, TMEDA
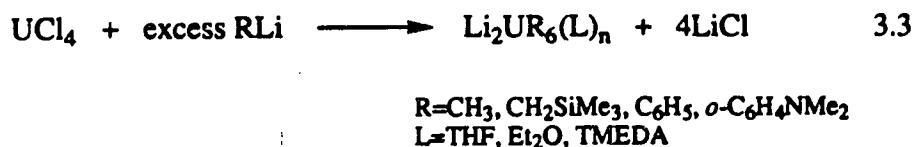
hydrocarbyl complexes has been extensively studied.[8] The research results show that the U(IV)-C bonds are very polarized and lead to high reactivities, such as hydrogenolysis, CO insertion, and polymerization of olefins. Compared to U(IV) hydrocarbyl complexes, the chemistry of U(III) hydrocarbyls is very limited. Marks et al.[9] reported the successful synthesis of $UCp^*_2CH(SiMe_3)_2$ by the reaction of $[U(\eta^5\text{-}Cp^*)_2(\mu\text{-}Cl)]_3$ with $LiCH(SiMe_3)_2$ and showed that it undergoes rapid hydrogenolysis to form the hydride $[UCp^*_2H]_x$.

Contrary to the hydrocarbyl derivatives, homoleptic uranium amido complexes are remarkably stable. For example, tetrakis(diethylamido)U(IV), $U(NEt_2)_4$, can be distilled at 120°C under high vacuum.[10] Uranium(IV) amide complexes were later successfully used by Jamerson et al.[11] for the preparation of a series of $UCp_2(NR_2)_2$ compounds; unlike "UCp_2Cl_2" these complexes were resistant to ligand redistribution. Although numerous uranium(IV) amido complexes have been prepared,[12] the number of U(III) amido complexes is still very small. The first U(III) amido complex, $U[N(SiMe_3)_2]_3$, was reported by Andersen[13] in 1979. Surprisingly, it showed no Lewis acidic behavior toward a series of Lewis bases (CO, PMe_3, $OPMe_3$, THF, NMe_3, pyridine, ${}^tBuNC$, and ${}^tBuCN$), but it did react with molecular oxygen or $ONMe_3$ to form the U(V) complex, $UO[N(SiMe_3)_2]_3$. Later, Marks et al.[9] reported the successful synthesis of $UCp^*_2N(SiMe_3)_2$ by the reaction of $[U(\eta^5\text{-}Cp^*)_2(\mu\text{-}Cl)]_3$ with $NaN(SiMe_3)_2$. The synthesis of the first U(III) hydrotris(pyrazolyl)borate amido complex,

U(Tp^{Me2})[N(SiMe$_3$)$_2$]Cl, was reported by Santos.[14] It was obtained by reduction of U(Tp^{Me2})[N(SiMe$_3$)$_2$]Cl$_2$ with sodium naphthalide. However, there is no further report on its derivative chemistry.

In view of the hard, oxophilic nature of U(IV) it is not surprising that there is a vast area of coordination[15,16] and organometallic[17-19] chemistry with oxygen donor ligands. Indeed, there are well documented examples of hydrotris(pyrazolyl)borate complexes, such as U(Tp^{Me2})(OR)$_x$Cl$_{3-x}$ (x=1-3; R=^{t}Bu, ^{i}Pr, C$_6$H$_2$Me$_3$-2,4,6),[20] U(Tp^{Me2})(OAr)$_x$Cl$_3$. $_x$Cl$_{3-x}$(THF)$_y$ (x=1-3; y=0,1; Ar=C$_6$H$_5$, C$_6$H$_2$Me$_3$-2,3,5),[21] and U(Tp^{Me2})(O$_2$CCH$_3$)$_3$.[22] In sharp contrast, there is still no report on the synthesis of hydrotris(pyrazolyl)borate U(III) alkoxides and aryloxides. Recently Isabel Santos[23] studied the reaction of U(Tp^{Me2})Cl$_2$ with aryloxides, but encountered difficulties. We hoped that use of the well characterized U(Tp^{Me2})I$_2$(THF)$_2$ may alleviate this problem.

In this chapter we report the successful synthesis of U(III) hydrotris(pyrazolyl)borate amido and hydrocarbyl complexes and summarize the results of their reactivity studies. Also reported are attempts to obtain U(Tp^{Me2})(OR)$_2$ type complexes

3.2. Results and Discussion

3.2.1. Synthetic Aspects: Amido and Hydrocarbyl Derivatives

Considering the dramatic thermal stability of uranium amido complexes over the hydrocarbyl analogues we decided to start our investigation of the derivative chemistry of U(Tp^{Me2})I$_2$(THF)$_2$ with the amido ligand. Reaction of U(Tp^{Me2})I$_2$(THF)$_2$ with two equiv of NaN(SiMe$_3$)$_2$, a very popular amido ligand with f-elements, proceeded readily and gave, after simple work-up, purple-blue crystalline U(Tp^{Me2})[N(SiMe$_3$)$_2$]$_2$ (5) in 80% isolated yield.

The preparation of the bis-hydrocarbyl derivative proved to be considerably more challenging and troublesome. From the initial reactions with the organolithio reagent,

LiCH$_2$SiMe$_3$, no pure compound could be isolated. Hexane diffusion into THF solution gave only an uncharacterizable, oily material. Solvent removal, followed by extraction of the residue with toluene and cooling the toluene extracts precipitated blue crystals which were identified as the starting material, U(Tp^{Me2})I$_2$(THF)$_2$, on the basis of ^{1}H NMR spectroscopy. Success was finally achieved by using the potassium salt of the bulky hydrocarbyl, CH(SiMe$_3$)$_2^-$; with this ligand, dark blue U(Tp^{Me2})[CH(SiMe$_3$)$_2$]$_2$(THF) (6) was obtained in 62% yield. Attempts to remove the coordinated THF by repeated dissolution of 6 in toluene, followed by solvent removal, failed. The synthetic procedures are summarized in Scheme 3.1.

^{a}Scheme 3.1 Derivative Chemistry of (Tp^{Me}2)UI$_2$(THF)$_2$

(Tp^{Me}2)U[N(SiMe$_3$)$_2$]I
7, purple-red (79%)

[(Tp^{Me}2)U[CH(SiMe$_3$)$_2$]I]
purple-red

NaN(SiMe$_3$)$_2$

KCH(SiMe$_3$)$_2$

Na$_v$(SiMe$_3$)$_2$

(Tp^{Me}2)UI$_2$(THF)$_2$

KCH(SiMe$_3$)$_2$

2NaN(SiMe$_3$)$_2$

2KCH(SiMe$_3$)$_2$

(Tp^{Me}2)U[N(SiMe$_3$)$_2$]$_2$
5, dark blue (83%)

(Tp^{Me}2)U[CH(SiMe$_3$)$_2$]$_2$(THF)
6, dark blue (62%)
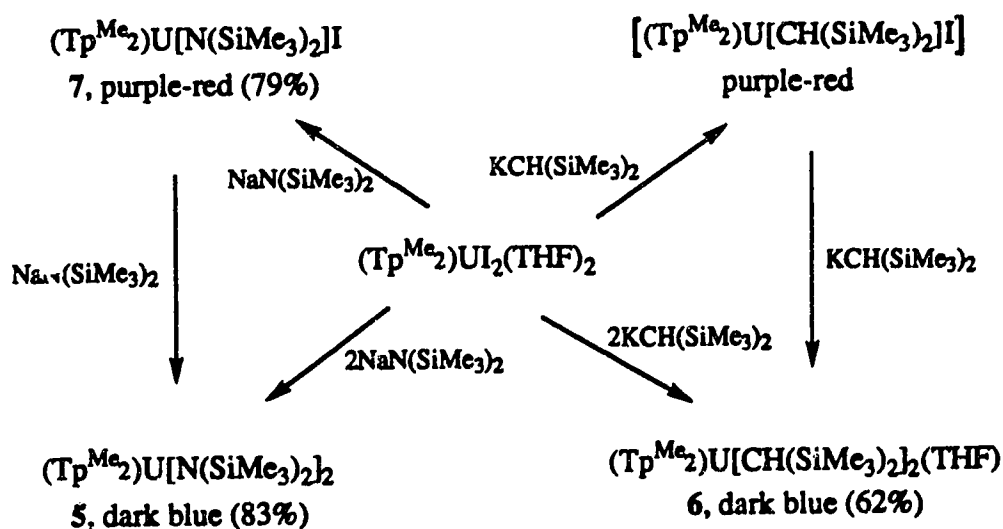
^{a}Condition: in toluene at -50°C

Anticipating that the products may be thermally unstable, the reactions were carried out at low temperature, ca. -50°C. In both cases, the interesting observation was made that

the reactions proceeded *via* an intermediate purple-red coloration. The color was maintained as long as the reaction mixture was kept at -50°C. Only upon warming the mixture did the dark blue color of the final products 5 and 6 develop. We assumed that the intermediate coloration was due to the monosubstituted derivatives and this was verified in the case of the amido reaction by the isolation of purple-red $U(Tp^{Me2})[N(SiMe_3)_2]I$ (7). Isolation of $U(Tp^{Me2})[CH(SiMe_3)_2]I$ was not attempted.

The THF adduct of complex 7, $U(Tp^{Me2})[N(SiMe_3)_2]I(THF)$, could be obtained readily by crystallization of $U(Tp^{Me2})[N(SiMe_3)_2]I$ from Et_2O/THF at -40°C. The coordinated THF is labile and can ... ·y repeated cycles of dissolution in toluene and evacuation, indicating that the c· ·· ·· dF is only loosely bonded to the U(III) metal center. $U(Tp^{Me2})(N(SiM\cdot$ ... ..iy stable both in solution and as a solid.

In contrast to $U(Tp^{Me2})[N(SiMe_3)_2]I$, complexes 5 and 6 are thermally unstable. Therefore, the yields of the products are closely related to the reaction conditions. The use of a donor solvent, such as THF or Et_2O, should be avoided because both compounds are thermally less stable in donor solvents than in non-donor solvents. It is recommended that after stirring the mixture at -50°C, the reaction vessel be evacuated while the mixture is allowed to warm naturally to r~~m temperature. This procedure results in preferential removal of liberated THF from $U(Tp^{Me2})I_2(THF)_2$ and decomposition is reduced. Indeed, in a particular preparation of complex 5 when, due to some technical difficulties, the solvent removal during warming-up was slow, the yield of $U(Tp^{Me2})[N(SiMe_3)_2]_2$ (5) was only 39% and $U(Tp^{Me2})[N(SiMe_3)_2](3,5-Me_2pz)$, one of the thermal decomposition product of complex 5, was also isolated in 41% yield.

With the availability of $U(Tp^{Me2})[N(SiMe_3)_2]I$ (7) it was of obvious interest to attempt the synthesis of the mixed amido/hydrocarbyl derivative. Gratifyingly, reaction of compound 7 with one equiv of $KCH(SiMe_3)_2$ in toluene readily gave $U(Tp^{Me2})[N(SiMe_3)_2][CH(SiMe_3)_2]$ (8) in 46% yield. Interestingly, the color of the complex, unlike the dark blue of 5 and 6, is dark blue-green. We also note that compound

8, like complex **5**, is THF-free. That is, two amido ligands, and one amido and one hydrocarbyl ligands are apparently sufficient to provide the necessary steric saturation to stabilize the five-coordinate uranium metal center, but two hydrocarbyl ligands are not and the six-coordinate $U(Tp^{Me2})[CH(SiMe_3)_2]_2(THF)$ (**6**) results.

The formulation of the complexes followed from elemental analysis. The IR spectra displayed the characteristic B-H stretching band around $2500cm^{-1}$. The room temperature ^1H NMR spectra of complexes **5** to **8** were uninformative as to the structures of the complexes. They all displayed similar features, a broad signal and very broad features almost hidden in the base line. The appearance of the spectra was best accommodated by flurional solution behavior. This is not a surprise for complexes **5**, **7**, and **8** since non-rigidity is the rule rather than exception for five-coordinate complexes,[24,25]. However, the fluxional nature of six-coordinate **6** was more unexpected.[26] In an effort to determine the solution structure of the complexes, VT ^1H NMR experiments were carried out.

3.2.2. Variable Temperature ^1H NMR Spectroscopic Studies

The VT ^1H NMR spectra of $U(Tp^{Me2})[N(SiMe_3)_2]_2$ are shown in Fig. 3.1. As mentioned, the room temperature ^1H NMR spectrum consists of broad, uninformative signals. Lowering the temperature results in the gradual emergence of the features hidden in the base line. The low temperature limiting spectrum (Fig. 3.1) is reached at $-100°C$ and consists of nine resonances in the approximate ratio of 18:9:9:6:6:3:3:2:1. The number and relative intensities of the signals indicate a C_S molecular symmetry which renders two $SiMe_3$ of one amido ligand (18H) and two pyrazolyl groups equivalent (6:6:2).

The VT ^1H NMR spectra of **8** are shown in Fig. 3.2. The LT limiting spectrum is already reached at $-50°C$, (Fig. 3.2) and shows 14 resonances with intensity ratio of 9:9:9:9:3:3:3:3:3:3:1:1:1:1. It is interesting that the introduction of the hydrocarbyl ligand slows down the fluxionality significantly and brings in sufficient asymmetry to render all
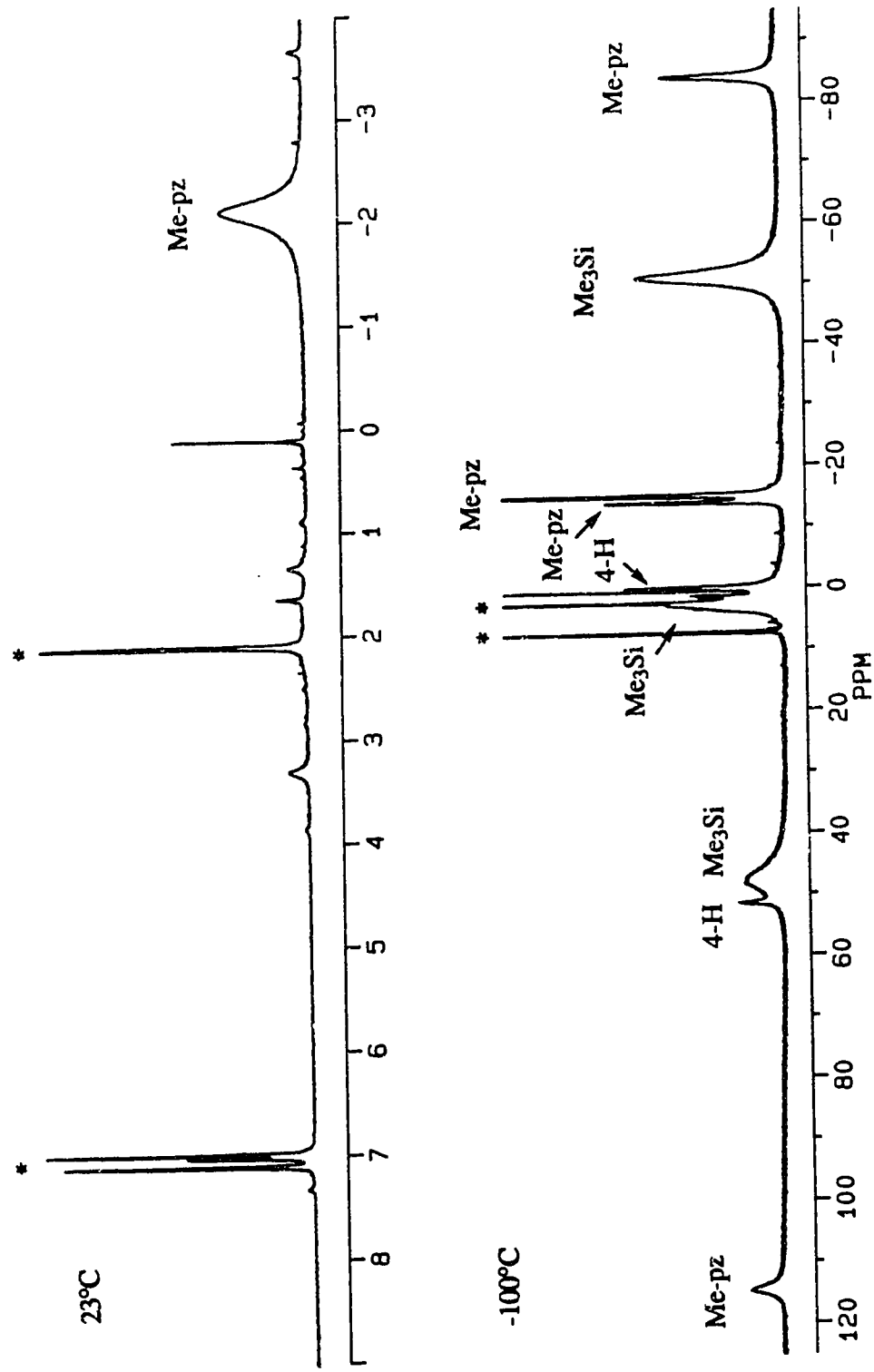
Fig. 3.1 ^{1}H NMR Spectrum of U(Tp^{Me_2})[N(SiMe$_3$)$_2$]$_2$ (5) (Toluene-d$_8$, 23°C, -100°C)
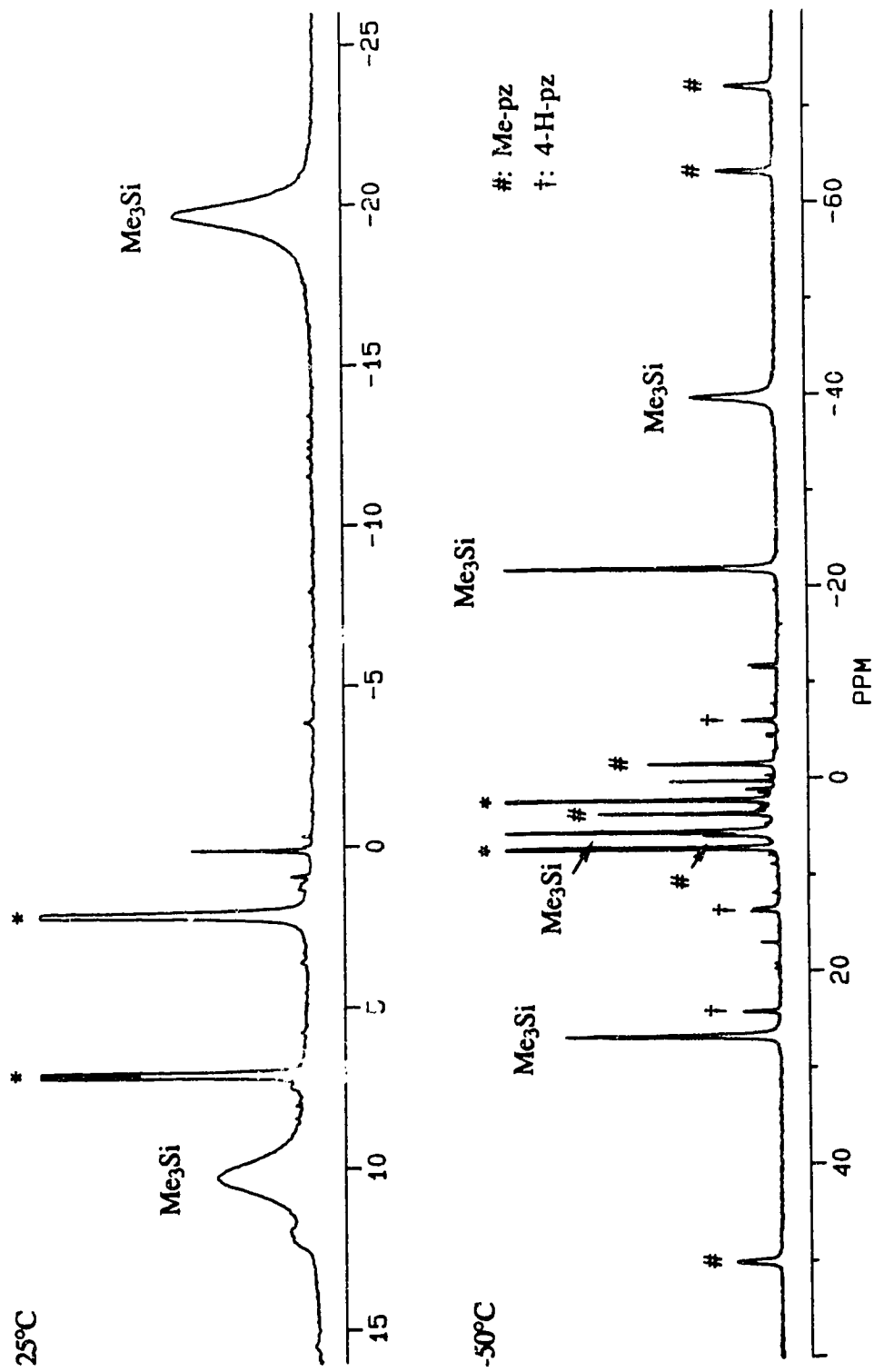
Fig. 3.2 ^{1}H NMR Spectrum of U(Tp^{Me_2})[N(SiMe$_3$)$_2$][HC(SiMe$_3$)$_2$] (8) (Toluene-d$_8$, 25°C, -50°C)

groups inequivalent. The reduced fluxionality is not totally unexpected since the rearrangement must now exchange the positions of two different ligands, one of which may have a preference for one particular type of coordination position.

Since six-coordinate structures are usually rigid,[26] the VT ^1H NMR behavior of $U(Tp^{Me2})[CH(SiMe_3)_2]_2(THF)$ (6) was somewhat unexpected. The decoalesence temperature was estimated to be around -70°C, and the low temperature limiting spectrum could not be reached down to -100°C. The high fluxionality of the complex may be due to the large degree of ionic and hence nondirectional bonding in the complex, or to the possibility of rapid THF dissociation-reassociation in solution.

3.2.3. Molecular Structures of $U(Tp^{Me2})[N(SiMe_3)_2]_2$ (5), $U(Tp^{Me2})[CH(SiMe_3)_2]_2(THF)$ (6), and $U(Tp^{Me2})[N(SiMe_3)_2]_2[CH(SiMe_3)_2]_2$ (8)

Although the composition of the complexes was secure and in fact the low temperature ^1H NMR spectra of 5 indicated a molecular symmetry close to C_s, to determine the detailed coordination geometries and precise structural parameters, sing crystal X-ray analysis on complexes 5, 6, and 8 was carried out. Perspective views of the structures are shown in Figures 3.3, 3.4, and 3.5. Relevant bond distances and angles are listed in Tables 3.1.

The crystals contain well separated, monomeric units with no unusual intermolecular contacts. In all three structures the Tp^{Me2} ligand is coordinated to the uranium metal center in an η^3-fashion. In complexes 5 and 8 the uranium is five coordinate; two $N(SiMe_3)_2^-$ or one $N(SiMe_3)_2^-$ and one $CH(SiMe_3)_2^-$ ligands providing sufficient steric bulk to stabilize the low coordination environment. Two $CH(SiMe_3)_2^-$ ligands apparently are not able to provide the same steric saturation and one THF molecule coordinates as well to give a six-coordinate uranium in complex 6, which has a distorted octahedral geometry.
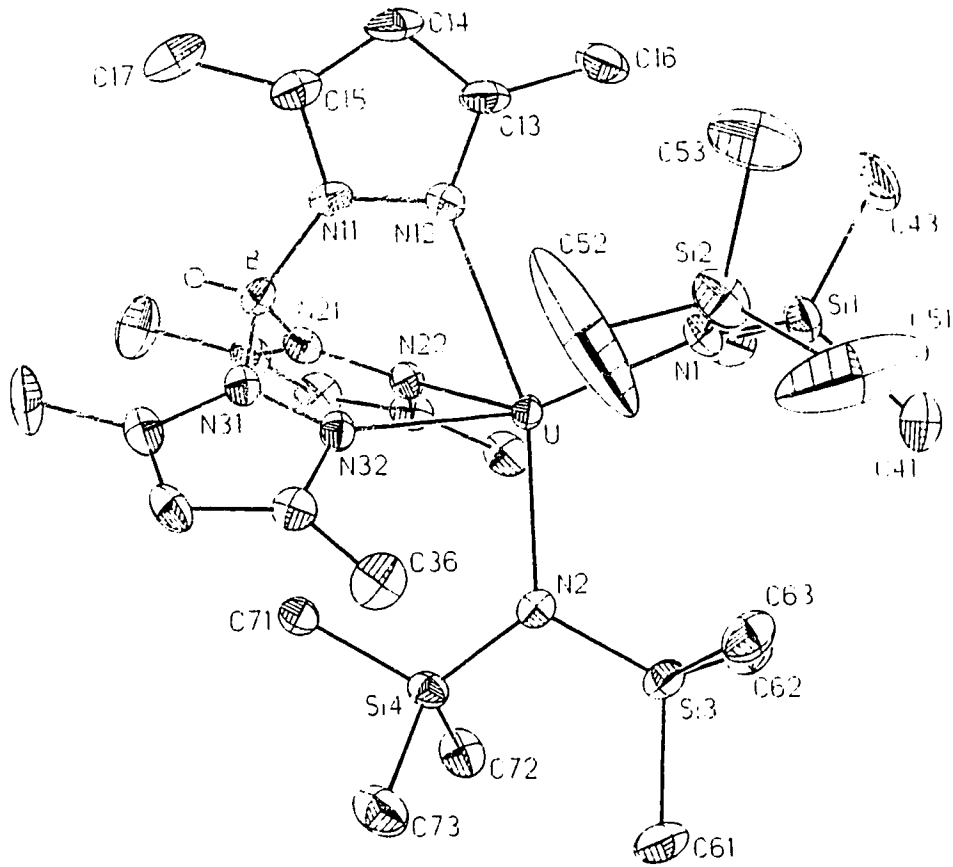
Fig. 3.3 Molecular Structure of U(Tp^Me2)[N(SiMe3)2]2 (5)

The coordination geometries of **5** and **8** are best described as distorted trigonal bipyramids. The tripodal nature of the Tp^{Me_2} ligand forces it to occupy one apical and two equatorial positions with one apical and one equatorial site vacant. In compound **5** these sites are occupied by the two identical amido ligands. As seen in Fig. 3.5, in compound **8** the hydrocarbyl group is in the apical position and the amido ligand is in the equatorial site.

The site preference is determined by steric and electronic factors. On the basis of calculations, or simple VSEPR[28] considel s, in a five-coordinate, trigonal bipyramidal ML_3X_2 compound, the larger ligands prefer the equatorial sites whereas smaller ligands occupy the apical positions, since the apical site has three nearest neighbors at 90°, but the equatorial sites have only two such close neighbors. Thus, the apical sites experience greater repulsion and this results in preferential occupation of these sites by the smaller ligands. Since the size of $N(SiMe_3)_2^-$ is almost the same as that of $CH(SiMe_3)_2^-$, the steric factors alone will not determine the site occupied by these ligands.

Hoffmann et al.[29] have carried out a unified molecular orbital treatment of pentacoordinate transition metal complexes. Considering σ-bonding only, the calculations show that in d^0-d^4 system the stronger σ-donor prefers equatorial sites. Since the hydrocarbyl ligand is a better σ donor than the amido group, it should occupy an equatorial position. But this is exactly the opposite of what is observed in the crystal structure of complex **8**. However, Hoffmann's analysis also points out that π-interaction may reverse the prediction of the σ-bonding model. The LUMO in these complexes is a metal d π-type orbital, thus strong π-donors should also prefer the equatorial sites due to stabilizing π-bonding interactions. Since $N(SiMe_3)_2^-$ is both a σ and a π donor, the equatorial disposition in compound **8** is probably due to the π-type interaction.

As mentioned earlier, an important feature of five-coordination is the difference between the ligand sites. The apical positions experience greater repulsion than the
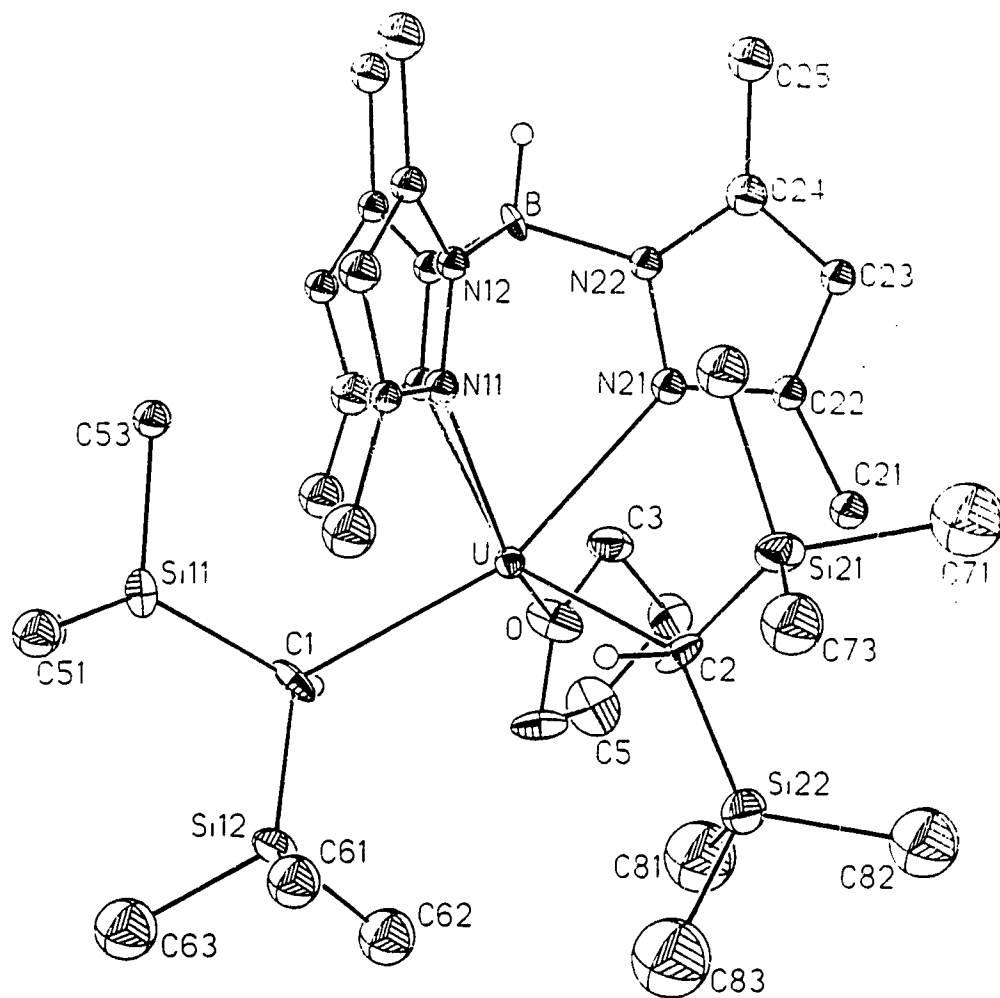
Fig. 3.4 Molecular Structure of U(Tp^{iMe2})[CH(SiMe_3)_2]_2(THF) (6)
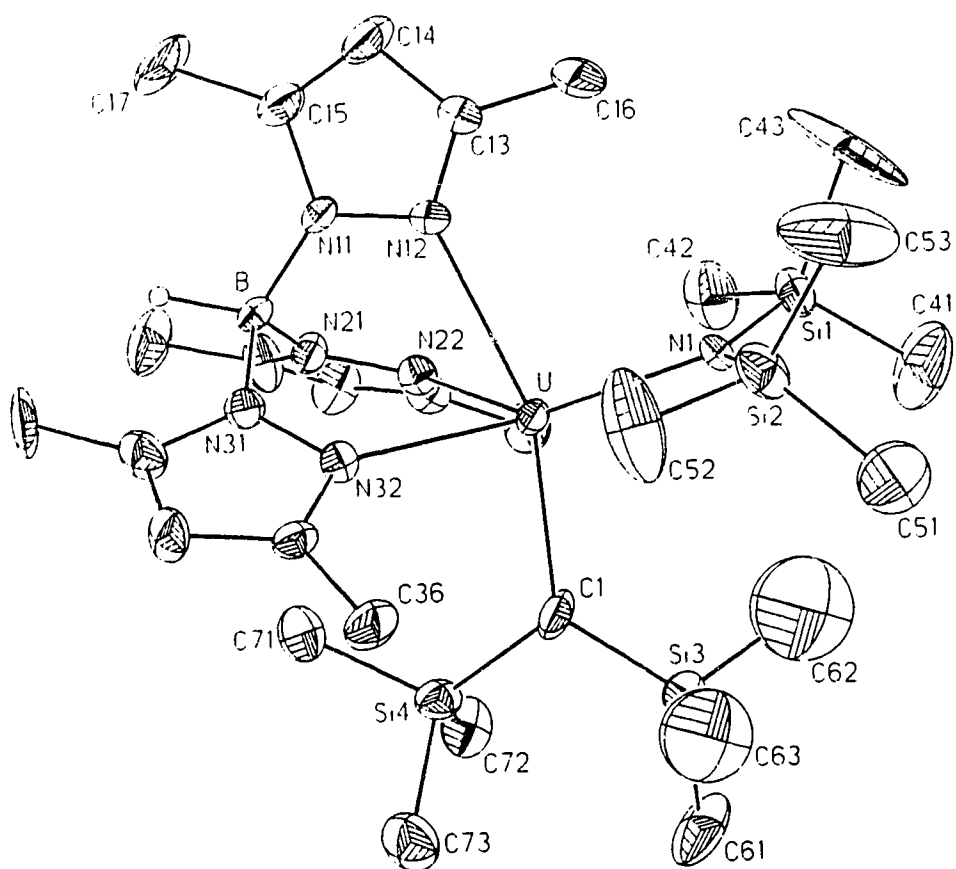
Fig. 3.5 Molecular Structure of U(Tp^{Me2})[N(SiMe$_3$)$_2$][HC(SiMe$_3$)$_2$] (8)

equatorial sites, and this leads to the prediction of longer apical metal-ligand bond lengths. Theoretical calculations, based on model five-coordinate compounds containing only unidentate ligands, give an $M\text{-}L_{apical}$ to $M\text{-}L_{equatorial}$ ratio of 1.21.[27] As expected the apical $U\text{-}N_{pz}$ bond distances (2.707(12)Å (5), 2.688(16)Å (8)) are significantly longer than the equatorial $U\text{-}N_{pz}$ bond lengths (2.541(10) and 2.535(10)Å (5); 2.568(16) and 2.546(16)Å (8)). However, the ratio of $U\text{-}N_{apical}:U\text{-}N_{equatorial}$ (1.07 (5), 1.04 (8)) is much less than the theoretical value. This is obviously due to the tridentate nature of Tp^{Me2} ligand. The rigidity of the Tp^{Me2} ligand prevents the apical pyrazolyl ring to freely move away from U(III) metal center to reduce the repulsion.

The bonding and steric influence of the Tp^{Me2} ligands in complexes 5 and 8 are very similar. This is suggested by the nearly equal $U\text{-}N_{pz}$ distances and $N_{pz}\text{-}U\text{-}N_{pz}$ angles, the sum of the these angles being almost equal (229.0(3)° (5), 230.9(5)° (8)). Since both compounds have one equatorial amido group, any difference in distortion will be caused by the apical ligand. The sizes of the $N(SiMe_3)_2^-$ and $CH(SiMe_3)_2^-$ groups are similar, but the amido group interacts more strongly with U(III), as evidenced by the shorter U-N bond, 2.393(9)Å compared to 2.527(24)Å for the U-C bond. Consequently, complex 5 is more congested than 8. The larger $U\text{-}N_{eq}$ bond distance (2.381(8)Å in 5 vs 2.369(16)Å in 8) and the larger $N_{eq}\text{-}U\text{-}N_{ax}$ angle (112.3(4)° in 5 vs 106.9(8)° in 8) are in accord with this analysis.

Another indication of the congested nature of the U(III) centers in these complexes comes from the values of the U-N-Si or U-C-Si angles. The two angles within individual ligands (117.2(5)°, 118.1(5)°, and 119.5(4)°, 125.7(6)° in 5; 116.7(7)°, 118.4(7)°, and 123.3(14)°, 124.8(13)° in 8) are almost equal, whereas in $U[CH(SiMe_3)_2]_3$ (101.8(8)°, 122(1)°),[30] $La[CH(SiMe_3)_2]_3$ (102.0(4)°, 121.0(4)°), and $Sm[CH(SiMe_3)_2]_3$ (107(1)°, 124(1)°)[31] they are significantly different due to the γ-agostic interaction with the silyl methyl groups. The saturated nature of the coordination sphere of complexes 5 and 8 prevents the occurrence of γ-agostic interactions. It is noteworthy that the two angles are

Table 3.1 Selected Bond Lengths (Å) and Angles (°) for Complexes 5, 6, and 8

5		6		8	
		Bond Lengths			
U-N ₂	2.707(12)	U-N11	2.50(1)	U-N12	2.688(16)
U-N22	2.541(10)	U-N21	2.60(1)	U-N22	2.568(16)
U-N32	2.535(10)	U-N41	2.69(1)	U-N32	2.546(16)
U-N$_{pz}$	2.594(98)*	U-N$_{pz}$	2.60(1)*	U-N$_{pz}$	2.601(76)*
U-N1	2.381(8)	U-C1	2.64(2)	U-C1	2.527(24)
U-N2	2.393(9)	U-C2	2.64(2)	U-N1	2.369(16)
U-N$_{amido}$	2.387(8)*	U-O	2.58(1)		
		Bond Angles			
N12-U-N22	66.2(3)	N11-U-N21	75.4(4)	N12-U-N22	73.6(5)
N12-U-N32	78.3(3)	N11-U-N31	72.4(4)	N12-U-N32	72.3(5)
N22-U-N32	84.3(3)	N21-U-N31	67.5(4)	N22-U-N32	85.0(5)
N1-U-N2	112.3(4)	C1-U-C2	113.4(5)	C1-U-N1	106.9(8)
N1-U-N22	136.4(3)	C1-U-N21	158.9(5)	N1-U-N22	134.4(5)
N1-U-N32	126.3(3)	C2-U-N31	151.4(5)	N1-U-N32	133.6(4)
N2-U-N12	158.8(3)	O-U-N11	147.1(4)	C1-U-N12	159.2(8)
		Torsional Angles			
B-N11-N12-U	-33(1)	B-N12-N11-U	1(2)	B-N11-N12-U	4(2)
B-N21-N22-U	14(1)	B-N22-N21-U	14(2)	B-N21-N22-U	20(2)
B-N31-N32-U	-21(1)	B-N32-N31-U	-15(2)	B-N31-N32-U	-12(2)
N22-U-N1-Si1	-45(1)			N22-U-N1-Si1	-18(1)
N32-U-N1-Si2	8(1)			N32-U-N1-Si2	22(1)

* Averaged bond lengths

also similar in complex 6 (120.7(8)°, 122(1)°, and 124.8(8)°, 117.5(9)° (6)). Here, besides steric saturation, the presence of the coordinated THF also negates the need for agostic interaction by electronically saturating the uranium.

The U-N$_{amide}$ bond distances are in the order 5 (2.387(8)Å) > 8 (2.369(16)Å) > U[N(SiMe$_3$)$_2$]$_3$ (2.320(4)Å), and follow the expected trend based on coordination number and steric hindrance. The relatively weaker U-C interaction in 8, to some extent, releases the congestion in this complex and allows for a slightly shorter U-N$_{amide}$ bond length than in 5. By the same steric arguments the trend in the U-C σ bond length (2.64(2)Å (6)>2.527(24)Å) (8)> 2.48(2)Å U[CH(SiMe$_3$)$_2$]$_3$[12]) can be rationalized. The U-O$_{THF}$ bond distance in 6 (2.58(1)Å) is comparable to 2.564(4)Å in [U(Tp^{Me2})$_2$THF][BPh$_4$] (4) but slightly longer than 2.52(4)Å in UI$_3$(THF)$_4$.

A closer examination of the structures reveals a very important structural feature for all these amido and hydrocarbyl complexes, that is, steric congestion occurs at the periphery of the molecules, not in the inner coordination sphere.

Reference to Fig. 3.4 shows that in compound 6 the two hydrocarbyl groups and the THF are roughly parallel to the local C$_3$ axis of the Tp^{Me2} ligand, and stagger the three pyrazolyl rings of Tp^{Me2} ligand. There is a pseudo mirror plane in the molecule: one of the pyrazolyl rings, the uranium center, and the oxygen atom of the THF ligand lie in the mirror plane which bisects two CH(SiMe$_3$)$_2$$^-$ groups and the other two pyrazolyl rings of Tp^{Me2} ligand. The symmetrical environment of the pyrazolyl ring in the mirror plane results in a negligible torsional angle, 1(2)°. However, due to the repulsion between the silyl methyl groups and the 3-methyl groups of the pyrazolyl rings, the other two pyrazolyl rings twist away from the CH(SiMe$_3$)$_2$$^-$ groups, giving torsional angles of 14(2)° and -15(2)°, respectively.

The inner coordination geometries of complexes 5 and 8 also possess approximate mirror symmetry, but the details of the distortion are significantly different. The pyrazolyl ring lying in the pseudo mirror plane of complex 8 has a small torsional angle of 4(2)°,

while the other two pyrazolyl rings twists 20(2)° and -12(2)°, respectively. However, the strong interaction of the apical $N(SiMe_3)_2^-$ with U(III) in complex 5 dramatically affects the orientation of the equatorial $N(SiMe_3)_2^-$ ligand. The N22-U-N1-Si1 and N32-U-N1-Si2 torsional angles, almost equal in compound 8 (-18(1)° and 22(1)°), change significantly and are also very different in compound 5 (-45(1)° and 8(1)°). Because of the nature of this well arranged locked-up structure, the orientation of the pyrazolyl ring lying in the pseudo mirror plane is also influenced by the twist of the equatorial $N(SiMe_3)_2^-$ ligand and its torsional angle increases to -33(1)°. Based on the above structural analysis it is clear that in these complexes the real congestion is between the silyl methyl and pyrazolyl 3-methyl groups.

With the molecular structure of complexes 5 and 8 at hand it is worthwhile to briefly return to the VT ^1H NMR studies and the solution structures of these molecules. Rearrangement of the ligands in complex 5 is expected to be facile, simple turnstile rotation exchanges the pyrazolyl rings of the Tp^{Me2} ligand and the axial-equatorial amido ligands. The situation in complex 8 is quite different. While the above mentioned turnstile rotation would exchange the positions of the amido and hydrocarbyl ligands, the preference of the latter for the apical site renders this an energetically less favorable situation. This is clearly reflect. in the higher energy barrier for exchange.

3.2.4. Thermal Behavior of $U(Tp^{Me2})[N(SiMe_3)_2]_2$ and $U(Tp^{Me2})[CH(SiMe_3)_2]_2(THF)$

As indicated in the introduction of this chapter, the instability of metal-carbon σ-bonds is mainly kinetic in origin, the most common decomposition pathway being β-hydrogen elimination. However, elimination of β-hydrogen is not the only decomposition pathway. With the bulky neopentyl $(CH_2C(Me_3)_3^-)$ and trimethylsilylmethyl $(CH_2Si(Me_3)_3^-)$ ligands γ-H abstraction is also possible. Marks et al.[32-34] have shown that $ThCp^*_2R_2$ complexes, with branched alkyl ligands, undergo intramolecular abstraction

$$Cp^* \diagdown \underset{\diagup}{\overset{\diagup}{Th}} \overset{\cdots CH_2CMe_3}{\diagdown CH_2CMe_3} \qquad \xrightarrow[\text{cyclohexane}]{50°C, 60h} \qquad Cp^* \diagdown \underset{Cp^*}{\overset{}{Th}} \overset{H_2}{\underset{\overset{\diagup}{C}}{\diagup}} CMe_2 \quad + \quad CMe_4 \qquad 3.5$$

$$Cp^* \diagdown \underset{\diagup}{\overset{\diagup}{Th}} \overset{\cdots CH_2SiMe_3}{\diagdown CH_2SiMe_3} \qquad \xrightarrow{80°C, 48h} \qquad Cp^* \diagdown \underset{Cp^*}{\overset{}{Th}} \overset{H_2}{\underset{\overset{\diagup}{C}}{\diagup}} SiMe_2 \quad + \quad SiMe_4 \qquad 3.6$$
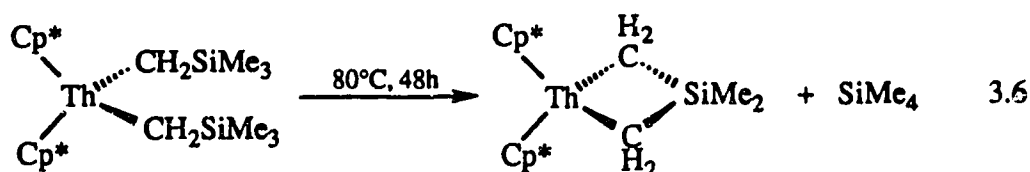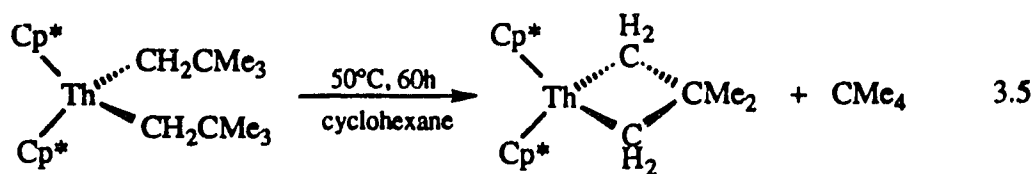
of a γ-hydrogen to form metallacycles (eq. 3.5 and 3.6). Andersen *et al.*[35,36] have also found that thermolysis of the amido-methyl compound $M[N(SiMe_3)_2]_3(Me)$ (M=Th, U) proceeds by γ-hydrogen elimination to yield a metallacycle (eq. 3.7), which reacts readily

$$M[N(SiMe_3)_2]_3(Me) \quad \xrightarrow[>130°C]{-CH_4} \quad [(Me_3Si)_2N]_2M \underset{N}{\overset{H_2}{\diagup}} \overset{C}{\underset{SiMe_3}{\diagup}} SiMe_2 \qquad 3.7$$
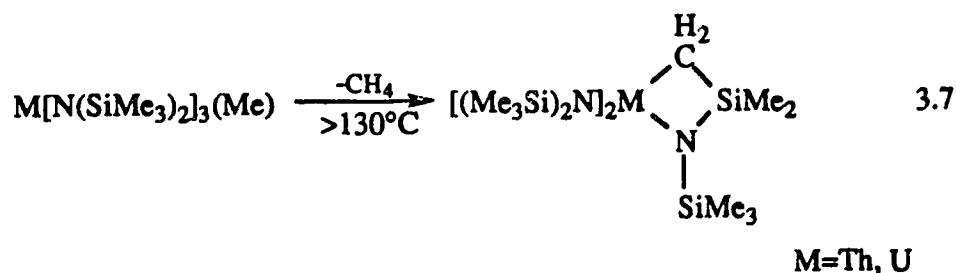
M=Th, U

with CO, ^tBuNC, and ^tBuCN (Scheme 3.2). Attempts to obtain the related alkyl derivatives, $M[N(SiMe_3)_2]_3(R)$, (M=Th, U; R=Et, CH_2SiMe_3) met with failure and direct conversion to the metallacycle was observed. It was argued that steric congestion in the hypothetical alkyl was very severe and this facilitated γ-H abstraction and subsequent formation of the metallacycle. The reaction of $M[N(SiMe_3)_2]_3Cl$ with excess $NaN(SiMe_3)_2$ in hydrocarbon solvents led to a recovery of the starting material. However, when the reaction was carried out in THF, the hydride, $M[N(SiMe_3)_2]_3H$, was isolated.[35]

Considering the congested nature and thermal instability of complexes 5, 6, and 8 it was of interest to see whether similar C-H activation could lead to the formation of metallacycles.

Scheme 3.2

$[(Me_3Si)_2N]_2M$ $O{-}C{\overset{CH_2}{\diagup}}$
$N{-}SiMe_2$
Me_3Si

$\uparrow$ CO

$[(Me_3Si)_2N]_2M$ $\overset{H_2}{C}$ $SiMe_2$
N
$SiMe_3$

^tBuNC ^tBuCN

^tBu
$N{-}C{\overset{CH_2}{\diagup}}$
$[(Me_3Si)_2N]_2M$
$N{-}SiMe_2$
Me_3Si

^tBu
$N{=}C$
$[(Me_3Si)_2N]_2M$ CH_2
$N{-}\underset{Me_2}{Si}$
Me_3Si
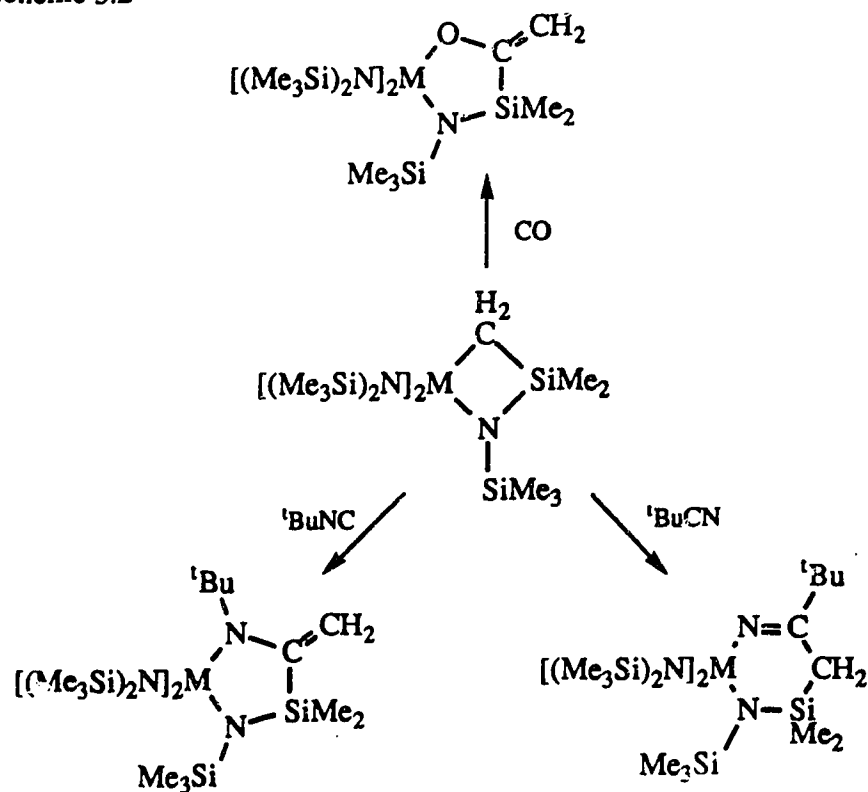
It was found that $U(Tp^{Me2})[N(SiMe_3)_2]_2$ is much less stable in donor solvents than in simple hydrocarbons. In DME at room temperature, complex 5 decomposes in a few hours, based on the observation of a color change from blue to dark brown. Cooling the brown solution at -40°C gave three kinds of crystals; black cluster-shaped, colorless, and some big brown brick-like crystals, which were manually separated. The black cluster-shaped and colorless crystals were identified as $U(Tp^{Me2})[N(SiMe_3)_2](3,5-Me_2pz)$ (9) and $[HB(3,5-Me_2pz)N(SiMe_3)_2]_2$, respectively. The ^1H NMR spectrum of the brown product was uninformative, thus the nature of this minor decomposition product could not be determined.

$U(Tp^{Me2})[N(SiMe_3)_2]_2$ is stable at room temperature in hexane; no color change was observed overnight. However, when the solution was heated at 40°C for a few hours, decomposition occured, as indicated by a color change from blue to brown. Cooling the brown solution gave three crystalline products; light-purple, colorless, and a small amount

of big blue crystals. The former two compounds were identified as $U[N(SiMe_3)_2]_2(3,5$-$Me_2pz)_2$ (10) and $[HB(3,5$-$Me_2pz)N(SiMe_3)_2]_2$, respectively. Due to the limited amount of blue crystals, the compound was only characterized by ^1H NMR spectroscopy and appears to be $U[N(SiMe_3)_2](3,5$-$Me_2pz)_3$.

Compared to the amide compound, the hydrocarbyl derivative 6 was much less stable; decomposition in DME occurred at -40°C. Although crystalline brown product was obtained, the ^1H NMR spectrum displayed a multitude of peaks and could not be interpreted. The nature of the decomposition product(s) is unknown.

The thermal reaction of complexes 5 and 6 were more complicated than hoped for, especially the redox reaction behavior of compound 5 in hexane which was unexpected. It is difficult to propose a convincing reaction pathway, but it is clear that B-N bond cleavage dominates. This is a commonly observed path and a feature that unfortunately complicates poly(pyrazolyl)borate chemistry.[37,38]

3.2.5. Molecular Structures of $U(Tp^{Me2})[N(SiMe_3)_2](3,5$-$Me_2pz)$ (9) and $U[N(SiMe_3)_2]_2(3,5$-$Me_2pz)_2$ (10)

To unambiguously determine the structures of 9 and 10 single crystal X-ray analyses were carried out. Perspective views of the structures are shown in Fig 3.6 and 3.7. Relevant bond lengths and angles are listed in Table 3.2.

In complex 9 the U(III) center is surrounded by an η^3-Tp^{Me2} ligand, η^2-$(3,5$-$Me_2pz)^-$ ligand, and the $N(SiMe_3)_2^-$ moiety, resulting in a formal coordination number of six. However, the coordination geometry is best described as distorted trigonal bipyramidal by taking the mid-point of the N41-N42 bond of the η^2-$(3,5$-$Me_2pz)^-$ ligand as occupying one of the apical sites. The η^3-Tp^{Me2} ligand (N11, N21, N31) occupies the other apical and two equatorial positions, with the amido nitrogen, N1, taking up the final equatorial site. The formal coordination number in complex 10 is also six, from two η^2-pyrazolides and two amido ligands. But again the geometry is best described as
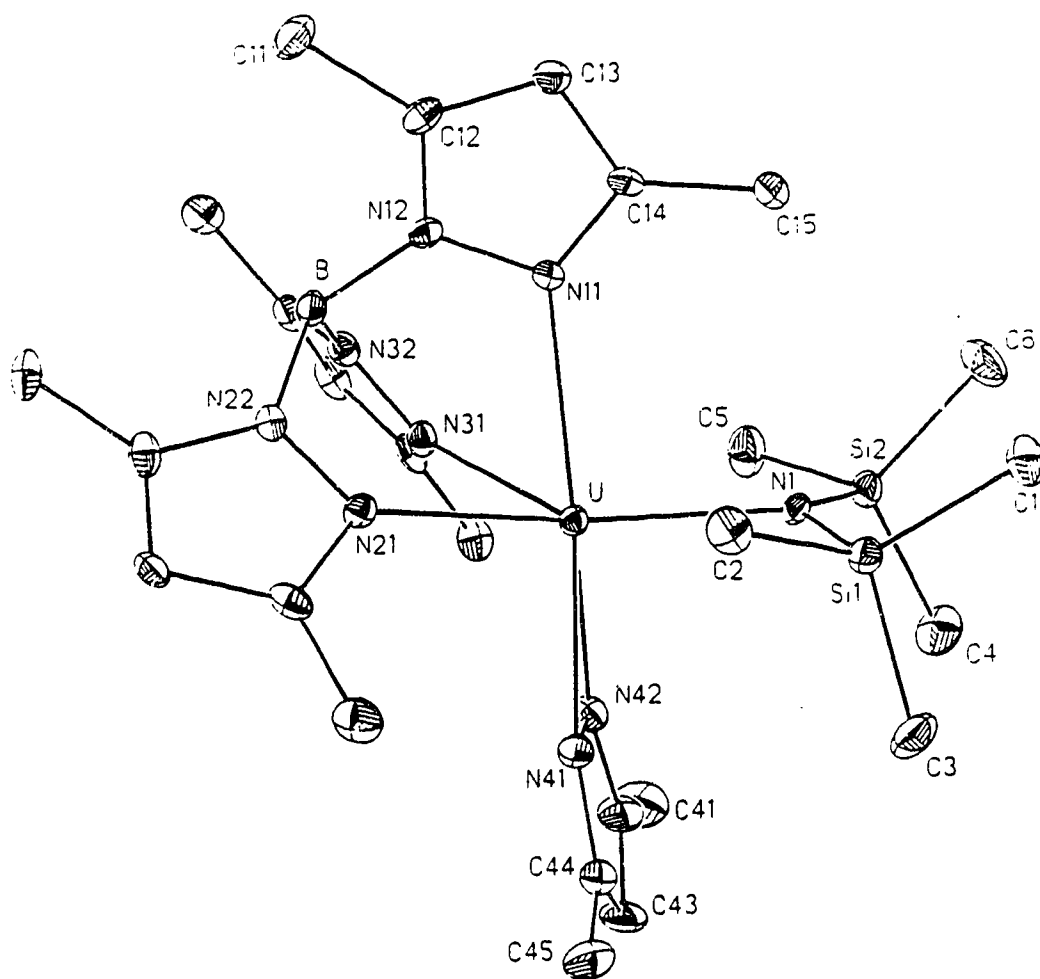
Fig. 3.6 Molecular Structure of U(Tp^{Me2})[N(SiMe$_3$)$_2$](3,5-Me$_2$pz) (9)
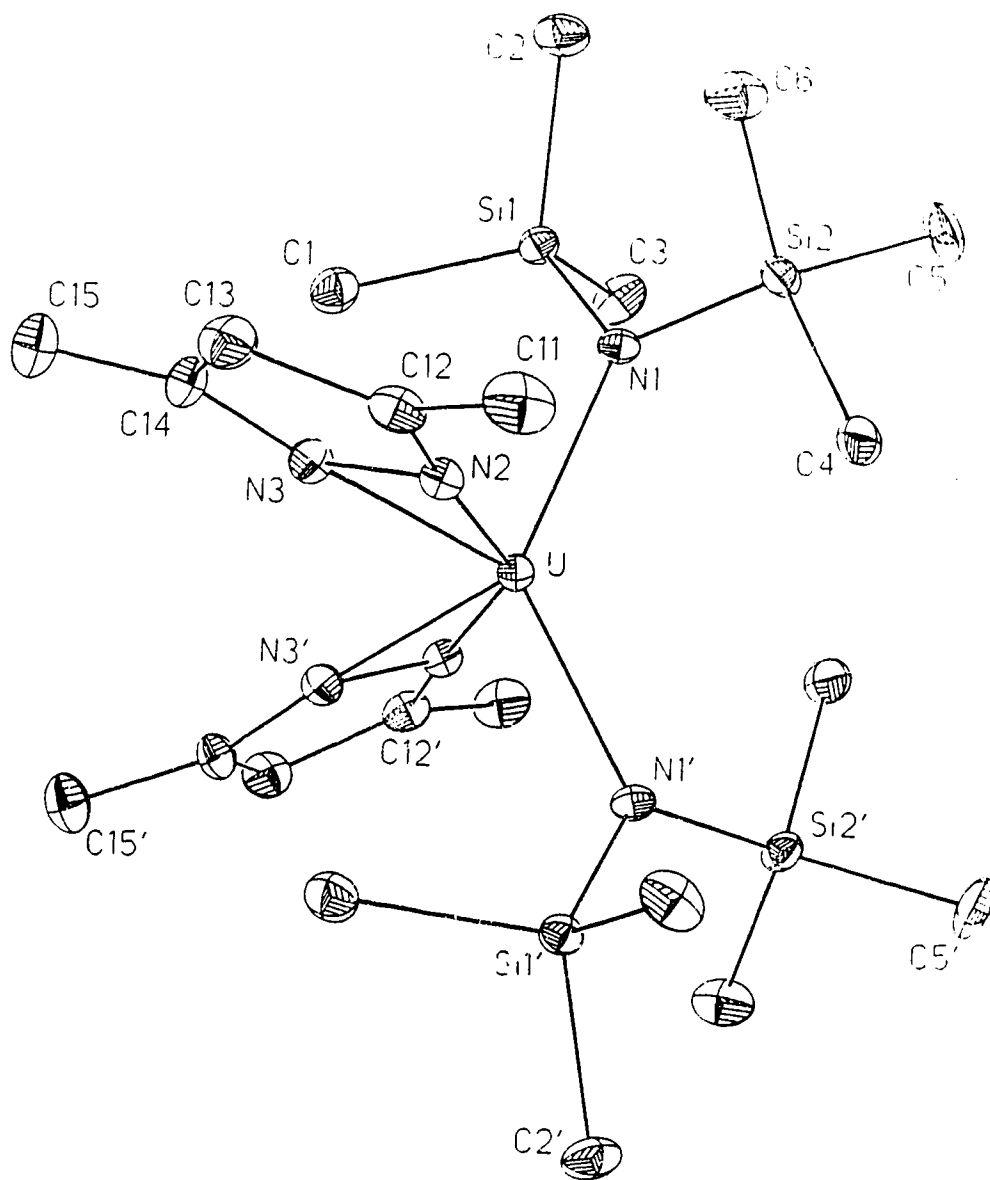
Fig. 3.7 Molecular Structure of U[N(SiMe₃)₂]₂(3,5-Me₂pz)₂ (19)

Table 3.2 Selected Bond Distances (Å) and Angles (°) for Complexes **9** and **10**

	9		**10**	
		Bond Distances		
U-N1	2.349(6)	U-N1	2.236(7)	
U-N11	2.657(7)	U-N2	2.395(7)	
U-N21	2.577(6)	U-N3	2.334(8)	
U-N31	2.572(7)	U-N$_{pz}$	2.37(4)*	
U-N$_{Tp}$Me₂	2.552(35)*			
U-N41	2.445(7)			
U-N42	2.434(7)			
U-N$_{pz}$	2.440(8)*			
		Bond Angles		
N11-U-N21	74.9(2)	N1-U-N1'	130.$^-$	
N11-U-N31	74.7(2)	N1-U-N@	9$_\angle$ $^?$	
N21-U-N31	77.6(2)	N1-U-N'@	110.3	
N1-U-N21	140.3(2)	N@-U-N'@	118.4	
N1-U-N31	135.6(2)			
N1-U-N@	91.3			
N11-U-N@	176.3			
		Torsional Angles		
B-N11-N12-U	22.7(9)			
B-N21-N22-U	21.4(9)			
B-N31-N32-U	15.5(9)			
Si1-N1-U-N21	-26.8(6)			
Si2-N1-U-N31	27.3(5)			

* Averaged bond lengths; @ Center of the N-N of the η^2-pyrazolide

dis d tetrahedral by considering the pyrazolides as occupying one coordination position, the distortion is manifested by the N1-U-N1', N1-U-Cent(N2-N3), N1-U-Cent(N2'-N3'), and Cent(N2-N3)-U-Cent(N2'-N3') angles (130.7, 94.7, 110.3, and 118.4°). Complex 10 has crystallographically imposed C_2 symmetry which renders both amide and pyrazolide groups equivalent.

As in compounds 5 the apical L-N$_{Tp}$Me bond length in the trigonal bipyramidal compound 9 (2.o₃, 1·¹) is substantially longer than the other two equatorial U-N$_{Tp}$Me bond distances (2.572(7) and 2.577(6)Å), for the same reason as mentioned earlier. The U-N$_{amide}$ lengths are in the order: 2.387(8)Å, 5 > 2.369(16)Å, 8 > 2.349(6)Å, 9 > 2.320(4)Å, U[N(SiMe₃)₂]₃ > 2.236(7)Å, 10 ≈ 2.235(5)Å, U[N(SiMe₃)₂]₂Cl₂(DME). Steric arguments can rationalize the pattern for compounds 5, 8, 9, and U[N(SiMe₃)₂]₃. The U-N$_{amide}$ bond distances of compound 10 are the same as those of U[N(SiMe₃)₂]₂Cl₂(DME), but shorter than those of U[N(SiMe₃)₂]₃. The short distance in 10 than in U[N(SiMe₃)₂]₃ can be explained by the higher oxidation state of uranium in 10.

Coordination of the pyrazolide ligand in an η^2-fashion, "endo-bidentate", has been seen also in the following uranium(IV) complexes; U(η^5-Cp)₃(η^2-pz),[39] U(η^5-Cp*)₂(η^2-pz)Cl, U(η^5-Cp*)₂(η^2-pz)₂.[40] The average U-N$_{\eta^2-pz}$ bond distance of 2.440(8)Å in 9 is almost 0.1Å longer than the average U-N$_{\eta^2-pz}$ bond distance of 2.38(3)Å in the above three complexes, after correction for the changes in oxidation state and coordination numbers.[41] The increase is presumably related to the congested nature of complex 9 due to the bulky Tp^{Me2} and amido ligands and the apical disposition of the η^2-pyrazolide moiety. In line with these arguments the average U-N$_{\eta^2-pz}$ bond length, (2.37(4)Å), in complex 10 is shorter than that in compound 9, (2.440(8)Å); this is in accord with the trend in U-N$_{amide}$ bond lengths.

Unlike in compounds 5 and 8 where the apical ligand lies in the approximate mirror plane of the molecule, the solid state structure of complex 9 shows that the orientation of

the η^2-pyrazolide ring in this case is perpendicular to this plane. Although there are a few short contacts between the pyrazolide and amido ligands, (H41A-H5B 2.73Å, H45C-H3B 2.80Å, H45A-H3B 2.92Å, and H41B-H4C 2.94Å), it is easy to imagine that the steric congestion will be greater if the η^2-pyrazolide ring was to rotate 90° along the apical axis. The orientation of the η^2-pyrazolide causes the three pyrazolyl rings of the Tp^{Me2} ligand to twist in one direction to minimize the repulsion between the silyl methyl and 3-methyl groups, the torsion angles being 22.7(9)°, 21.4(9)°, and 15.5(9). Similar uni-directional twisting has been observed in $Sm(Tp^{Me2})_2$ and $Yb(Tp^{Me2})_2$ complexes, where the average torsional angles are 21.0(3), and 20.3(4)°, respectively.[42]

3.2.6. Reactivity Studies of $U(Tp^{Me2})[CH(Si \ e_3)_2]$ (TSIF)

The chemistry of organo uranium complexes containing U-C σ bond has been extensively studied. Since U-C σ bonds are much more polarized than the analogous transition metal to carbon σ bonds, the complexes containing such bonds are very reactive. Marks et al.[43,44] have demonstrated that $U(Cp^*)_2R_2$ compounds react with H_2 or CO rapidly as shown in eq. 3.8-3.10. They have also shown that $UCp^*_2CH_2CH_3$, generated

$$2(\eta^5\text{-}Cp^*)_2UR_2 + 4H_2 \xrightarrow[\text{25°C}]{\text{toluene}} \{[\eta^5\text{-}Cp^*)_2UH_2]_2 + 4RH \qquad 3.8$$

$$\qquad\qquad\qquad\qquad\qquad\qquad\qquad\qquad 3.9$$

$$\qquad\qquad\qquad\qquad\qquad\qquad\qquad\qquad 3.10$$
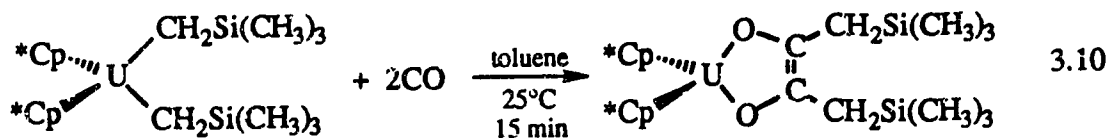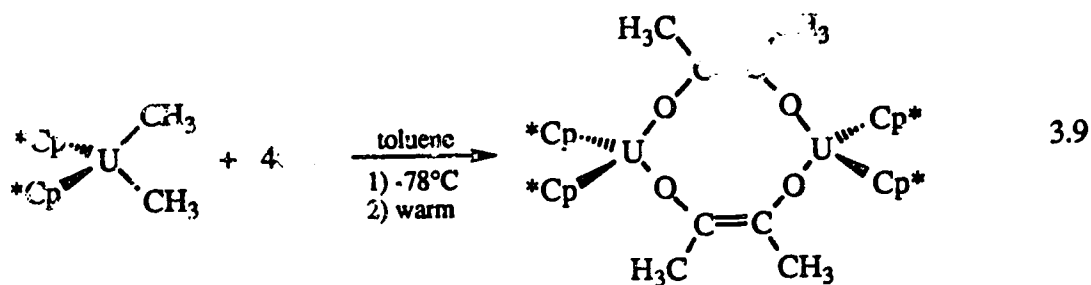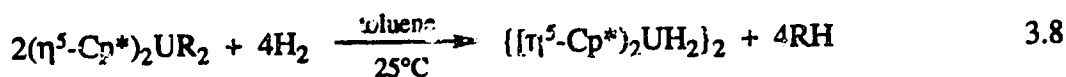
in situ from the reaction of UCp^*_2H and ethylene, is an effective catalyst for ethylene polymerization producing a high-melting, narrow polydispersity polyethylene, eq. 3.11.

$$Cp^*_2UCH_2CH_3 + nCH_2=CH_2 \longrightarrow Cp^*_2U(CH_2CH_2)_nCH_2CH_3 \qquad 3.11$$

As expected, $U(Tp^{Me2})[CH(SiMe_3)_2]_2(THF)$ (6) did react with H_2 and CO rapidly at room temperature, and a color change from blue to brown was observed. Both reactions were monitored by ^1H MR spectroscopy. Unfortunately, the ^1H NMR spectra were uninformative, and the nature of the formed product(s) could not be deduced. Furthermore, due to the high solubility of the product(s) in pentane, so far we have not been able to grow single crystals suitable for X-ray diffraction analysis. In preliminary studies, it was also observed that $U(Tp^{Me2})[CH(SiMe_3)_2]_2(THF)$ polymerizes ethylene, but not propylene.

3.2.7. Reactions of $U(Tp^{Me2})I_2(THF)_2$ with Oxygen Donor Ligands

Attempts to prepare $U(Tp^{Me2})(OR)_2/(OAr)_2$ type complexes were unsuccessful. From the reaction with two equiv of NaOEt only a small amount of black crystalline product was obtained. Although the mass spectrum did show a peak consistent with the formulation "$U(Tp^{Me2})(OEt)_2(THF)_2$", the ^1H NMR spectrum displayed numerous peaks and could not be assigned. Since the reaction appeared not to be simple and clean, further studies were not pursued.

To help to saturate the coordination sphere of U(III), the reaction with bulky KO^tBu was carried out. However, after simple work-up, a green crystalline powder was obtained from a hexane solution by cooling at -40°C. The compound was identified as the known U(IV) complex, $U(Tp^{Me2})(O^tBu)_3$.[20] Complications due to redox behavior are not new in metal-alkoxide chemistry. For instance, Minhas *et al.*[45] reported that when NaO^tBu or $NaOC_6H_3-R_2-2,6$ (R=H, Me) ligands were used to prepare V(II) alkoxides, only V(III) complexes were isolated. The desired, neutral $V(OAr)_2(L)_x$ complexes only were obtained

when bulky aryloxides, such as $NaOC_6H_3-R_2-2,6$ (R=^tBu, Ph) were used. Therefore, the reactions of $U(Tp^{Me2})I_2(THF)_2$ with $KOC_6H_3-R_2-2,6$ (R=Me, ^iPr) were carried out. Unfortunately, only the U(IV) complexes, $U(Tp^{Me2})(OC_6H_2Me_3-2,4,6)_3$[20] and $U(Tp^{Me2})(OC_6H_3{}^iPr_2-2,6)_3THF$, were obtained. Considering the greater oxophilicity and larger ionic radius of U(III) (1.17Å compared to 0.97Å for V(II)), and the stronger reducing power of U(III) ($E°(U^{+4}/U^{+3})$=-0.631V compared to $E°(V^{+3}/V^{+2})$= -0.255V),[46] perhaps the outcome is not a complete surprise.

The chelate effect has been widely used to enhance the stability of complexes.[47] To investigate whether this strategy would allow the isolation of $U(Tp^{Me2})(chelate)_2$ type complexes the reactions with $K^tBuC(O)CHC(O)^tBu$ (Kdpm) and KO_2C^tBu were carried out and finally the redox complication was eliminated. However, the desire of U(III) for oxygen donors apparently proved too strong, and dpm⁻ not only substituted the iodides but also the Tp^{Me2} ligand and gave $U(dpm)_3$ (11). The reaction with $^tBuCO_2^-$ gave a complex whose M.S. and elemental analysis data are in full accord with the molecular formulation of $U(Tp^{Me2})(O_2C^tBu)_2$ (12). However, the ^1H NMR spectrum displayed many peaks, not consistent with the simple monomeric formulation. Structure analysis on the complex was performed but, so far, the X-ray data has not been refined satisfactorily. The structure of the complex is still not clear.

In view of all the problems associated with oxygen donors, including the chelating ligands, it was decided to try the chelating dihydrobis(pyrazolyl)borate ligand, $H_2B(pz)_2^-$, since the $H_2B(pz)_2^-$ and $H_2B(3,5-Me_2pz)_2^-$ ligands have been successfully used to prepare $U[H(\mu-H)B(pz)_2]_3(THF)$[48] and $U[H(\mu-H)B(3,5-Me_2pz)_2]_3$.[49] The reaction was successful and $U(Tp^{Me2})[H_2B(pz)_2]_2$ (13) was isolated in 45% yield.

3.3. Conclusions

The reactions of $U(Tp^{Me2})I_2(THF)_2$ with $NaN(SiMe_3)_2$ and $KCH(SiMe_3)_2$ in 1:1 and 1:2 molar ratios readily gave $U(Tp^{Me2})[N(SiMe_3)_2]_2$ (5), $U(Tp^{Me2})[N(SiMe_3)_2]I$ (7),

and U(Tp^{Me2})[CH(SiMe$_3$)$_2$]$_2$(THF) (6). The mixed amido/hydrocarbyl derivative, U(Tp^{Me2})[N(SiMe$_3$)$_2$][CH(SiMe$_3$)$_2$]$_2$ (8) was also successfully prepared. The structures of complexes 5, 6, and 8 were determined by X-ray analysis, which demonstrated that the coordination congestion is in the outer coordination sphere rather than in the inner coordination sphere. In solution all the complexes are fluxional, and the slower rearrangement of 8 compared to 5 was attributed to the site preference of the hydrocarbyl ligand for an apical position in a trigonal bipyramidal coordination geometry. The complexes 5 and 6 are thermally unstable in solution and the decomposition processes are solvent dependent. Complex 5 decomposes more readily in a donor solvent, such as DME, than in hydrocarbon. From DME decomposition, U(Tp^{Me2})[N(SiMe$_3$)$_2$](3,5-Me$_2$pz) (9) was obtained. Surprisingly, the thermal decomposition in hexane was accompanied by redox behavior and gave U[N(SiMe$_3$)$_2$]$_2$(3,5-Me$_2$pz)$_2$. In both cases B-N bond cleavage of the Tp^{Me2} ligand dominates the thermal process. Although U(Tp^{Me2})[CH(SiMe$_3$)$_2$]$_2$(THF) reacts readily with H$_2$ and CO, the nature of the products could not be elucidated due to the uninformative ^{1}H NMR spectra.

Contrary to the simple metathesis observed with amido and hydrocarbyl ligands, the reactions with alkoxides and aryloxides were accompanied by redox behavior and only the U(IV) complexes, U(IV)(Tp^{Me2})(O^{t}Bu)$_3$, U(Tp^{Me2})(OC$_6$H$_2$Me$_3$-2,4,6)$_3$, and U(Tp^{Me2})(OC$_6$H$_3^i$Pr$_2$-2,6)$_3$THF, could be isolated. The redox complication could be eliminated by using the chelating ligands, ^{t}BuCO$_2^-$, H$_2$B(pz)$_2^-$, and dpm$^-$. However, the dpm$^-$ ligand also displaced Tp^{Me2} ligand and gave U(dpm)$_3$. Only with the former two were U(III) complexes, U(Tp^{Me2})(O$_2$C^{t}Bu)$_2$ and U(Tp^{Me2})[H$_2$B(pz)$_2$]$_2$, isolated.

3.4. Experimental Section

3.4.1. Preparation of Starting Materials

The preparation of $U(Tp^{Me2})I_2(THF)_2$ was described in Chapter 2. $KCH(SiMe_3)_2$[50-52] and $NaN(SiMe_3)_2$[53] were prepared according to the literature methods and purified by crystallization from Et_2O and toluene solution at -40°C, respectively.

3.4.2. Synthetic Procedures

$U(Tp^{Me2})[N(SiMe_3)_2]_2$ (5)

A solution of $NaN(SiMe_3)_2$ (207mg, 1.13mmol) in toluene (5mL) was cooled in a -50°C cold bath for 30 minutes and added dropwise to a slurry of $U(Tp^{Me2})I_2(THF)_2$ (526mg, 0.564mmol) in toluene (6mL) at -50°C. The mixture was stirred for 3 hours at -50°C. At this point the color was purple-red. The reaction flask was evacuated, and the

r.   llowed to warm to room temperature during 20 minutes, the color changed

a   e red to dark blue. Filtration, followed by solvent removal under vacuum produced dark blue, almost black, crystalline material. The solid was washed with cold hexane (2x1mL) to give $U(Tp^{Me2})[N(SiMe_3)_2]_2$ (402mg, 83% yield). IR (KBr, cm^{-1}): v(B-H) 2560. ^1H NMR (C_6D_6, 25°C, δ ppm): -2.19(br, Me-pz). ^1H NMR (toluene-d$_8$, -100°C, δ ppm): 47.5, 3.2, -51.2 (br, 9H, 9H, 18H, $(SiMe_3)_2N^-$); -15.4, -84.0 -14.5, 114.7 (s, 6H, 6H, 3H, 3H, Me-pz); -0.2, 51.3 (s, 2H, 1H, 4-H-pz). ^{11}B NMR (C_6D_6, 25°C, δ ppm): -3.65. Anal. Calc. for $C_{27}H_{58}BN_8Si_4U$: C, 37.89; H, 6.83; N, 13.09. Found: C, 37.76; H, 6.28; N, 12.63%.

$U(Tp^{Me2})[CH(SiMe_3)_2]_2(THF)$ (6)

Toluene (ca. 5mL), cooled in a -50°C cold well, was added to $KCH(SiMe_3)_2$ (207mg, 1.04mmol). The slurry of $KCH(SiMe_3)_2$ prepared in this way was added dropwise to a slurry of $U(Tp^{Me2})I_2(THF)_2$ (487mg, 0.522mmol) in toluene (5mL) at -50°C. The mixture was stirred for 3 hours at -50°C and the color changed from blue to

purple-red. While the mixture was allowed to warm to room temperature the toluene solvent was removed quickly under vacuum: during this process the color changed from purple-red to dark blue. The residue was extracted with toluene (2x5mL). The solvent was stripped off from the extracts and the black solid residue was triturated and washed with cold hexane (-40°C; 2x4mL) to give $U(Tp^{Me2})[CH(SiMe_3)_2]_2(THF)$ (300mg; 62% yield). IR (KBr, cm^{-1}): v(B-H) 2560. ^1H NMR (toluene-d$_8$, 25°C, δ ppm): -4.83(br, SiMe$_3$); 95.10(s, $HC(SiMe_3)_2$); 1.79 (br, 9H, Me-pz). ^{11}B NMR (toluene-d$_8$, 25°C, δ ppm): 23.04. Anal. Calc. for $C_{33}H_{68}BN_6OSi_4U$: C, 42.80; H, 7.40; N, 9.07. Found: C, 42.22; H, 7.38; N, 9.00%.

$U(Tp^{Me2})[N(SiMe_3)_2]I$ (7) and $U(Tp^{Me2})[N(SiMe_3)_2]I(THF)$

A solution of NaN(SiMe$_3$)$_2$ (65mg, 0.356mmol) in toluene (4mL) was kept in a cold bath at -50°C for 30 minutes and added dropwise to a slurry of $U(Tp^{Me2})I_2(THF)_2$ (332mg, 0.356mmol) in the same solvent (5mL) at -50°C. The mixture was stirred at this temperature for two hours, the color char... from blue to purple-red. The coloration remained while the mixture was allowed to warm under vacuum for 20 minutes. Filtration gave quantitative amount of white NaI and a purple-red filtrate. The solvent was removed from the filtrate under vacuum and trituration with pentane (2mL) gave $U(Tp^{Me2})[N(SiMe_3)_2]I$ as a dark purple-red, almost black, powder (232mg, 79% yield). IR (KBr, cm^{-1}): v(B-H) 2558. ^1H NMR (toluene-d$_8$, 25°C, δ ppm): -11.07(br, N(SiMe$_3$)$_2$). ^{11}B NMR (toluene-d$_8$, 25°C, δ ppm): 62.09. Anal. Calc. for $C_{21}H_{40}BN_7ISi_2U$: C, 30.67; H, 4.9; N, 11.92; I, 15.43. Found: C, 32.30; H, 5.04; N, 11.11; I, 16.83%.

Crystallization of $U(Tp^{Me2})[N(SiMe_3)_2]I$ from a 2:1 Et$_2$O/THF mixture at -40°C gave purple-red, almost black crystals of $U(Tp^{Me2})[N(SiMe_3)_2]I(THF)$. M.S. (16eV, 240°C): (M-THF)$^+$=822. ^1H NMR (toluene-d$_8$, 25°C, δ ppm): One main resonance at 5.30 ppm and several other very broad features between -4.0 and 12.0 ppm. ^{11}B NMR

spectrum (toluene-d$_8$, 25°C, δ ppm): 9.08. Anal. Calc. for C$_{25}$H$_{48}$BON$_7$ISi$_2$U: C, 33.60; H, 5.41; N, 10.97; I, 14.20. Found: C, 33.58; H, 5.00; N, 11.15; I, 15.11%.

U(Tp^{Me2})[N(SiMe$_3$)$_2$][CH(SiMe$_3$)$_2$] (8)

A slurry of KCH(SiMe$_3$)$_2$ (41mg, 0.207mmol) in ca. 4mL of toluene, prepared as above, was added dropwise to a slurry of U(Tp^{Me2})[N(SiMe$_3$)$_2$]I (170mg, 0.207mmol) in toluene (2mL) at -50°C. The mixture was stirred for two hours at -50°C and the color changed from purple red to dark blue-green. The mixture was filtered, the filtrate was concentrated to 1mL, and cooled at -40°C for three days to give dark blue-green crystals of U(Tp^{Me2})[N(SiMe$_3$)$_2$][CH(SiMe$_3$)$_2$] (82mg, 46% yield). IR (KBr, cm^{-1}): v(B-H) 2557. ^{1}H NMR (toluene-d$_8$, 25°C, δ ppm): 10.28, -20.52(br, br, N(SiMe$_3$)$_2$/CH(SiMe$_3$)$_2$). ^{1}H NMR (toluene-d$_8$, -50°C, δ ppm): 26.6, 5.4, -22.0, -39.8 (s, 9H, 9H, 9H, 9H, N(SiMe$_3$)$_2$/CH(SiMe$_3$)$_2$); 50.0, 3.5, 2.0, -1.7, -52.3, -72.2 (s, 3H, 3H, 3H, 3H, 3H, 3H, Me-pz); 24.0, 13.4, -6.2 (s, 1H, 1H, 1H, 4-H-pz). ^{11}B NMR spectrum (toluene-d$_8$, 25°C, δ ppm): 21.35. Anal. Calc. for C$_{28}$H$_{59}$BN$_7$ISi$_4$U: C, 39.33; H, 6.96; N, 11.47. Found: C, 41.43; H, 6.16; N, 10.37%.

U(Tp^{Me2})[N(SiMe$_3$)$_2$](3,5-Me$_2$pz) (9)

The same procedure as for the preparation of compound 5 was carried out. After filtering off the white NaI precipitate, the toulene solvent was removed slowly under vacuum. The crystalline residue was washed with hexane (3x2mL) to give complex 5 (229mg, 39% yield). The dark purple-red hexane washings were cooled at -40°C for a few days. Filtration gave crystalline U(Tp^{Me2})[N(SiMe$_3$)$_2$](3,5-Me$_2$pz) (143mg). The filtrate was concentrated and cooled at -40°C for days. Filtration gave a second crop crystalline U(Tp^{Me2})[N(SiMe$_3$)$_2$](3,5-Me$_2$pz) (83mg). The total yield is 41%. IR (KBr, cm^{-1}): v(B-H) 2554, 2440. ^{1}H NMR (toluene-d$_8$, 25°C, δ ppm): -22.03(s, 18H, SiMe$_3$); -24.91, 3.60(s, s 9H, 9H, Me-Tp^{Me2}); 7.79(s, 3H, 4-H-Tp^{Me2}); -0.57(s, 6H, Me-pz);

31.30(s. 1H, 4-H-pz). ^{11}B NMR (toluene-d$_8$, 25°C, δ ppm): 49.60. Anal. Calc. for $C_{26}H_{47}BN_9Si_2U$: C, 39.49; H, 5.99; N, 15.84. Found: C, 38.40; H, 96; N, 15.24%.

3.4.3. Thermal Behavior of Complexes 5 and 6
U(Tp^{Me2})[N(SiMe$_3$)$_2$]$_2$ in DME

Complex 5 (198mg) was dissolved in DME (1mL). During two days at room temperature the color of the solution changed gradually from blue to brown and precipitation of colorless crystals was observed. Inverse filtration gave colorless crystals (16mg) which were washed with hexane (1mL) and dried under vacuum. The solvent was removed from the filtrate and the residue redissolved in pentane (3mL). Cooling the pentane solution at -40°C gave a mixture of crystals which were manually separated: black cluster-shaped crystals (53mg), big brown crystals (23mg), and a very small amount of black needle-like crystals which were not studied further.

The decomposition products were identified as follows:

Colorless crystals were [HB(3,5-Me$_2$pz)N(SiMe$_3$)$_2$]$_2$: ^{1}H NMR (toluene-d$_8$, 25°C, δ ppm): 0.39, -0.30(br, 18H, 18H, SiMe$_3$); 2.33, 2H, Me-pz); 5.61(s, 2H, 4-H-pz); 4.40(br. 2H, H-B). ^{11}B NMR (toluene-d$_8$, 25°C, δ ppm): -2.31(d, J$_{B-H}$=102.7Hz).

Black cluster-shaped crystals were shown to be U(Tp^{Me2})[N(SiMe$_3$)$_2$](3,5-Me$_2$pz) (9) by comparison of the ^{1}H NMR spectrum with authentic sample. ^{1}H NMR (toluene-d$_8$, 25°C, δ ppm): -21.74(s, 18H, SiMe$_3$); -24.76, 3.45(s, s, 9H, 9H, Me-Tp^{Me2}); 7.79(s, 3H, 4-H-Tp^{Me2}); -0.63(s, 6H, Me-pz); 30.98(s, 1H, 4-H-pz); ^{11}B NMR (toluene-d$_8$, 25°C, δ ppm): 48.67.

Brown crystals did not show ^{11}B NMR resonance and the ^{1}H NMR spectrum was simple and could not be interpreted. The identity of this compound is not known.

U(Tp^{Me2})[N(SiMe$_3$)$_2$]$_2$ in Hexane

A slurry of complex 5 (300mg) in 4mL hexane was stored in drybox at room temperature for a day. Very little color change was observed, indicating that the decomposition process is slow at room temperature. The slurry was then stirred at 40°C. This resulted in a gradual dissolution and a color change from blue to brown. The solution was concentrated under vacuum to 2mL and cooled at -40°C for a few days. Filtration gave light purple red crystals (111mg) together with a small amount of yellowish crystalline powder. The latter was identified as [HB(3,5-Me$_2$pz)N(SiMe$_3$)$_2$]$_2$, by comparison of its ^{1}H NMR spectrum with the colorless crystals isolated from the decomposition in DME . Further concentration and cooling of the filtrate at -40°C gave a second crop of light purple red crystals (19mg) together with a few brick-like blue crystals. The brick-like blue crystals became opaque when exposed to the N$_2$ atmosphere of the drybox

The light purple-red crystals were identified as U[N(SiMe$_3$)$_2$]$_2$(3,5-Me$_2$pz)$_2$ (10): IR (KBr, cm^{-1}) ν 2954, 2438, 1521, 1431, 1251, 843. ^{1}H NMR (toluene-d$_8$, 25°C, δ ppm): -5.18(s, 36H, SiMe$_3$); -13.26(s 12H, Me-pz); 10.60(s, 2H, 4-H pz). ^{11}B NMR (toluene-d$_8$, 25°C, δ ppm): no signal was observed. Anal. Calc. for C$_{28}$H$_{50}$N$_7$ISi$_4$U: C, 35.28; H, 6.73; N, 11.22. Found: C, 34.60; H, 6.67; N, 10.81%.

Blue crystals: did not show ^{11}B NMR resonance. The ^{1}H NMR spectrum appeared to be consistent with U[N(SiMe$_3$)$_2$](3,5-Me$_2$pz)$_3$. Due to the small amount, further identification was not attempted.

U(Tp^{Me2})[CH(SiMe$_3$)$_2$]$_2$(THF) in DME

Complex 6 (118mg) was dissolved in DME (4mL) at -40°C. After a few days at -40°C the color of the solution changed gradually from blue to brown, and a brown microcrystalline precipitate was formed. The brown solid (50mg) was isolated by filtration. Unfortunately the ^{1}H NMR spectrum displayed too many peaks to be interpreted.

3.4.4. Reactivity of U(Tp^{Me2})[CH(SiMe$_3$)$_2$]$_2$(THF)
toward Small Molecules

Reaction with H$_2$

^{1}H NMR Monitoring: After H$_2$ was injected into the NMR tube, which contained U(Tp^{Me2})[CH(SiMe$_3$)$_2$]$_2$(THF), the data acquisition started as quickly as possible. After 15 minutes, the intensities of the resonances at -4.83 and 1.79 ppm, due to U(Tp^{Me2})[CH(SiMe$_3$)$_2$]$_2$(THF), decreased gradually and two new resonances at -1.2 and 0.00 ppm appeared. The resonance at 0.00 ppm is presumably due to free H$_2$C(SiMe$_3$)$_2$. After 25 minutes, the intensity of the resonances at -4.83 and 1.79 ppm kept decreasing, while that of the resonances at -1.2 and 0.00 ppm increased. After 40 minutes, the resonances at -4.83 and 1.79 ppm have disappeared and the peak at -1.2 ppm decreased in intensity. The resonance at 0.00 ppm dominated the spectrum, and the color of the solution has changed from blue to brown.

Bench-top Reaction: A hexane solution of U(Tp^{Me2})[CH(SiMe$_3$)$_2$]$_2$(THF) (162mg, 1.75x10^{-4}mol, (6mL)) was frozen in a liquid N$_2$ bath. DMPE (0.03mL) was injected with a syringe and the N$_2$ atmosphere was replaced with H$_2$. The reaction vessel was allowed to warm to -78°C and the mixture was stirred for half hour. No obvious color change was observed. Further warming to room temperature, with stirring, produced, during four hours, a gradual color change from blue to brown and the formation of some brown precipitate. The solvent was removed under vacuum and an oily material was obtained. The residue was redissolved in pentane, but cooling the pentane solution failed to give a solid material. The ^{1}H NMR spectrum of the crude product could not be interpreted.

Reaction with CO

^{1}H NMR Monitoring: The same procedure as for the hydrogenolysis was carried out. Immediately, the resonances at -4.83 and 1.79 ppm began to decrease while a

resonance at 0.00 ppm appeared. After the resonances at –4.83 and 1.79 ppm have completely disappeared the dominant peak in the spectrum was at 0.00 ppm, with a broad band between 2.4 and 0.0 ppm.

Bench-top Reaction: A hexane solution of $U(Tp^{Me2})[CH(SiMe_3)_2]_2(THF)$ (113mg, 1.22×10^{-4}mol, (8mL)) was frozen in a liquid N_2 bath and the reaction flask was evacuated and the stopcock closed. The reaction vessel was warmed to -78°C and was put under a CO atmosphere. Stirring the mixture at -78°C for ca. one hour resulted in no observable color change. The mixture was allowed to warm to room temperature during four hours and the color gradually changed from blue to red-brown. Cooling the hexane solution failed to give crystalline material.

3.4.5. Reactions of $U(Tp^{Me2})I_2(THF)_2$ with Oxygen Donor Ligands

Two Equiv of NaOEt

Addition of a solution of NaOEt (29mg, 0.424mmol) in THF (6mL) to a slurry of $U(Tp^{Me2})I_2(THF)_2$ (198mg, 0.212mmol) in THF (4mL) resulted in a slow color change from blue to brownish red. After stirring for 2 hours, the solvent was stripped off, and the residue was extracted with toluene. Filtration, followed by diffusion of pentane into the toluene solution led to the isolation of 17mg black, microcrystalline powder. The ^1H NMR spectrum of this product contained a multitude of peaks and could not be assigned. The spectrum was also complicated. Although a mass envelope with appropriate isotope for $U(Tp^{Me2})(OEt)_2(THF)_2$ could be detected, the highest intensity peak was at , two mass units higher than expected. No other pure product could be isolated from this reaction.

Two Equiv of KO^{t}Bu

A solution of KO^{t}Bu (63mg, 0.566mmol) in THF (3mL) was added to a slurry of $U(Tp^{Me2})I_2(THF)_2$ (264mg, 0.283mmol) in THF (5mL) at -50°C. The color changed

from blue to red. After stirring for 3 hours at -50°C the formation of a large amount of brown precipitate was observed. The mixture was allowed to warm to room temperature and stirring continued overnight. Filtration gave 94mg of an off-white precipitate (calculated KI, 60mg). The solvent was stripped off. After extraction with hexane (2mL + 1mL) the residue was redissolved in THF. Cooling the hexane solution at -40°C gave 52mg of green microcrystalline powder identified as $U(Tp^{Me_2})(O^tBu)_3$.[20] ^1H NMR $(C_6D_6, 23°C, \delta$ ppm): 2.74 (27H, ^tBu); -2.05, 7.05 (9H, 9H, Me-pz); 6.86 (3H, 4-H, pz). ^{11}B NMR $(C_6D_6, 23°C, \delta$ ppm): -24.1. No pure material could be isolated from the THF solution.

Two Equiv of $KOC_6H_2Me_3$-2,4,6

A solution of KOC_6H_2... (141mg, 0.808mmol) in THF (3mL) was added to a slurry of $U(Tp^{Me_2})I_2(THF)_2$ (... mg, 0.404mmol) in THF (2mL) in 3 portions at -50°C. The mixture was stirred for 3 hours, producing a gradual color change from purple blue to dark brownish red. Stirring was continued for another one and half hour while the mixture was allowed to warm to room temperature. Filtration gave a brownish red solution and almost quantitative amount of white KI precipitate. The solvent was stripped off and the residue was washed with hexane (2x5mL), and Et_2O (2x4mL). Both hexane and Et_2O washings had a dark brownish red color. The residue was a pale-green crystalline powder which was redissolved in THF. The solutions were cooled at -40°C and gave 87mg and 22mg of green crystalline powder from the THF and Et_2O solutions, respectively. ^1H NMR analysis indicated that both solids were $U(Tp^{Me_2})(OC_6H_2Me_3$-2,4,6$)_3$.[20] ^1H NMR (toluene-d_8, 23°C, δ ppm): 8.26 (6H, m-H, mesityl); 2.86 (9H, p-Me, mesityl); -0.96 (18H, o-Me, mesityl); 7.54 (3H, 4-H-pz); 6.19, -2.27 (9H, 9H, Me-pz). ^{11}B NMR (toluene-d_8, 23°C, δ ppm): -26.2. No pure product could be isolated from hexane solution.

Two Equiv of $KOC_6H_3{}^iPr_2$-2,6

A solution of $KOC_6H_3{}^iPr_2$-2,6 (79mg, 0.364mmol) in THF (3mL) was added to a slurry of $U(Tp^{Me2})I_2(THF)_2$ (170mg, 0.182mmol) in THF (4mL) at -50°C. Stirring the mixture for half an hour did not result in any significant color change. The mixture was allowed to warm to room temperature and stirring continued overnight. Filtration gave quantitative amount of white KI precipitate. The THF solvent was stripped off. After extraction with 4mL of hexane, the residue was redissolved in THF. Cooling the hexane solution at -40°C gave black crystals and some pale green microcrystalline powder. The ^1H NMR spectrum of black crystals could not be interpreted. Cooling the THF solution at -40°C gave green crystals of $U(Tp^{Me2})(OC_6H_3{}^iPr_2$-2,6)_3THF (14mg). ^1H NMR (toluene-d_8, 23°C, δ ppm): 6.95, -2.79 (9H, 9H, 3,5-Me-pz); 7.26 (3H, 4-H-pz); 2.50, (d, 18H, Me-^iPr_a); 12.85 (heptet, 3H, H-^iPr_a); -2.31 (d, 18H, Me-^iPr_b); -16.02 (heptet, 3H, H-^iPr_b); 10.25, 7.47 (dd, dd, 3H, 3H, 3,5-H-phenoxide); 8.55 (t, 3H, 4-H-phenoxide); 3.56, 1.46 (m, m, 4H, 4H, THF), ^{11}B NMR (toluene-d_8, 23°C, δ ppm): -27.57. Anal. Calc. for $C_{55}H_{81}BN_6O_4U$: C, 57.99; H, 7.17; N, 7.38. Found. C, 58.52; H, 7.05; N, 7.37%.

Two Equiv of Kdpm; Formation of $U(dpm)_3$ (11)

A solution of Kdpm (118mg, 0.530mmol) in THF (4mL) was added to a slurry of $U(Tp^{Me2})I_2(THF)_2$ (247mg, 0.265mmol) in THF (3mL). After stirring for 2 hours at -50°C, a color change from blue to brown and the formation of white precipitate were observed. Following filtration, the residue was extracted with THF (3mL). The solvent was stripped off from the combined THF solutions and the residue was redissolved in hexane. Cooling the hexane solution at -40°C gave brown crystals identified as $U(dpm)_3$ (11) ^1H NMR (toluene-d_8, 25°C, δ ppm): -1.80(s, 54H, ^tBu); 13.21(s, 3H, HC). M.S.: 788(M$^+$). Anal. Calc. for $C_{33}H_{57}BO_6U$: C, 50.31; H, 7.29. Found: C, 54.49; H, 7.61%.

Two Equiv of KO_2C^tBu

A solution of KO_2C^tBu (69mg, 0.492mmol) in THF (4mL) was added to a slurry of $U(Tp^{Me2})I_2(THF)_2$ (230mg, 0.246mmol) in THF (3mL) at -50°C. An immediate color change from blue to dark green and the formation of precipitate were observed. After stirring for 2 hours at -50°C, filtration gave almost quantitative KI precipitate. The THF solvent was removed under vacuum and the residue was washed with heptane (3mL) and hexane (3mL), both washings had a light blue color. The powder was redissolved in a 3:1 mixture of THF and hexane (by volume). Crystallization at -40°C gave 50mg (27%) of $U(Tp^{Me2})(O_2C^tBu)_2$ (12) as dark green, almost black crystals. IR (KBr, cm^{-1}): ν(B-H): 2556; 2363 (s), 2340 (s). M.S.: 738(M$^+$). The ^{1}H NMR spectrum contained numerous peaks and could not be assigned. Anal. Calc. for $C_{25}H_{40}BN_6O_4U$: C, 40.72; H, 5.47; N, 11.40. Found: C, 40.92; H, 5.50; N, 10.34%.

Preparation of $U(Tp^{Me2})[H_2B(pz)_2]_2$ (13)

A solution of $KH_2B(pz)_2$ (85mg, 0.440mmol) in THF (2mL) was added to a slurry of $U(Tp^{Me2})I_2(THF)_2$ (205mg, 0.220mmol) in THF (4mL). The mixture was stirred for three hours. No significant color change was observed. Inverse filtration through a cannula gave a dark colored solution and almost quantitative white KI precipitate. The THF solvent was removed under vacuum and the residue was triturated with pentane (2mL), then dissolved in Et_2O. Gas phase diffusion of pentane into the Et_2O solution at -40°C gave $U(Tp^{Me2})[H_2B(pz)_2]_2$ (13) as a dark, almost black crystalline powder in 45% yield. IR (KBr, cm^{-1}): ν(B-H) 2430; 2283, 2251. M.S.: 830(M$^+$). ^{1}H NMR (C_6D_6, 25°C, δ ppm): -2.68, -6.12 (s, s, 6H, 6H, Me-Tp^{Me2}); 2.97, -5.63 (s, s, 3H, 3H, Me-Tp^{Me2}); 16.17, 14.33, 10.63, 9.03, 7.54, 5.48, 5.09 (s, 2H); 11.92 (s, 1H, 4-H-Tp^{Me2}). Anal. Calc. for $C_{27}H_{38}N_{14}B_3U$: C, 39.11; H, 4.62; N, 23.65. Found: C, 39.70; H, 4.35; N, 22.91.

3.4.6. X-ray Data Collection, Structure Solution and Refinement:

Single crystals suitable for X-ray analysis were obtained by cooling a toluene solution (5, 6, and 8) and hexane solution (9 and 10) over a few days at -40°C. A summary of the crystallographic data is listed in Table 3.3.

Table 3.3 Crystallographic Data for Complexes 5, 8, 6, 9, and 10

compounds	5	8	6	9	10
mol formula	$C_{27}H_{58}BN_9Si_4U$	$C_{28}H_{59}BN_7Si_4U$	$C_{33}H_{68}BN_6OSi_4U$	$C_{26}H_{47}BN_9Si_2U$	$C_{22}H_{50}N_6Si_4U$
formula weight	959.32	925.19	926.13	790.75	749.07
space group	$P\bar{1}$	$P2_1/c$	$P2_12_12_1$	$P\bar{1}$(No. 2)	$C2/c$(No. 15)
a,Å	11.866(2)	9.996(5)	12.518(2)	11.502(2)	18.506(3)
b,Å	15.062(2)	18.575(6)	17.599(3)	11.608(2)	14.209(3)
c,Å	11.423(2)	16.663(5)	19.508(5)	13.167(2)	12.850(2)
α,deg	93.12(1)	90	90	97.90(1)	90
β,deg	115.32(1)	93.99(4)	90	92.61(1)	99.398(12)
γ,deg	82.84(1)	90	90	102.03(1)	90
V,Å³	1831.1(5)	3086(4)	4332(2)	1697.9(5)	3333.7(9)
Z	2	4	4	2	4
diffractometer	P1	P1	Enraf-Nonius CAD4	Siemens P4/RA	Siemens P4/RA
radiation(λ,Å)			MoKα(0.7107) from graphite monochromater		
scan mode	θ-2θ	ω-2θ	θ-2θ	θ-2θ	θ-2θ
2θ limits(deg)	2.0-50.0	3.0-56.0	3.0-50.0	50.0	50.0
temp, °C	23	23	23	-100	-100
no. of unique data	5068	3441	2945	5944	2911
no. of variables	415	316	250	352	150
R1	0.043[a]	0.056[a]	0.063[a]	0.0452[b]	0.0433[b]
R2	0.053[a]	0.060[a]	0.072[a]		
wR2				0.1130[b]	0.0938[b]

[a]$(I>3\sigma(I))$; [b]$(I>2\sigma(I))$; $R_1 = \Sigma||F_o|-|F_c||/\Sigma|F_o|$; $R_2 = [\Sigma w_1(|F_o|-|F_c|)^2/\Sigma w_1 F_o^2]^{1/2}$, $wR_2 = [\Sigma w_2(F_o^2 - F_c^2)^2/\Sigma w_2 F_o^4]^{1/2}$

3.5. References

(1) Gilman, H.; Jones, E.; Bindschadler, E.; Blume, D.; Karmas, G.; Martin, J., G. A.; Nobis, J. F.; Thirtle, J. R.; Yale, H. L.; Yoeman, F. A. *J. Am. Chem. Soc.* 1956, *78*, 2790.

(2) Gilman, H. *Adv. Organomet. Chem.* 1968, 7, 33.

(3) Marks, T. J.; Seyam, A. M. *J. Organomet. Chem.* 1974, 67, 61.

(4) Brandi, G.; Brunelli, M.; Lugli, G.; Mazzei, A. *Inorg. Chim. Acta* 1973, 7, 319.

(5) Cotala, A. E.; Tsutsui, M. *J. Am. Chem. Soc.* 1973, 95, 91.

(6) Marks, T. J.; Seyam, A. M.; Kolb, J. R. *J. Am. Chem. Soc.* 1973, 95, 5529.

(7) Sigurdson, E. R.; Wilkinson, G. *J. Chem. Soc., Dalton Trans.* 1977, 812.

(8) Marks, T. J., Day, V. W. In *Fundamental and Technological Aspects of Organo-f-Element Chemistry*; T. J. Marks and I. L. Fragala, Ed.; D. Reidel Publishing Company: Dordrecht Boston Lancaster, 1984; pp 115.

(9) Fagan, P. J., Manriquez, J. M.; Marks, T. J.; Day, C. S.; Vollmer, S. H.; Day, V. W. *Organometallics* 1982, 7, 170-180.

(10) Jones, R. G.; Karmas, G., Martin, G. A.; Jr.; Gilman, H. *J. Am. Chem. Soc.* 1956, 78, 4285.

(11) Jamerson, J. D. Ph. D. Thesis, University of Alberta, 1974.

(12) Takats, J. In *Fundamental and Technological Aspects of Organo-f-Element Chemistry*; T. J. Marks and I. L. Fragala, Ed.; D. Reidel Publishing Company: Dordrecht Boston Lancaster, 1984; pp 159.

(13) Andersen, R. A. *Inorg. Chem.* 1979, 18, 1507-1509.

(14) Sartain, I., Marquez, N., Pires de Matos, A. *Inorg. Chim. Acta* 1987, 139, 57-66.

(15) Calderazzo, F., Vitali, M., Vigato, P. A. *Inorg. Chim. Acta* 1978, 28, 77-122.

(16) Cotton, F. A., Wilkinson, G. *Advanced Inorganic Chemistry* Fifth ed.; John Wiley & Sons, Inc.: New York, 1988; pp 877.

(17) Sigurdson, E. R., Thomas, J. L.; *Organomet. Chem. Soc.* 4 1971, 7, 1-58.

(18) Cernia, E.; Mazzei, A. *Inorg. Chim. Acta* **1974**, *10*, 239-252.

(19) Marks, T. J.; Ernst, R. D. In *Comprehensive Organometallic Chemistry*; S. G. Wilkinson, F. G. A. Stone and E. W. Abel, Ed.; Pergamon Press: Oxford, 1982; Vol. 3; pp 173.

(20) Marques, N.; Marcalo, J.; Pires de Matos, A.; Bagnall, K. W. *Inorg. Chim. Acta* **1987**, *134*, 309.

(21) Domingos, A.; Marcalo, J.; Marques, N.; Pires de Matos, A. *J. Less-Common. Met.* **1989**, *149*, 271-277.

(22) Domingos, A.; Marcalo, J.; Marques, N.; Pires de Matos, A. *Polyhedron* **1992**, *11*, 501-506.

(23) Santos, I. **1993**, personal communication.

(24) Muetterties, E. L.; Mahler, W.; Packer, K. J.; Schmutzler, R. *Inorg. Chem.* **1964**, *3*, 1298.

(25) Muetterties, E. L. *Acc. Chem. Res.* **1970**, *3*, 266.

(26) Cotton, F. A.; Wilkinson, G. *Advanced Inorganic Chemistry*; Fifth ed.; John Wiley & Sons, Inc.: New York, 1988, pp 1318.

(27) Kepert, D. L. In *Inorganic Stereochemistry*Springer-Verlag: Berlin, 1982; Vol. 6; pp 36.

(28) Huheey, J. E. In *Inorganic Chemistry*; Third ed.Harper & Row, Publishers, New York: Cambridge, 1983; pp 208.

(29) Rossi, A. R.; Hoffmann, R. *Inorg. Chem.* **1975**, *14*, 365-374.

(30) Van Der Sluys, W. G.; Burns, C. J.; Sattelberger, A. P. *Organometallics* **1989**, *8*, 855-857.

(31) Hitchcock, P. B.; Lappert, M. F.; Smith, R. G.; Bartlett, R. A.; Power, P. P. *J. Chem. Soc., Chem. Commun.* **1988**, 1007-1009.

(32) Bruno, J. W.; Marks, T. J.; Day, V. W. *J. Am. Chem. Soc.* **1982**, *104*, 7357.

(33) Bruno, J. W.; Day, V. W.; Marks, T. J. *J. Organomet. Chem.* **1983**, *250*, 237.

(34) Bruño, J. W.; Duttera, M. R.; Fendrick, C. M.; Smith, G. M.; Marks, T. J. *Inorg. Chim. Acta* **1984**, *94*, 271.

(35) Simpson, S. J.; Turner, H. W.; Andersen, R. A. *Inorg. Chem.* **1981**, *20*, 2991-2995.

(36) Simpson, S. J.; Andersen, R. A. *J. Am. Chem. Soc.* **1981**, *103*, 4063-4066.

(37) Bradley, D. C.; Hursthouse, M. B.; Newton, J.; Walker, N. P. C. *J. Chem. Soc., Chem. Commun.* **1984**, 188.

(38) Kime-Hunt, E.; Spartalian, K.; DeRusha, M.; Nunn, C. M.; Carrano, C. J. *Inorg. Chem.* **1989**, *28*, 4392-4399.

(39) Eigenbrot, J., C. W.; Raymond, K. N. *Inorg. Chem.* **1981**, *20*, 1553-1556.

(40) Eigenbrot, J., C. W.; Raymond, K. N. *Inorg. Chem.* **1982**, *21*, 2653-2660.

(41) Shannon, R. D. *Acta Crystallogr.* **1976**, *A32*, 751.

(42) Zhang, X. Ph. D. Thesis, University of Alberta, 1995.

(43) Manriquez, J. M.; Fagan, P. J.; Marks, T. J. *J. Am. Chem. Soc.* **1978**, *100*, 3939.

(44) Manriquez, J. M.; Fagan, P. J.; Marks, T. J.; Day, C. S.; Day, V. W. *J. Am. Chem. Soc.* **1978**, *100*, 7112.

(45) Minhas, R. K.; Edema, J. J. H.; Gambarotta, S.; Meetsma, A. *J. Am. Chem. Soc.* **1993**, *115*, 6710.

(46) Cotton, F. A.; Wilkinson, G. In *Advanced Inorganic Chemistry*; Fifth ed.John Wiley & Sons, Inc.: New York, 1988; pp 981, 1388, 988, 651.

(47) Huheey, J. E. In *Inorganic Chemistry*; Third ed.Harper & Row, Publishers, New York: Cambridge, 1983; pp 527.

(48) Sun, Y.; Takats, J.; Eberspacher, T.; Day, V. *Inorg. Chim. Acta* **1995**, *229*, 315-322.

(49) Carvalho, A.; Domingos, A.; Gaspar, P.; Marques, N.; Pires de Matos, A.; Santos, I. *Polyhedron* **1992**, *11*, 1481.

(50) Pi, R.; Bauer, W.; Brix, B.: Schade, C.; Von Rague Schleyer, P. *J. Organomet. Chem.* **1986**, *306*, C1-C4.

(51) Davidson, P. J.; Harris, D. H.; Lappert, M. F. *J. Chem. Soc. Dalton Trans.* **1976**, 2268-2274.

(52) Schaverien, C. J.; Meuselen, J. B. v. *Organometallics* **1991**, *10*, 1704-1709.

(53) Avens, L. R.; Bott, S. G.; Clark, D. L.; Sattelberger, A. P.; Watkin, J. G.; Zwick, B. D. *Inorg. Chem.* **1994**, *33*, 2248-2256.

Chapter 4

Synthesis and Structure of Uranium(III) Complexes Containing
Dihydrobis(pyrazolyl)borate Ligand

4.1. Introduction

The poly(pyrazolyl)borate ligands provide a flexible and versatile coordination environment for both transition metal ions[1] and the f-elements.[2] For the large f-elements the chemistry has been dominated by the hydrotris(pyrazolyl)borate ligands. However, recently a series of interesting complexes with dihydrobis(pyrazolyl)borate ligands have been described. Reger et $al.$[3] reported the synthesis of $Y[H(\mu-H)B(pz)_2]_3$ and $Y[H(\mu-H)B(3,5-Me_2pz)_2]_3$ and determined the solid state structure of the former complex. Domingos et $al.$[4] have demonstrated that the complexes $M[H(\mu-H)B(3,5-Me_2pz)_2]_3$, (M=U, Ce, Sm, and Yb) also featured three-center B-H···M bridge type interactions and tricapped trigonal prismatic geometry.

Since steric effects play a dominant role in determining the coordination number and geometry of f-element complexes it was of interest to determine what effect, if any, the less bulky $H_2B(pz)_2^-$ ligand would have on the nature of the tris-chelate U(III) complex. Reported here is the synthesis, characterization, and X-ray structure of uranium(III) complexes containing the $H_2B(pz)_2^-$ ligand. The results of this chapter have been published.[5]

4.2. Results and Discussion

4.2.1. Synthesis and Spectroscopic Characterization

Reaction of a slurry of $UI_3(THF)_4$ with three equivalents of $KH_2B(pz)_2$ gave $U[H(\mu-H)B(pz)_2]_3(THF)$ (14) in good yield (eq. 4.1). Complex 14 is a dark, almost black solid, which is very soluble in THF and toluene, soluble in Et_2O, but only sparingly

$$UI_3(THF)_4 + 3KH_2B(pz)_2 \xrightarrow[\text{2 hr}]{\text{THF/r.t.}} U[H(\mu\text{-}H)B(pz)_2]_3(THF) + 3KI \qquad 4.1$$

14 (black crystals)
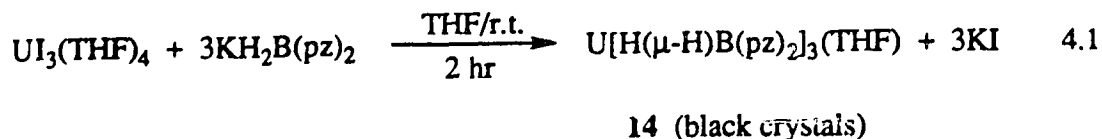
soluble in hexane. Elemental analysis is consistent with the presence of one THF molecule per uranium center. An attempt to remove the THF by heating the compound at 70°C under dynamic vacuum was unsuccessful, but repeated cycles of dissolution of 14 in toluene and solvent removal did result in the formation of the THF-free complex, $U[H(\mu\text{-}H)B(pz)_2]_3$ (15).

The IR spectrum of 14 in the solid state shows a complex B-H stretching pattern at 2430 and ca. 2282, 2251 cm^{-1}. The higher frequency band can be assigned to a normal terminal B-H stretch, while the bands at lower frequencies are indicative of bridging B-H⋯U(III) interactions. A similar type of interaction has been described by Domingos for $U[H(\mu\text{-}H)B(3,5\text{-}Me_2pz)_2]_3$, (16), although the shifts in 14 are smaller than those found in the latter complex[4] (B-H⋯U stretches are at: 2270, 2240, 2190, 2090 cm^{-1}). We propose that coordination of the THF ligand causes increased steric and electronic saturation of the U(III) center in 14 and weakens the B-H⋯U interaction. The B-H stretching region of the unsolvated complex $U[H(\mu\text{-}H)B(pz)_2]_3$, (15), shows a main band at 2432 cm^{-1} (B-H terminal) with a broad multiplet envelop extending down to 2219 cm^{-1}. The presence of low frequency features is expected based on the analogous 3,5-dimethylpyrazolyl complex 16. Unfortunately, a comparison between the nature and strength of the agostic B-H⋯U(III) interactions between complexes 15 and 16 is not possible due to the ill defined shape of the broad envelop.

The ^1H NMR spectrum of 14 shows only one set of signals for the protons of pyrazolyl rings and one for the THF molecule. The resonances of the latter are shifted from their normal diamagnetic positions and provide further indication for THF coordination. The observation of only one set of resonances is indicative of fluxional

behavior. The ^{11}B NMR spectrum also shows only a single peak, consistent with the ^{1}H NMR results. The fluxional nature of 14 was ascertained by a variable temperature ^{1}H NMR study. Decoalescence of the signals is observed around -60°C, but the low temperature limiting spectrum could not be reached even at -100°C. Thus the mechanism of the rearrangement process remains unknown.

The ^{1}H NMR spectrum of complex 15 at room temperature also shows one set of resonances for the pyrazolyl protons (23.73, 11.12, and 11.05 ppm), but contrary to the behavior of complex 16 the BH_2 signal could not be detected. In view of this observation and the known fluxional nature of complexes 14 and 16 a variable temperature ^{1}H NMR study was carried out, as shown in Figure 4.1. Interestingly, already at -20°C two distinct B-H resonances were detected at 29.31 ppm and 1.10 ppm. The signals were assigned to B-H···U(III) bridge and B-H terminal units, respectively, on the basis of the much broadened and more shifted nature of the former signal, signifying the influence of the paramagnetic U(III) center. Warming the sample to 80°C resulted in the emergence of a broad averaged BH_2 signal at δ 12.7 ppm, a value close to that observed for the averaged BH_2 signal in the dimethylpyrazolyl analogue 16.[4] The lineshape changes are reversible and we calculate a free energy of activation at the coalescence temperature (T_c=40°C) of 51 kJ/mol for the process that equilibrates the environments of the two B-H hydrogens. It is interesting to note that Reger et al.[3] reported a very similar energetic barrier for the same process in Y[H(μ-H)B(pz)$_2$]$_3$, 47.7 kJ/mol. However in that case the energetics were based on ^{13}C NMR data of slightly different pyrazolyl rings in the solution ground state structure, as the BH_2 hydrogens could not be differentiated in this diamagnetic molecule even at low temperature. The observation of well separated B-H signals in 15 for a virtually identical $\Delta G^{\ddagger}$ is of course due to the paramagnetic U(III) center and represents another interesting application of chemical shift expansion in paramagnetic complexes to the study of fast rate processes.[6] Finally, we note that the ^{1}H NMR spectrum of U[H(μ-H)B(3,5-Me$_2$pz)$_2$]$_3$ (16) showed only one broad BH_2 resonance
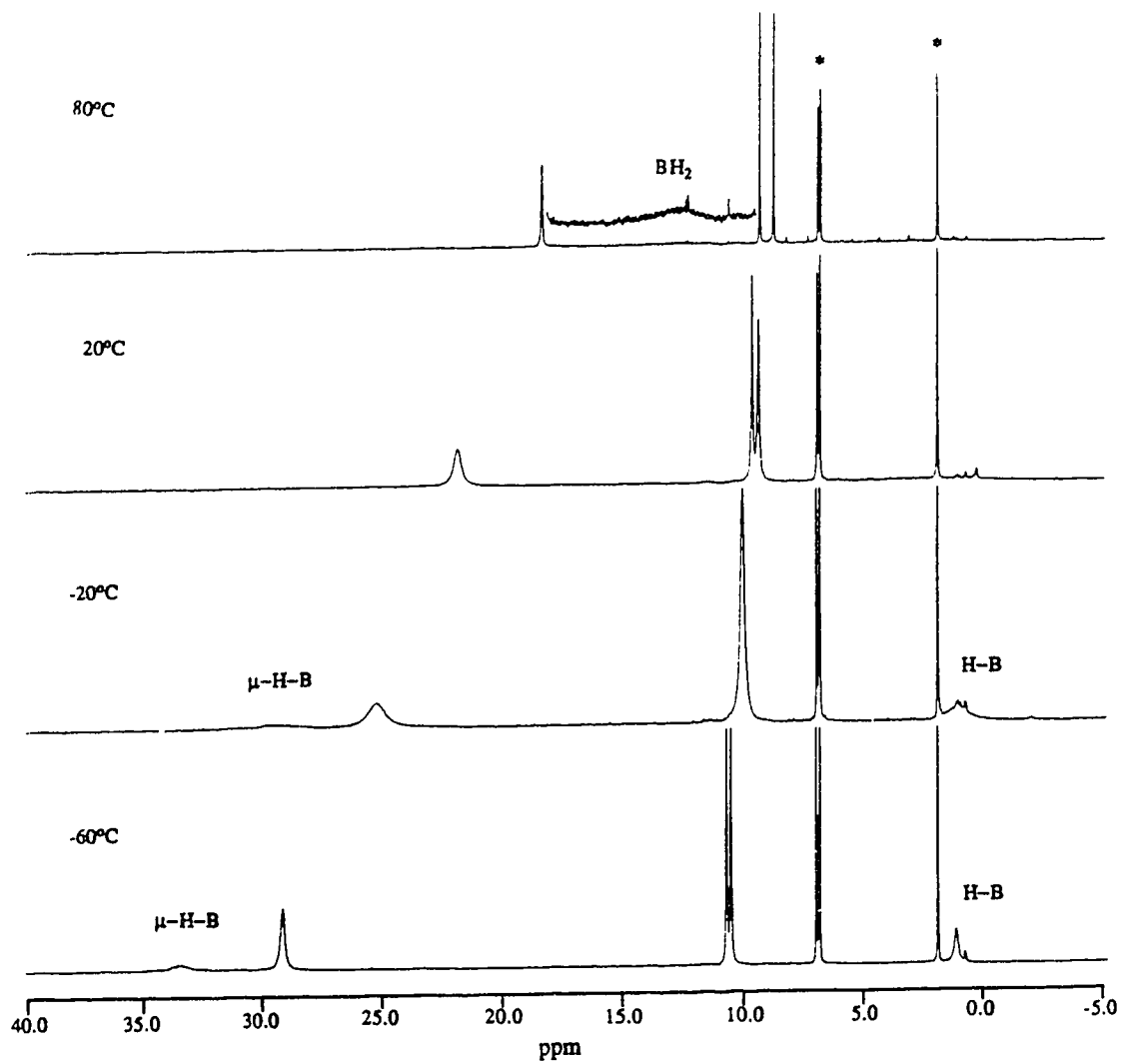
Fig. 4.1 Variable Temperature ^{1}H NMR Spectra (400 MHz) of U[H(μ-H)B(pz)$_2$]$_3$
(15) in Toluene-d$_8$; the Spectrum at -60°C is ^{1}H{^{11}B}

down to $-63°C$.[4] It thus appears that the agostic B-H$\cdots$U(III) interactions are stronger in complex 15 than in 16, which may not be unexpected in view of the more sterically crowded nature of the dimethylpyrazolyl derivative 16.

4.2.2. Molecular Structure of U[H(μ-H)B(pz)$_2$]$_3$(THF) (14)

In order to corroborate the presence of B-H$\cdots$U(III) interaction and to determine the precise geometry of the molecule, a single crystal X-ray analysis was performed. The analysis revealed that in the solid state complex 14 is composed of discrete U[H(μ-H)B(pz)$_2$]$_3$(THF) molecules (Figure 4.2) in which each U(III) ion is coordinated to a pair of nitrogens from each of the three bidentate H$_2$B(pz)$_2^-$ ligands and the oxygen of a THF ligand. As shown in Figure 4.3, the THF oxygen caps one square face of a (necessarily) distorted trigonal prismatic coordination polyhedron described by the six nitrogen donors. The three H$_2$B(pz)$_2^-$ ligands span two triangular edges and one square edge of this trigonal prism. The pair of ligands which span triangular edges occupy opposite sides of a square face not capped by the THF ligand; the third bidentate H$_2$B(pz)$_2^-$ ligand spans the vertical edge which is common to the remaining two square faces. Consistent with the solid-state IR data mentioned above, each of the H$_2$B(pz)$_2^-$ ligands engages in a three-center two-electron B-H$\cdots$U agostic bonding interaction by folding along its edge of the coordination polyhedron, buckling the six-membered UN$_4$B ring[7] and tipping the B-H group toward the metal. This results in hydrogen atoms which cap three of the remaining four uncapped faces of the trigonal prism. As shown in Fig. 4.3, the "lower" triangular face of the trigonal prism is the only "uncapped" face. H$_{1bb}$ caps the "upper" triangular face and H$_{2bb}$ and H$_{3bb}$ cap square faces. U[H(μ-H)B(pz)$_2$]$_3$(THF) is therefore formally ten-coordinate in the solid state and probably in solution as well. Selected bond lengths and angles involving nonhydrogen atoms of 14 are given in Table 4.1. Ligand$\cdots$ligand contacts on the coordination sphere of crystalline 14 are given in Table 4.2.

Fig. 4.2 Perspective Drawing of the Solid-state Structure for U[H(μ-H)B(pz)₂]₃(THF)
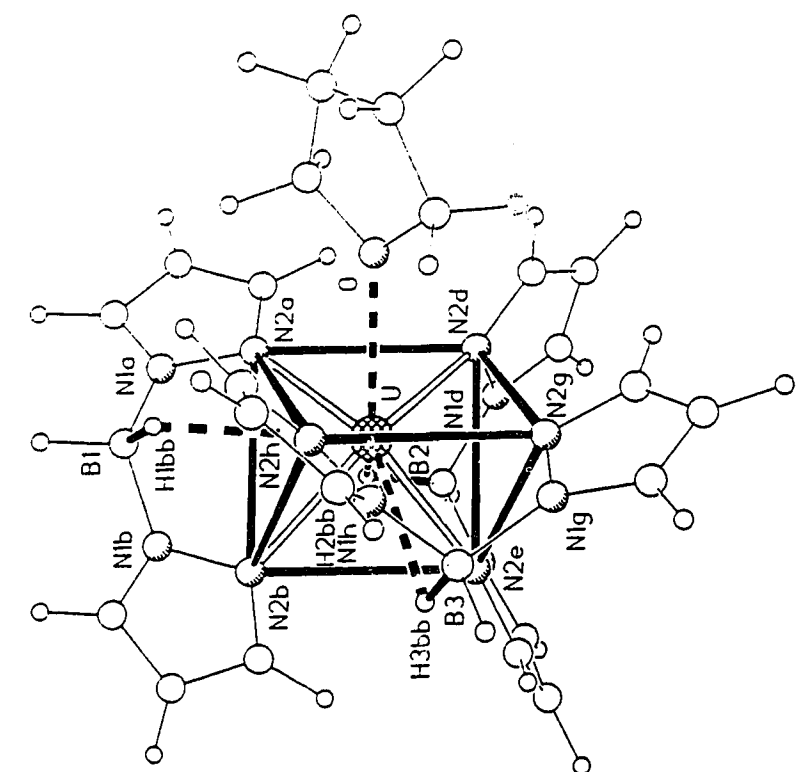
Fig. 4.3 Perspective Drawing of the Solid-state Structure for U[H(μ-H)B(pz)₂]₃(THF) with the Trigonal Prismatic Coordination Polyhedron Included
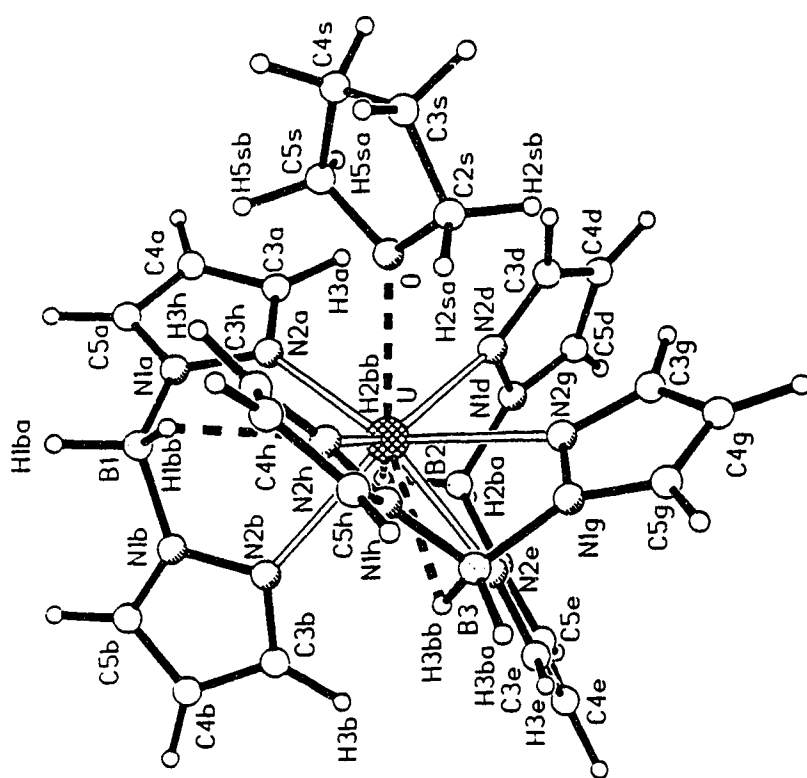
Table 4.1 Selected Bond Lengths (Å) and Angles (°) for Complex **14**

Bond Lengths

U-N2a	2.576(10)	U-N2e	2.607(9)
U-N2b	2.567(11)	U-N2g	2.601(11)
U-N2d	2.568(9)	U-N2h	2.608(9)
U-O	2.625(8)	U···H1bb	3.01[a]
		U···H2bb	3.01[a]
		U···H3bb	2.88[a]

Bond Angles

N2a-U-N2b	77.4(3)	N2d-U-N2g	79.0(3)
N2a-U-N2d	75.4(3)	N2e-U-N2g	73.8(3)
N2b-U-N2d	124.3(3)	N2a-U-N2h	111.6(3)
N2a-U-N2e	117.5(3)	N2b-U-N2h	92.2(3)
N2b-U-N2e	75.1(3)	N2d-U-N2h	143.1(3)
N2d-U-N2e	76.0(3)	N2e-U-N2h	124.3(3)
N2a-U-N2g	147.8(3)	N2g-U-N2h	78.6(3)
N2b-U-N2g	134.1(3)	N2a-U-N2b	77.4(3)
N2a-U-N2b	77.4(3)	N2a-U-N2b	77.4(3)
N2a-U-O	75.7(3)	N2e-U-O	144.3(3)
N2b-U-O	140.0(3)	N2g-U-O	79.4(3)
N2d-U-O	76.1(3)	N2h-U-O	71.2(3)

[a] This parameter was calculated using the idealized coodinates for the BH₂ hydrogen atoms

Table 4.2 Ligand···Ligand Contacts (Å) along Edges of the Coordination Polyhedron

N2a···N2b	3.22	N2d···N2g	3.29	N2d···N2e	3.19
N2e···N2g	3.13	N2g···N2h	3.30	N2a···N2d	3.14
N2a···N2h	4.29	N2b···N2e	3.15	N2b···N2h	3.73
O···N2a	3.19	O···N2d	3.20	O···N2g	3.34
O···N2h	3.05	H1bb···N2a	2.75	H1bb···N2b	2.73
H1bb···N2h	2.80	H2bb···N2a	2.85	H2bb···N2b	3.16
H2bb···N2d	2.75	H2bb···N2e	2.81	H3bb···N2b	3.40
H3bb···N2e	2.99	H3bb···N2g	2.74	H3bb···N2h	2.69

As shown in Fig. 4.4, the capped "square" faces of the trigonal prism are defined by the following three groups of four nearly coplanar nitrogen atoms: I: N_{2a}, N_{2b}, N_{2d} and N_{2e}, coplanar to $0.07Å$; II: N_{2a}, N_{2d}, N_{2g} and N_{2h}, coplanar to $0.08Å$; and III: N_{2b}, N_{2c}, N_{2g} and N_{2h}, coplanar to within $0.12Å$. Least-squares mean planes through these "square" groups of atoms make the following dihedral angles with each other: I-II, $57.9°$; I-III, $71.0°$; and II-III, $51.6°$. The triangular faces of the polyhedron are within $3.1°$ of being parallel. The "upper" triangle defined by N_{2a}, N_{2b} and N_{2h} makes dihedral angles of $81.4°$, $85.7°$ and $85.7°$ with the mean planes for "squares" I, II and III, respectively; the "lower" triangle defined by N_{2d}, N_{2e} and N_{2g} makes dihedral angles of $78.5°$; $85.1°$ and $87.7°$ with them.

The THF oxygen atom is displaced by $1.96Å$ out of its "square" face and capping hydrogen atoms H_{2bb} and H_{3bb} are displaced by $1.81Å$ and $1.75Å$, respectively, out of theirs. H_{1bb} is displaced by $1.66Å$ out of the "upper" triangular face. The U-O bond length is $2.625(8)Å$ and the U···H distances average $3.00(11)Å$. (A fixed B-H bond length of $1.14Å$ was used for these calculations.)

The six U-N bonds in **14** have an average length of $2.588(20)Å$ which is the same as the average length $(2.582(33)Å)$ observed in the solid state for the U-N bonds in the two crystallographically-independent molecules of $U[H(\mu-H)B(3,5-Me_2pz)_2]_3$ (**16**).[4] Compound **16** is the nonsolvated analogue of **14** that incorporates the sterically more-demanding $H_2B(3,5-Me_2pz)_2^-$ ligand. The six nitrogens in **16** also describe a trigonal prism and each of the $H_2B(3,5-Me_2pz)_2^-$ ligands is involved in three-center two-electron bonding interactions with the metal. The most obvious difference between the U(III) coordination in **16** and **14** is therefore a formal increase by one in coordination number from nine in **16** to ten in **14**. A change in coordination number from nine to ten is expected to involve a ~$0.05Å$ uniform increase in all metal-ligand bond lengths.[8] This does not seem to have occurred in the present case since the U-N bond lengths for **14** and **16** are quite similar. Although this result might loosely be interpreted as indicating that
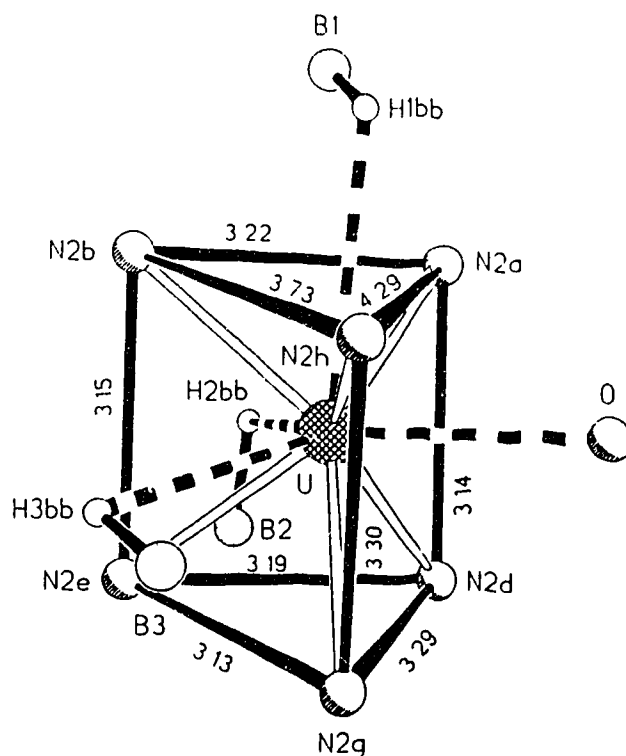
Fig. 4.4 Perspective Drawing of the Trigonal Prismatic Coordination
Polyhedron Observed for U(III) in the Solid-state Structure of
U[H(μ-H)B(pz)$_2$]$_3$(THF)

binding a THF ligand to the U(III) ion in U[H(μ-H)B(pz)$_2$]$_3$ (15) is sterically equivalent

to replacing the hydrogens by methyls at the 3- and 5-positions in each of its six

pyrazolyl rings, this would be an oversimplification. The U-O distance is similar to the

values observed in U(Tp^{Me2})I$_2$(THF)$_2$ (2.58(1) and 2.65(1)Å), (see Chapter 2), but as

expected, longer than the average bond length of 2.52(1)Å in the seven-coordinate

UI$_3$(THF)$_4$ complex.[9] As noted above, the solid-state IR bands associated with the

B-H···U interactions are shifted less in 14 than in 16 relative to the normal terminal B-H

stretch. This indicates weaker (and longer) three-center agostic U···H-B bonding

interactions with the metal in 14. The U···H bridge bonds are indeed weaker in 14 than 16

since the U···B separations average 3.42Å in 14 and 3.20Å in 16. The steric and/or

electronic differences between **14** and **16** therefore seem to affect the agostic B-H⋯U bonds much more than the U-N bonds (which were quite similar in the two compounds). This should probably not be surprising since these agostic bonds are the weakest ones to the metal. The steric and/or electronic factors which are responsible for lengthening these weak agostic bonds in **14** relative to **16** should also affect, although probably to a less noticeable degree, the other structural features of **14**.

The solid-state structure of **16** has approximate C_{3h} molecular symmetry with the bidentate ligands spanning the three vertical edges between triangular faces of the trigonal prism. This arrangement allows the ligands to pack efficiently by wrapping around the girdle of the trigonal prism with the BH_2 of one ligand nestled in between the pyrazolyl rings of the adjacent one. The BH_2 group of the $H_2B(3,5-Me_2pz)_2^-$ ligands can easily move toward the metal in this structure.

If a trigonal prismatic arrangement of six nitrogens is preferred for U(III) in these complexes, a different wrapping pattern must exist for the $H_2B(pz)_2^-$ ligands in **14** because of the coordinated THF ligand. Being the largest donor atom of a "capping" ligand, the THF oxygen will cap a "square" face of the trigonal prism. Maximum utilization of available agostic B-H⋯U bonding interactions will then require the capping of a triangular face and consequently the spanning of a triangular edge by at least one $H_2B(pz)_2^-$ ligand. This will determine which edges are spanned and which faces are capped by the remaining two ligands.

The data in Tables 4.1 and 4.2 reveal two trends which may help our analysis. Three of the six U-N bonds (U-N$_{2e}$, U-N$_{2g}$ and U-N$_{2h}$) are systematically longer (average length of 2.605(4)Å) than the other three (average length of 2.570(5)Å) and two edges (N$_{2a}$⋯N$_{2h}$ and N$_{2b}$⋯N$_{2h}$) of the trigonal prism are much (>0.40Å) longer than the others. Both of these effects can be attributed to steric crowding on the coordination sphere which manifests itself in ligand⋯ligand contacts which are short even after these distortions have occurred. These same interactions should weaken the agostic B-H⋯U

bonds, particularly since two of the face-capping hydrogen (H_{1bb} and H_{3bb}) are directly involved in these short contacts. With B-H and C-H bond lengths of 1.14Å and 1.09Å, respectively, hydrogen atom H_{1bb} is 2.96Å away from C_{3h} and points directly at it (the B_1-H_{1bb}···C_{3h} angle is 177°). Hydrogen atom H_{3bb} is 2.31Å away from hydrogen atom H_{3c} and 2.91Å away from C_{3e}. Both of these separations are less than or equal to the respective sums of van der Waals[10] radii: 1.2Å for hydrogen, 1.5Å for nitrogen and 1.7Å for carbon. Interligand H···H, N···H and C···H contacts equal to or less than the van der Waals values of 2.4Å, 2.7Å and 2.9Å, respectively, also exist between the THF ligand and adjacent pyrazolyl rings: H_{2sa}···C_{3h}, 2.80Å; H_{2sa}···N_{2h}, 2.68Å; H_{2sb}···C_{3g}, 2.90Å; and H_{5sa}···C_{3a}, 2.71Å. Pyrazolyl hydrogen atom H_{3b} is also involved in two short interligand contacts: H_{3b}···N_{2e} at 2.77Å and H_{3b}···C_{3c} at 2.83Å. Shortening the three long U-N bonds and/or the two long N···N polyhedral edges would make all of these short contacts even shorter.

Steric factors thus appear to be playing a significant role in weakening the agostic U···H-B bonding interactions in **14** relative to **16**. The U(III) ion in **14** maintains strong bonding interactions with the $H_2B(pz)_2^-$ nitrogens and the THF oxygen at the expense of the agostic B-H···U bonds. It is interesting to note that if the total elongation experienced by the agostic U···H bonds (~0.6Å) on going from **16** to **14** is distributed equally over all ten U··· ligand bonds in **14**, a more normal lengthening would be observed for the U-N bonds.

4.3. Conclusions

The nature of U[H(μ-H)B(pz)$_2$]$_3$(THF) (**14**) and U[H(μ-H)B(3,5-Me$_2$pz)$_2$]$_3$ (**16**) complexes underscores the role that steric effects play in the coordination chemistry of the f-elements. Use of the sterically less-demanding $H_2B(pz)_2^-$ ligands allows THF coordination in **14**. It is noteworthy that with the smaller Y(III) center both ligands give the same tris-chelate complex, Y[H(μ-H)B(pz')$_2$]$_3$. It is also interesting that despite the

presence of coordinated THF, complex **14** maintains three agostic B-H⋯U bonds. Not surprisingly the strength of these interactions is weaker in **14** than in **16**. The coordinated THF ligand is not firmly anchored in complex **14** and the THF-free complex, U[H(μ-H)B(pz)$_2$]$_3$ (**15**) is also readily available. This apparent solution lability may allow the synthesis of various U[H$_2$B(pz)$_2$]$_3$(L) complexes and to study the steric and electronic effect of these ligands on the strength of the agostic B-H⋯U bonding.

4.4. Experimental Section

4.4.1. Preparation of Starting Material

The ligand KH$_2$B(pz)$_2$ was prepared according to published methods.[11]

4.4.2. Synthesis of the Complexes

U[H(μ-H)B(pz)$_2$]$_3$(THF) (14)

To a slurry of UI$_3$(THF)$_4$ (183 mg, 0.202 mmol) in THF (4 mL) was added a solution of KH$_2$B(pz)$_2$ (113 mg, 0.606 mmol) in THF (2 mL). The mixture was stirred for two hours. Inverse filtration through a cannula gave a dark red solution and almost quantitative white precipitate of KI. The THF solvent was removed under vacuum and the residue was washed with hexane (2 mL). Complex **14** was isolated as a dark, almost black solid in 73% yield. Crystals could be obtained by redissolving in Et$_2$O (4 mL) and cooling the concentrated solution at -40°C for a few days. IR (KBr, cm^{-1}): v(B-H) 2430; 2283, 2251. ^{1}H NMR (toluene-d$_8$, 23°C, δ ppm): 21.02, 10.01, 9.57 (*H*, pz), 1.67, 0.82 (C*H$_2$*, THF). ^{11}B NMR (toluene-d$_8$, 23°C, δ ppm): -19.2. Anal. Calc. for C$_{22}$H$_{32}$N$_{12}$B$_3$OU: C, 35.18; H, 4.29; N, 22.38. Found: C, 35.05; H, 4.55; N, 21.85.

U[H(μ-H)B(pz)$_2$]$_3$ (15)

Complex **14** was dissolved in toluene (1mL) and the solvent was removed under vacuum, the process was repeated twice. The residue was triturated with hexane (2mL)

and dried under vacuum. Complex 15, black solid was obtained in 66% yield. IR (KBr, cm^{-1}): v(B-H) 2432; 2292, 2238 . ^{1}H NMR (toluene-d$_8$, 23°C, δ ppm): 23.73, 11.23, 11.05 (H, pz). ^{11}B NMR (toluene-d$_8$, 23°C, δ ppm): -21.5. Anal. Calc. for C$_{18}$H$_{24}$N$_{12}$B$_3$U: C, 31.84; H, 3.56; N, 24.76. Found: C, 32.36; H, 3.44; N, 23.94.

4.4.3. Variable Temperature ^{1}H NMR NMR Spectroscopic Studies

Due to the presence of paramagnetic U(III) center the ^{1}H chemical shifts are temperature dependent. The chemical shifts of the μ-BH and BH protons of complex 2 in the absence of exchange at the coalescence temperature were calculated from a plot of δ(ppm) *versus* 1/T; ^{1}H NMR (toluene-d$_8$, δ ppm) (253 K): 29.31 (μ-B-H), 1.10 (B-H); (213 K) 33.36 (μ-B-H), 1.24 (B-H); (203 K): 34.90 (μ-B-H), 1.39 (B-H); (193 K): 36.65 (μ-B-H), 1.59 (B-H). The relevant data are: coalescence temperature (T$_c$) 40±10°C (313 K); δ(ppm) 24.75 (μ-BH), 0.78 (BH) and δv = 9600 Hz. The free energy of activation based on the formula $\Delta G_c^{\ddagger}$ = 1.914×10^{-2} T [9.972 + log (T/δv)] kJ/mol^{12} is 51 kJ/mol.

4.4.4. Crystallographic Analysis.

Single crystals of U[H(μ-H)B(N$_2$C$_3$H$_3$)$_2$]$_3$(OC$_4$H$_8$) (14) were obtained by cooling Et$_2$O solution at -40°C slowly. The intensity data were corrected empirically for variable absorption effects using ψ scans for 6 reflections having 2θ(MoK$_{\bar{\alpha}}$) between 8.64° and 25.64°. Even though it was possible to locate the hydrogens on all three boron atoms from difference Fourier syntheses and satisfactorily vary their positions in least-squares refinement cycles, their refined positions gave a sufficiently distorted geometry at the borons that it was decided to place the hydrogens at idealized sp^3-hybridized positions with a B-H bond length of 1.01Å and only refine their isotropic thermal parameters.

Table 4.3 Crystallographic Data for $U[H(\mu\text{-}H)B(pz)_2]_3(THF)$ (**14**)

molecular formula	$U[H(\mu\text{-}H)B(N_2C_3H_3)_2]_3(OC_4H_8)$
molecular weight	751.06
color of crystal	black
crystal system	monoclinic
space group	$P2_1/c$ - C_{2h}^5 (No. 14)
cell dimensions	
a (Å)	10.662(2)
b (Å)	13.586(3)
c (Å)	20.868(6)
β (°)	103.32(2)
Z	4
volume(Å^3)	2941(1)
calculated density (g cm^{-3})	1.696
wavelength (Å)	0.71073
linear absorption coefficient (mm^{-1})	5.56
empirical absorption correction	ψ scans for 6 reflections
scan type	ω
2θ range	3.0-50.8
temperature	20°C
total no. reflections collected	5564
No. unique reflections	5396
R	0.042
Rw	0.049
GOF	1.100
data to parameter ratio	9.2:1

4.5. References

(1) Trofimenko, S. *Chem. Rev.* 1993, *93*, 943.

(2) Domingos, A.; Leal, J. P.; Marcalo, J.; Marques, N.; Kanellakopulos, B.; Maier, R.; Apostolidis, C. .; Simoes, J. A. M. *Eur. J. Solid State Inorg. Chem.* 1991, *28*, 413.

(3) Reger, D. L.; Lindeman, J. A.; Lebioda, L. *Inorg. Chem.* 1988, *27*, 1890.

(4) Carvalho, A.; Domingos, A.; Gaspar, P.; Marques, N.; Pires de Matos, A.; Santos, I. *Polyhedron* 1992, *11*, 1481.

(5) Sun, Y.; Takats, J.; Eberspacher, T.; Day, V. *Inorg. Chim. Acta* 1995, *229*, 315-322.

(6) Marks, T. J.; Kolb, J. R. *J. Am. Chem. Soc.* 1975, *97*, 27.

(7) Cotton, F. A.; Frenz, B. A.; Murillo, C. A. *J. Am. Chem. Soc.* 1975, *87*, 2118.

(8) Shannon, R. D. *Acta Crystallogr.* 1976, 751.

(9) Clark, D. L.; Sattelberger, A. P.; Bott, S. G.; Vrtis, R. N. *Inorg. Chem.* 1989, *28*, 1771-1773.

(10) Pauling, L. In *The Nature of the Chemical Bond*; Third ed.Cornell University Press: Ithaca, New York, 1960; pp 260.

(11) Trofimenko, S. *J. Am. Chem. Soc.* 1967, *89*, 3170.

(12) Sandstrom, J. *Dynamic NMR Spectroscopy*; Academic Press: London, 1982, pp 96.

Chapter 5

Chemical Behavior of a Klaui Ligand towards
U(III) Metal Center

5.1. Introduction

In Chapter 3, it was shown that the tripodal, six-electron nitrogen-donor hydrotris(pyrazolyl)borate ligands are capable of stabilizing U(III) complexes, allowing the isolation of a series of highly reactive complexes containing U-C and U-N σ bonds. Similar Sm(II) and Yb(II) compounds have also been prepared in our laboratory.[1]

In 1978 Klaui[2] reported the synthesis of the oxygen donor ligands, $[(\eta^5\text{-Cp})Co\{P(=O)(OR)_2\}_3]^-$, designated as L_{OR}, which may be considered electronically and geometrically analogous to the $Tp^{R,R'}$ ligand system because they are both 6-electron tripodal ligands with C_{3v} symmetry. However, their positions in the spectrochemical series[3] are quite different; Klaui ligands[4] occupy a low position next to F^-, while the $Tp^{R,R'}$ ligands[5] are moderately strong field ligands comparable to 1,10-phenanthroline. Klaui ligands have been used widely in the synthesis of a great number of transition metal complexes in various oxidation states; from low valent organometallic complexes, such as $Cu(L_{OR})CO$ and $Cu(L_{OR})(CH_2CH_2)$ (R=Me, Et, and ^iPr)[6] to high oxidation state compounds, $M(L_{OMe})O_3$ (M=Re, Tc).[7] However, the application of these ligands to f-element chemistry has received scant attention. Klaui[8] was the first to introduce his ligands to f-element chemistry. Reaction of LnX_3 (X=Cl$^-$, NO$_3^-$) with 2 equiv of HL_{OR} (R=Me, Et) in aqueous solution gave, after anion exchange, $[Ln(L_{OR})_2]Y$ (Ln=La, Eu, Pr; Y=BF$_4^-$, BPh$_4^-$). Nolan et al.[11] found that under anaerobic conditions the reaction of YCl$_3$ with 2 equivalents of NaL$_{OEt}$ gave the dimeric complex, $[(L_{OEt})Y(III)(CpCo\{P(=O)(OEt)_2\}_2\{P(=O)(OEt)(O)\})]_2$. The successful synthesis of the first uranium complexes, $U(L_{OEt})_2Cl_2$ and $U(L_{OEt})Cl_3(THF)$, via simple metathesis

reaction of UCl_4 with NaL_{OEt} was reported independently by two research groups.[9,10] U(III) complexes have not been reported to date.

It was of interest to synthesize U(III) complexes with the Klaui ligand that are analogous to the Tp^{Me2} derivatives and to compare their structures and chemical reactivities. In this chapter are reported the results of the reaction of the Klaui ligand, L_{OEt}, with $UI_3(THF)_4$.

5.2. Results and Discussion

5.2.1. Reactions of $UI_3(THF)_4$ with Anhydrous NaL_{OEt}

The reaction of $UI_3(THF)_4$ with one equivalent of NaL_{OEt} in THF proved to be complicated. The color of the solution changed from dark blue to brown upon addition of the ligand. Removal of the solvent, followed by extraction with toluene gave almost quantitative precipitation of NaI, seemingly indicating that the metathesis reaction proceeded as expected. Diffusion of hexane into the brown toluene solution resulted in the formation of brownish yellow, needle-like crystals together with some brownish powder. Upon drying, the crystals lost their shape and luster and became powdery. The ^1H NMR spectrum of the powder could not be interpreted. Due to these difficulties no further work was carried out with the 1:1 reaction.

The reaction of $UI_3(THF)_4$ with two equiv of NaL_{OEt} was carried out in the same way and proceeded with similar color changes. After similar work-up, cooling a toluene solution at -40°C gave only an oily material. However, cooling a very concentrated, syrup -like toluene solution at -40°C gave green crystals (17). The difficulty in separating the crystals from the thick syrup may be one of the reasons for the low yield (24%). The green color of the product, more typical for a U(IV) complex, was disturbing.

Characterization of the product proved problematic. The ^{31}P and ^1H NMR spectra are shown in Fig. 5.1. On the basis of our experience with $U(Tp^{Me2})_2I$, a simple "$U(L_{OEt})_2I$" complex was expected to be fluxional and to show a single line in the ^{31}P
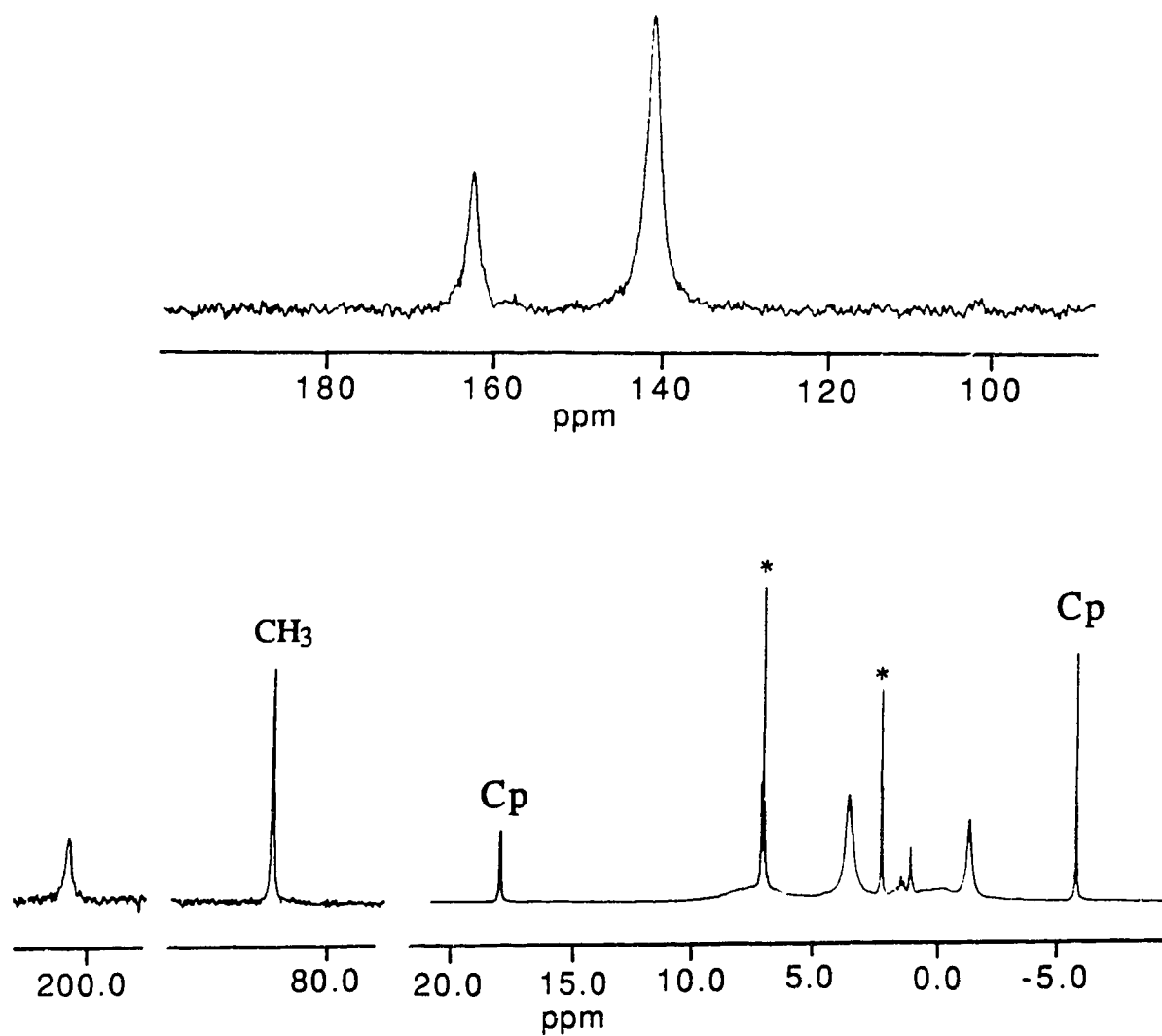
Fig. 5.1 ^{31}P and ^1H NMR Spectra of Product 17

NMR spectrum and three signals in a 5:12:18 ratio ($Cp:6CH_2:6CH_3$) in the ^1H NMR spectrum, respectively. The appearance of two signals in a 2:1 ratio in the ^{31}P NMR spectrum was clearly not consistent with a time-averaged symmetrical " $U(L_{OEt})_2I$" species, and pointed to either a rigid C_{2v} symmetrical structure or a mixture of two products. The ^1H NMR spectrum ruled out the former possibility. The spectrum at room temperature showed two sharp peaks at -5.84 and 17.95 ppm in a 2:1 ratio, two small peaks at very low field, 82.20 and 200.72 ppm in a 3:2 ratio, and five featureless broad signals at 7.5, 3.4, 0.1, -0.5, and -1.5 ppm. The sharp peaks at -5.84 and 17.95 ppm are most reasonably assigned to the Cp protons of the Klaui ligand; the appearance of two signals is not compatible with the rigid C_{2v} symmetric structure where both Cp rings would still be equivalent. The ratio of these two peaks is the same as the ^{31}P NMR signals and implies that the product is a mixture of two compounds in a 2:1 ratio. The very low field signals were unexpected for a U(III) complex, as was the green color.

In an attempt to get a better handle on the situation we decided to abstract iodide from the *in situ* generated product of the 1:2 reaction. As mentioned in Chapter 2, $U(Tp^{Me2})_2I$ reacted readily with $TlBPh_4$ to form the cationic complex, $[U(Tp^{Me2})_2THF][BPh_4]$, which was easily crystallized. We hoped the same strategy would help with the Klaui ligand as well.

Addition of $TlBPh_4$ to a THF solution containing one equiv of $UI_3(THF)_4$ and two equiv of NaL_{OEt} caused immediate precipitation of yellow TlI. Filtration followed by cooling the THF solution at -40°C gave a grass-green crystalline product (18).

The ^1H NMR spectrum of compound 18 (Fig. 5.2) shows a sharp peak at 13.64 ppm, one triplet at 0.22 ppm, two equal intensity broad signals at 3.10 and 2.77 ppm, a set of three multiplets at 7.14, 6.69, and 6.54 ppm in a 2:2:1 ratio, and two multiplets near the solvent peaks of THF-d_8 indicating that THF is also coordinated to the uranium metal center. The sharp resonance at 13.64 ppm is assigned to the Cp protons while the triplet (0.22 ppm) and the two broad signals (3.10 and 2.77 ppm) are due to the methyl and
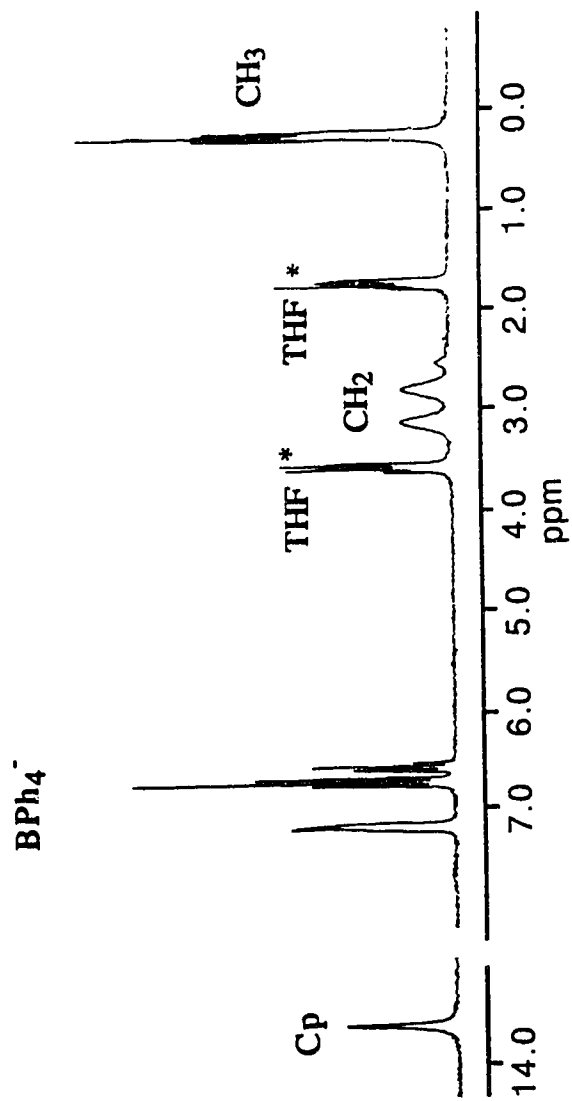
Fig. 5.2 ^{1}H NMR Spectrum of [U(L$_{-OEt}$)$_2$(THF)$_2$][BPh$_4$]$_2$ (18) (THF-d$_8$, 24°C)

methylene protons of L_{OEt}, respectively. The peaks at 7.14, 6.69 and 6.54 ppm, with the requisite 2:2:1 ratio, are assigned to BPh_4^-. The single resonance seen in the ^{31}P and ^{11}B NMR spectra is also consistent with a pure and symmetrical product. Integration of the ^1H NMR spectrum reveals that there are two BPh_4^- counter ions per uranium complex. Thus, during the reaction, uranium was oxidized from the +3 to the +4 oxidation state. This is consistent with the characteristic green color of the crystals. Because there was no Tl metal formed in this reaction it is reasonable to postulate that the redox reaction occurred between $UI_3(THF)_4$ and NaL_{OEt}. The nature of the reduction product is not known.

Although the iodide abstraction reaction clearly showed that oxidation complicates the reaction of $UI_3(THF)_4$ and NaL_{OEt}, it did not clarify the nature of the previously observed mixture. To resolve this issue and to corroborate the NMR deduction the structures of **17** and **18** were determined by single crystal X-ray diffraction.

5.2.2. Crystal Structural Analysis

Perspective views of the molecular structures of complexes **17** and **18** are shown in Fig. 5.3 and 5.4, respectively. Selected bond distances and angles are given in Table 5.1. It is immediately clear that both compounds contain eight-coordinate uranium metal centers with two η^3-Klaui ligands. The analysis also show that the oxidation state of uranium in both complexes is +4.

The structure of compound **17** is C_2 related. In the crystal lattice the I^- and EtO^- ligands are disordered over the two C_2-related coordination sites. The refined values of the occupancy factors for the nonhydrogen atoms of the I^- and EtO^- ligands indicate that 64.9% of the sites are occupied by I^- and 35.1% by EtO^-. The real chemical composition of the crystals could not be determined by X-ray diffraction analysis. In the structure of **18**, besides two η^3-L_{OEt} ligands there are two coordinated THF molecules.

The simplified inner coordination diagram of complex **18** is shown in Fig. 5.5. The coordination geometry is best described as a square anti-prism; the two square faces
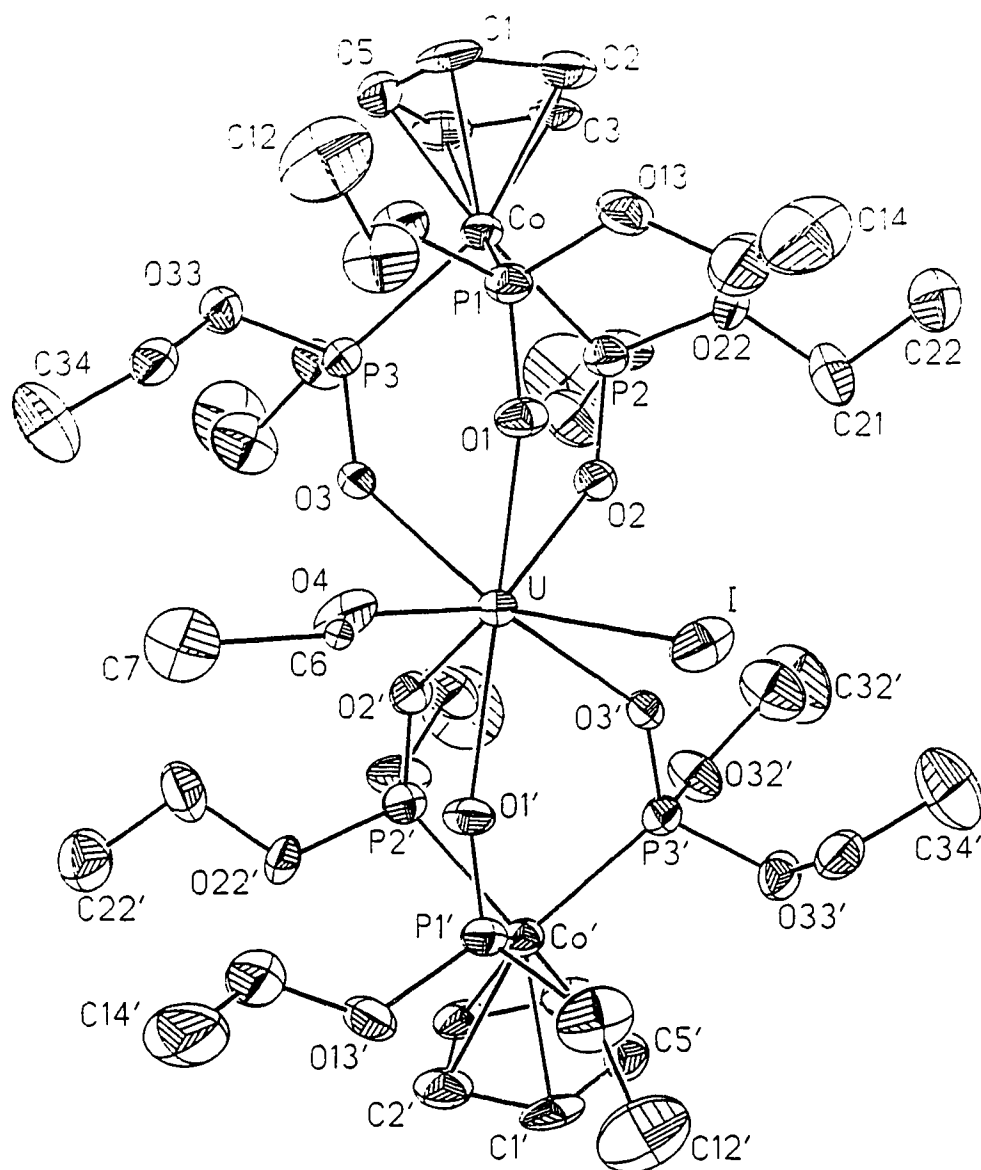
Fig. 5.3 Molecular Structure of U(L_OEt)_2(OEt)I/U(L_OEt)_2I_2 (17)
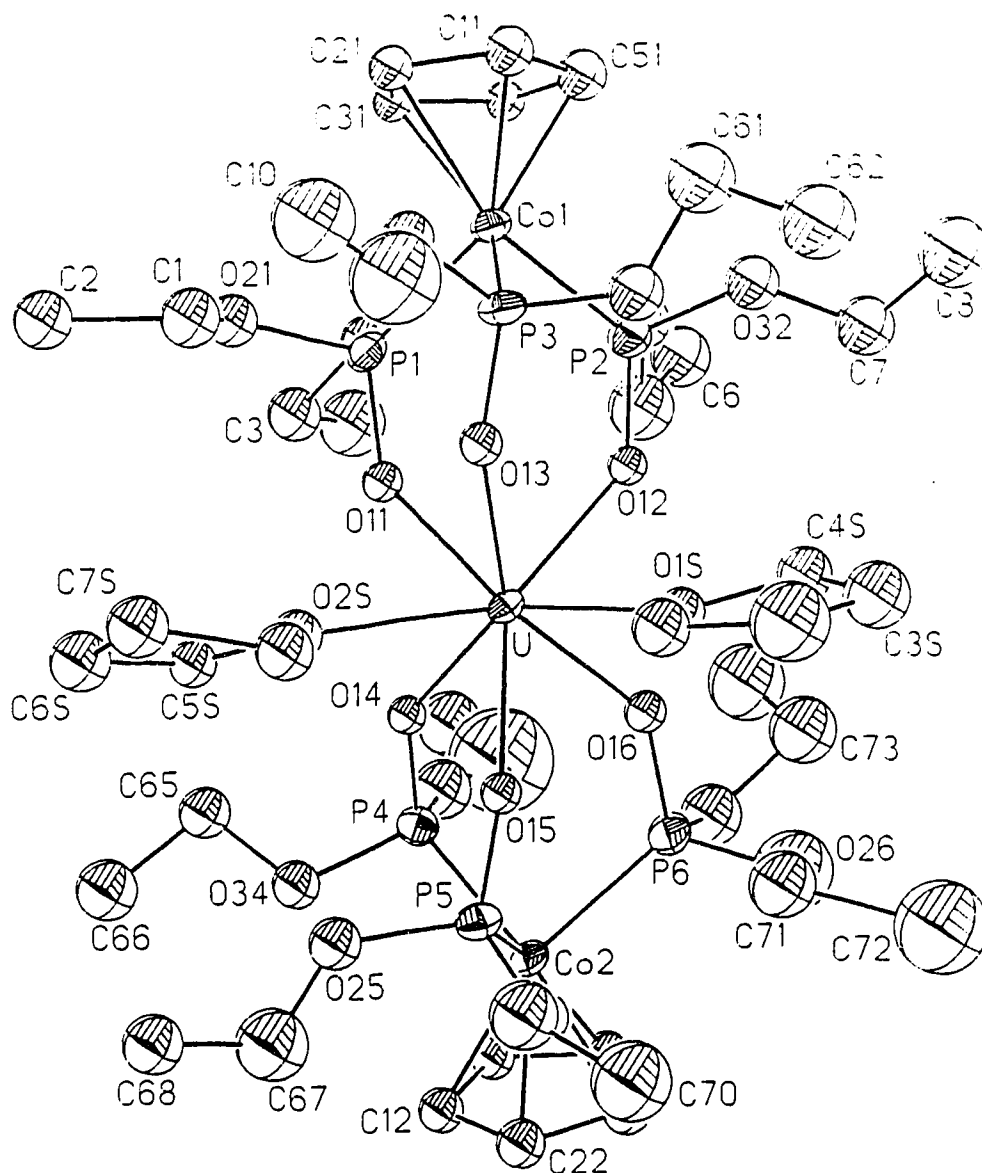
Fig. 5.4 Molecular Structure of [U(L$_{OEt}$)(THF)$_2$]$^{2+}$ (18)
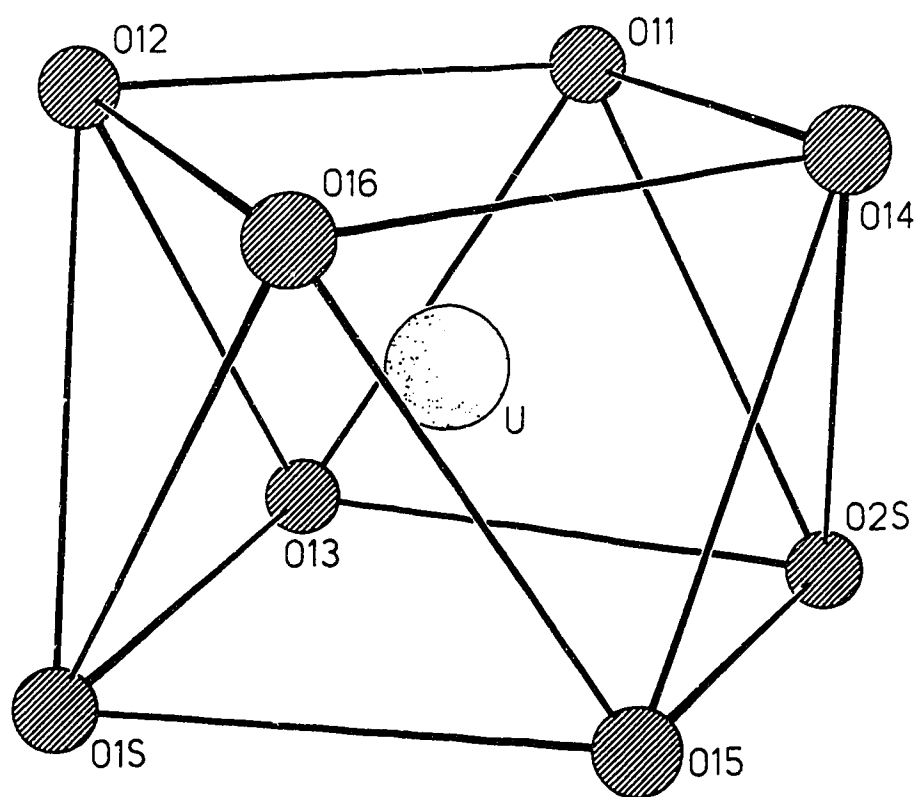
Fig. 5.5 Inner Coordination Geometry of $[U(L_{OEt})_2(THF)_2]^{2+}$ (18)

(O1s, O13, O2s, and O15) and (O11, O12, O16, and O14) are nearly coplanar to within ±0.064Å and ±0.062Å, respectively and the angle between the two planes is only 1.1°. The regularity of the geometry is also manifested by the almost equal angles of O1s-U-O2s, O13-U-O15, O11-U-O16, and O12-U-O14 (112.7(7), 112.8(6), 121.9(7), and 115.2(6)°). The uranium atom is 1.347 and 1.162Å from these two planes, respectively. Like compound **18**, complex **17** is also eight-coordinate. Due to the structural similarity between the two complexes, a first quick glance seems to indicate that complex **17** also adopts the same square anti-prismatic geometry. However, the structural parameters indicate that this is not the case. The larger size and the ensuing steric congestion caused by the iodide ligand are the reasons for the distortion. In order to minimize the repulsion, the two L_{OEt} ligands bend and twist away from iodide. The order of the Co-U-Co' angles, 137.7(1)° (**17**) < 141.90° (U(L_{OEt})$_2$Cl$_2$) < 155.8° (**18**), is consistent with this analysis and the widely different angles defining the "square anti-prism" of complex **17**, I-U-O4, O1-U-O1', O2-U-O2', and O3-U-O3' (94.1(7), 139.2(4), 87.3(4), and 128.7(4)°), are evidences of the distortion.

The average U-O$_{L_{OEt}}$ distance in compound **17** (2.384(5)Å) is longer than in compound **18** (2.31(2)Å), but is similar to the average U-O$_{L_{OEt}}$ bond length in U(L_{OEt})$_2$Cl$_2$ (2.36(3)Å), although the range of U-O$_{L_{OEt}}$ bond lengths is large in the latter complex. The shorter U-O$_{L_{OEt}}$ distance in complex **18** can be explained by the higher charge of the complex which increases the Lewis acidity of uranium and results in shorter U-O$_{L_{OEt}}$ bond lengths. A similar trend can be seen in the U···Co distances, 4.460(3)Å (**17**) > 4.436Å (U(L_{OEt})$_2$Cl$_2$) > 4.325Å (**18**), and indicates that the coordination around uranium is the most crowded in compound **17** and the least in compound **18**; a conclusion which is in agreement with the previous discussion and with the long U-I bond distance in compound **17**. The distance, (3.275(3)Å), is ca. 0.14Å longer than the U-Cl bond distance in complex U(L_{OEt})$_2$Cl$_2$ after correcting for the ionic radii difference between I⁻ and Cl⁻.

Table 5.1 Selected Bond Distances (Å) and Angles for Complexes 17 and 18

	17		18
Bond Distances			
U-O1	2.387(8)	U-O11	2.300(15)
U-O2	2.387(9)	U-O12	2.316(16)
U-O3	2.378(7)	U-O13	2.316(20)
U-O	2.384(5)*	U-O14	2.283(19)
U-O4	2.099(27)	U-O15	2.292(14)
U-I	3.275(3)	U-O16	2.325(18)
		U-O	2.305(16)*
		U-O1s	2.486(20)
		U-O2s	2.581(20)
Bond Angles			
O1-U-O2	73.4(3)	O1-U-O2	75.8(6)
O1-U-O3	73.1(3)	O1-U-O3	75.5(6)
O2-U-O3	73.1(3)	O2-U-O3	78.4(6)
		O4-U-O5	77.9(6)
I-U-O4	94.1(7)	O4-U-O6	74.4(6)
O1-U-O1'	139.2(4)	O5-U-O6	76.6(6)
O2-U-O2'	87.3(4)		
O3-U-O3'	128.7(4)	O1s-U-O2s	112.7(7)
		O13-U-O15	112.8(6)
		O12-U-O14	115.2(6)
		O11-U-O16	121.9(7)

* Averaged bond length

5.2.3. Chemical Confirmation of Compound 17

The X-ray structural analysis of compound **17** could only provide information about the ratio of I^- and EtO^- in the crystal lattice. The actual composition, whether a mixture of $U(L_{OEt})_2I_2/U(L_{OEt})_2(OEt)_2$ or $U(L_{OEt})_2I_2/U(L_{OEt})_2(OEt)I$, could not be determined unambiguously by X-ray analysis. To ascertain the chemical composition by spectroscopic means the compounds $U(L_{OEt})_2I_2$ (**19**) and $U(L_{OEt})_2(OEt)_2$ (**20**) were synthesized.

The preparation of the complexes is straightforward. Simple metathesis of $U(L_{OEt})_2Cl_2$ with excess NaI gives $U(L_{OEt})_2I_2$ (**19**), eq. 5.1, which could be easily

$$U(L_{OEt})_2Cl_2 \ + \ 2NaI(excess) \ \xrightarrow[\text{r.t.}]{\text{THF}} \ U(L_{OEt})_2I_2 \ + \ 2NaCl \qquad 5.1$$
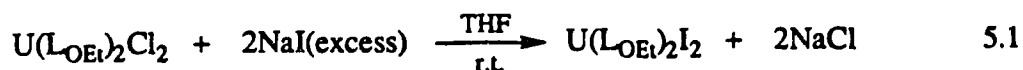
19 (olive crystals)

separated from NaCl and excess NaI by toluene extraction. Cooling the toluene solution at -40°C gave olive crystals in 31% yield. Reaction of $U(L_{OEt})_2Cl_2$ with 2 equiv of NaOEt in THF (eq. 5.2) gave light green crystals of $U(L_{OEt})_2(EtO)_2$ (**20**) in 71% yield by hexane extraction and cooling the hexane solution at -40°C.

$$U(L_{OEt})_2Cl_2 \ + \ 2NaOEt \ \xrightarrow[\text{r.t.}]{\text{THF}} \ U(L_{OEt})_2(OEt)_2 \ + \ 2NaCl \qquad 5.2$$
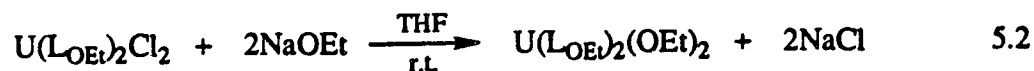
20 (light green crystals)

The ^{31}P NMR spectra of compounds **19** and **20** are shown in Fig. 5.6 and display single peaks at 163.3 and 114.0 ppm , respectively.

The composition of the mixture was elucidated by comparing the ^{31}P NMR spectra of the different products. This NMR probe was chosen because of the simplicity of the spectra. As mentioned above the ^{31}P NMR spectrum of complex **19** displays a single peak at 163.3 ppm. This peak corresponds to one of the signals seen in the ^{31}P NMR spectrum of the mixture **17**. However, the other signal in the mixture at 141.2 ppm does not

Crystals (17) from $UI_3(THF)_4$ + $2NaL_{OEt}$

$U(L_{OEt})_2I_2$ (19)

$U(L_{OEt})_2(OEt)_2$ (20)

$2U(L_{OEt})_2I_2$ + $(U(L_{OEt})_2(OEt)_2$

180   160   140   120   100
                        ppm

$U(L_{OEt})_2I_2$ $U(L_{OEt})_2(OEt)I$
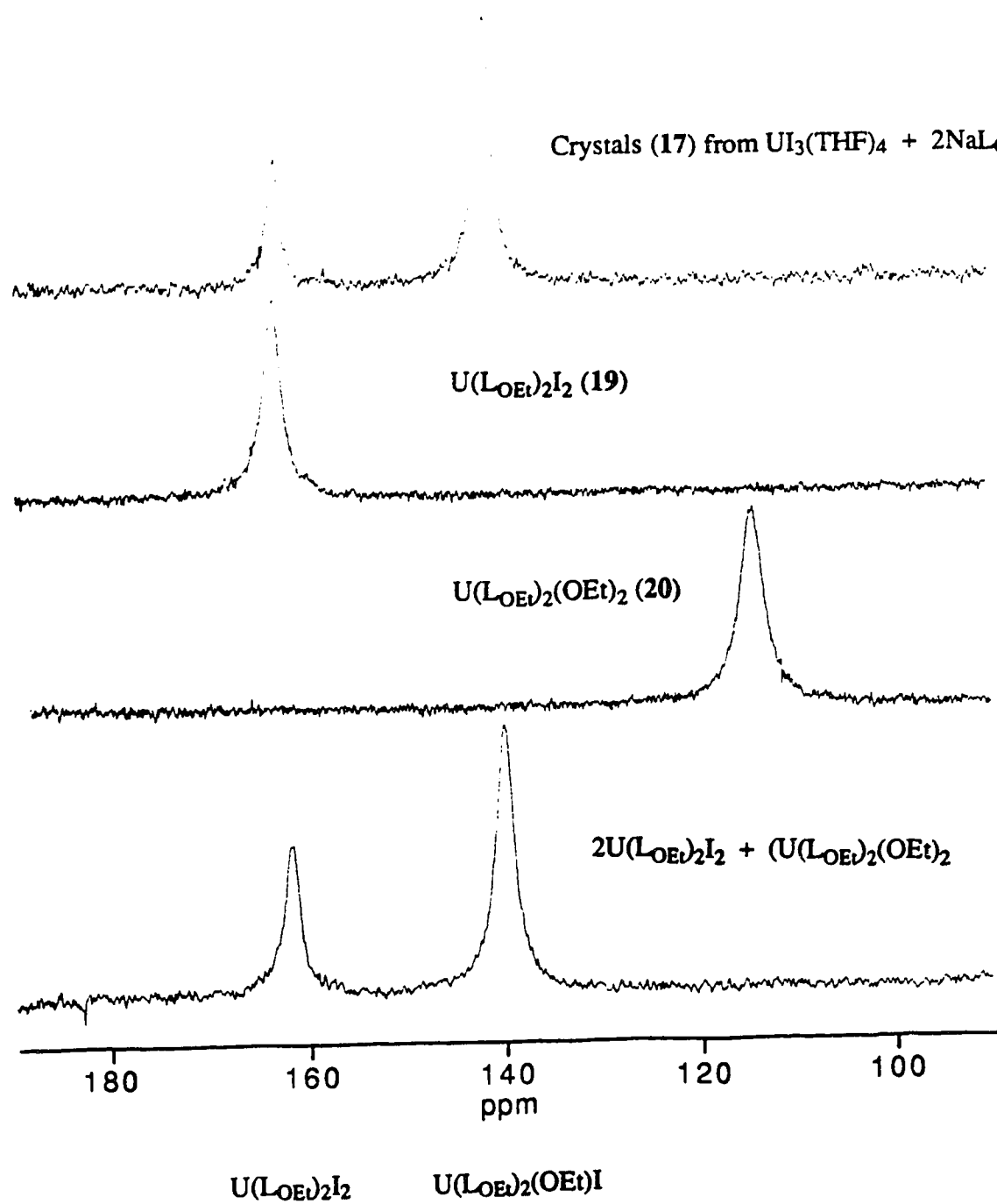
Fig. 5.6 ^{31}P NMR Spectral Characterization of Complex 17

correspond to the 114.0 ppm resonance of complex **20**. Therefore, at this point it was clear that complex **17** was not a mixture of $U(L_{OEt})_2I_2/U(L_{OEt})_2(OEt)_2$, but it contained $U(L_{OEt})_2I_2$. In an attempt to find the missing peak, complexes **19** and **20** were mixed. When half equiv of **20** was added to **19** the intensity of the ^{31}P NMR resonance of the latter decreased while that of complex **20** disappeared, simultaneously a new peak appeared at 141.2 ppm (Fig. 5.6). The ^1H NMR spectrum was consistent with ^{31}P NMR spectrum. The NMR observations clearly show a ligand exchange process as illustrated in eq. 5.3.

$$2U(L_{OEt})_2I_2 + U(L_{OEt})_2(OEt)_2 \longrightarrow 2U(L_{OEt})_2I(OEt) + U(L_{OEt})_2I_2 \qquad 5.3$$
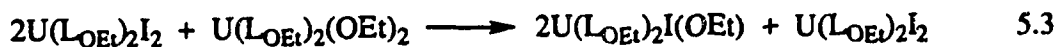
The new ^{31}P NMR resonance is due to the ligand exchange product $U(L_{OEt})_2(EtO)I$ (**21**). The ^{31}P NMR spectrum matches that of complex **17** and therefore shows that the product is a 2:1 mixture of $U(L_{OEt})_2(OEt)/IU(L_{OEt})_2I_2$.

Not surprisingly, when $U(L_{OEt})_2Cl_2$ and $U(L_{OEt})_2(EtO)_2$ were mixed a similar ligand redistribution process to form $U(L_{OEt})_2(EtO)Cl$ occurred.

5.2.4. Reaction of $UI_3(THF)_4$ with Hydrated NaL_{OEt}

Since redox reaction and formation of a mixture of $U(L_{OEt})_2I_2/U(L_{OEt})_2(OEt)I$ complicated the reaction of $UI_3(THF)_4$ with 2 equiv of anhydrous NaL_{OEt}, it was decided to examine the reaction with hydrated Klaui ligand as well. We did not expect elimination of the redox reaction behavior, but we were hoping that formation of a mixture and cleavage of P-OEt bond could perhaps be avoided.

The reaction of $UI_3(THF)_4$ with two equiv of hydrated NaL_{OEt} was carried out in the same way as the anhydrous reaction. A color change from blue to green was observed, different from the brown color seen previously. The ^{31}P NMR spectrum of the crude solid after separation of NaI indicated that the main component was $U(L_{OEt})_2I_2$, (**19**), one of the products of the reaction with the anhydrous ligand. The ^1H NMR spectrum was consistent

with the ^{31}P NMR spectrum. However, storing the solution at room temperature in the dry-box overnight resulted in the formation of green crystals (22), which were only soluble in CH_2Cl_2 and were insoluble in toluene, and hexane, and even in THF. The solubility behavior suggested that this compound was different from any of the products obtained from the anhydrous Klaui reaction.

The ^1H NMR spectrum recorded in CD_2Cl_2 was complicated, displaying many peaks, and could not be assigned. The ^{31}P NMR spectrum (Fig. 5.7) displayed four inequivalent phosphorus resonances, one single peak and three triplets in a ratio of 3:1:1:1. This could be interpreted as one L_{OEt} ligand with C_{3v} symmetry and one L_{OEt} ligand with no symmetry around the uranium metal center.
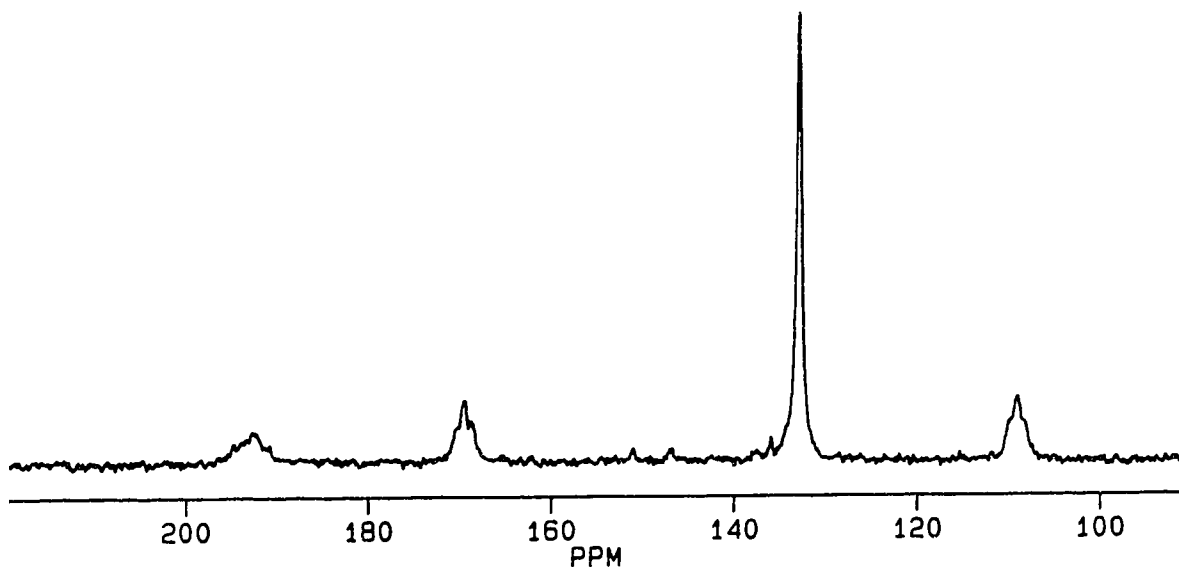
Fig. 5.7 ^{31}P NMR Spectrum of Complex 22 (CD_2Cl_2, 24°C)

5.2.5. X-ray Structural Analysis

A single-crystal X-ray diffraction analysis was carried out to establish the molecular structure of complex 22. A perspective view of the molecular structure is shown in Fig 5.8, which also defines the atomic labelling scheme. Selected bond distances and angles
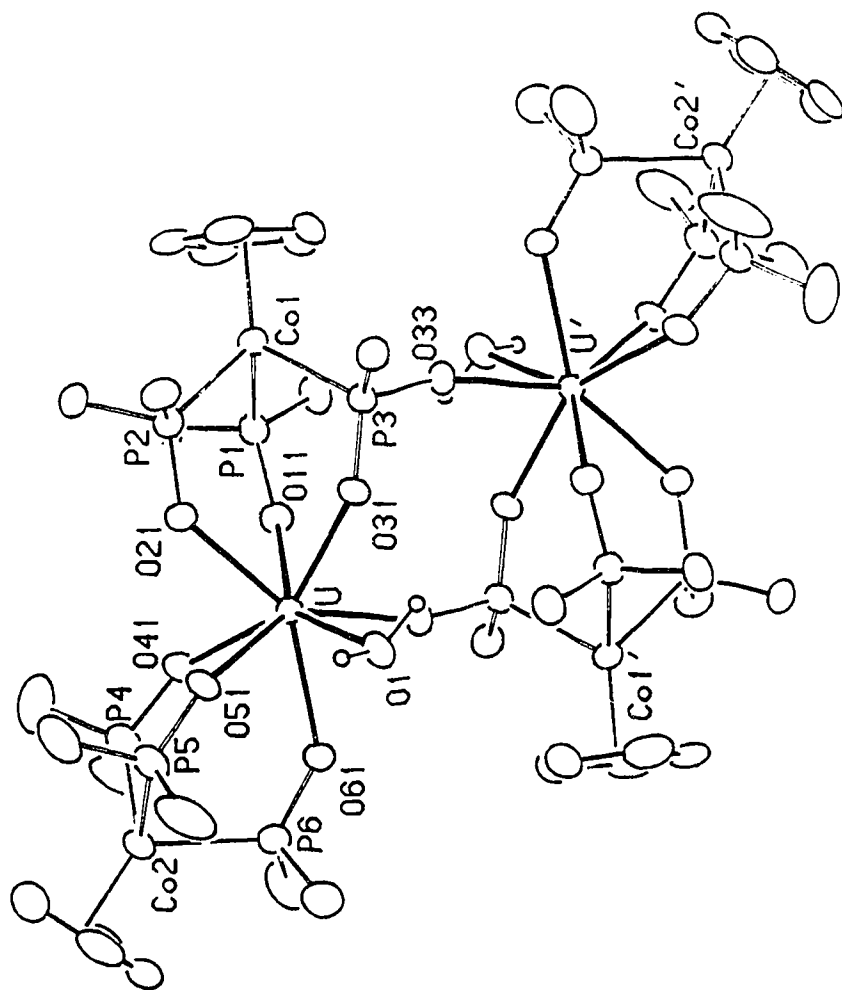
Fig. 5.8 Molecular Structure of [(L$_{OEt}$)U(CpCo{P(=O)(OEt)$_2$}$_2${P(=O)(OEt)(O)})(H$_2$O)]$_2^{2+}$ (22); the Et groups have been omitted from the P(OEt) moieties for clearity

are given in Table 5.2. Surprisingly, the molecule consists of a dimeric arrangement of two eight-coordinate U(IV) centers, which is symmetrical about an inversion center. One Klaui ligand is intact and interacts with the U(IV) metal center via three O donor in an η^3-fashion; the other ligand experienced a cleavage of a phosphonate ethyl groups (O33), making possible the dimeric linkage. A similar structure has been observed by Nolan and coworkers[11] where the metal center is Y(III). The geometry for the inner coordination around uranium is best described as square anti-prism. A simplified diagram of the coordination geometry for compound 22 is shown in Fig. 5.9. The two square faces (O1, O31, O21, and O51) and (O11, O33', O61, and O41) are nearly coplanar to within ±0.076Å and ±0.035Å, respectively. The U atom is 1.305(3) and 1.213(3)Å from these planes, respectively.
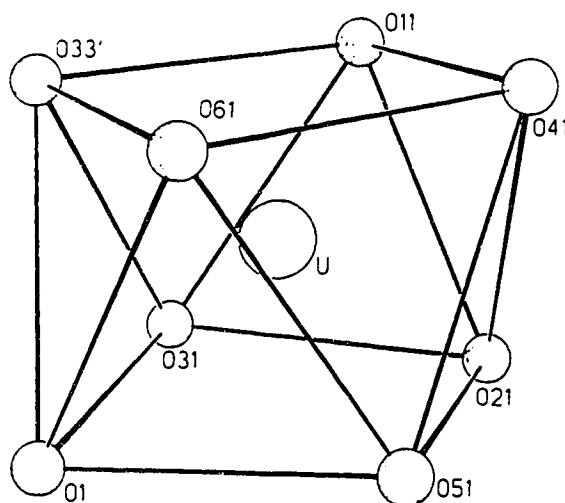
Fig. 5.9 Inner Coordination Geometry of Complex 22

Although the similarity of the structural frame-work between compound 22 and $[(L_{OEt})Y(III)(CpCo\{P(O)(OEt)_2\}_2\{P(=O)(OEt)(O)\})]_2$ is obvious the uranium complex is eight coordinate with one extra H_2O ligand coordinated to U(IV) ion while Y(III) is only seven coordinate. The larger ionic radius of U(IV) is the obvious reason for this

Table 5.2 Selected Bond Lengths (Å) and Angles for 22

Bond Lengths			
U-O11	2.335(6)	U-O21	2.367(6)
U-O31	2.290(6)	U-O41	2.361(7)
U-O51	2.345(6)	U-O61	2.412(7)
U-O$_{ave}$	2.35(4)	U-O33'	2.265(6)
U-O$_{H_2O}$	2.509(7)		

Bond Angles			
O11-U-O21	75.0(2)	O11-U-O31	78.5(2)
O21-U-O31	73.1(2)	O41-U-O51	76.8(2)
O41-U-O61	71.8(3)	O51-U-O61	74.3(2)
O1-U-O21	110.9(2)	O31-U-O51	115.7(2)
O11-U-O61	120.2(2)	O41-U-O33'	114.4(2)

observation. The average Y-O bond distance (2.32(8) Å) in Yttrium complex is about the same as the average U-O bond distance in complex 22. However, the large spread of the M-O bond lengths in both compounds prevents attaching any significance to this comparison.

5.2.6. ^{31}P and ^{1}H NMR Spectra of Complex 22

With the knowledge of the solid state structure, the ^{31}P NMR spectrum could be easily interpreted. The resonance at 132.7 ppm with an integration of 3P is assigned to the terminal L$_{OEt}$ ligand. The appearance of an averaged signal for the three phosphorus atoms indicates facile rotation along the local C$_3$ axis. Due to the rigid bridge structure and the asymmetric nature of the U(IV) metal center, the three phosphorus atoms of the bridging

L_{OEt} are inequivalent, giving three apparent triplets due to P-P coupling. The ^{1}H NMR spectrum can be also assigned on the basis of the solid-state structure. Even though the terminal Klaui ligand rotates rapidly along the local C_3 axis, the asymmetry of the U(IV) metal center renders the two ethoxide groups on each phosphorus inequivalent, giving two equal intensity resonances for the methyl groups with an integration of 9H. Moreover, since the two methylene protons are diastereotopic, they show up as four peaks each with a 3H integration. Due to the rigid bridge structure, all the five ethoxide groups on the bridging Klaui ligand are inequivalent and result in five methyl resonances with an integration of 3H and ten peaks for methylene protons with 1H integration. The unique feature of the ^{1}H NMR spectrum for this complex is that, due to the paramagnetic U(IV) metal center, all the ^{1}H NMR resonances are well separated.

5.3. Conclusions

Reactions of $UI_3(THF)_4$ with the Klaui ligand, NaL_{OEt}, proved to be complicated, and were accompanied by oxidation of uranium from the +3 to the +4 oxidation state. Thus, unfortunately, U(III) complexes with Klaui ligand could not be prepared. Therefore, the structural and chemical reactivity comparison between the two ligand systems, Trofimenko and Klaui ligands, could not be made.

5.4. Experimental Section

5.4.1. Preparation of Starting Materials

Hydrated sodium salt of the Klaui ligand was obtained as a gift from F. T. Edlemann. The anhydrous sodium salt was obtained by dehydration of hydrated salt by stirring a toluene solution over 4Å molecular sieves for a few hours, followed by filtration and removal of toluene from the filtrate under vacuum. Complex $U(L_{OEt})_2Cl_2$ was prepared according to the published method.[9] The preparation of $UI_3(THF)_4$ and $TlBPh_4$

were described in the Experimental Section, Chapter 2. Solid NaOEt was prepared by reaction of EtOH with excess Na metal in THF followed by stripping off THF.

5.4.2. Synthetic Procedures

Reaction of $UI_3(THF)_4$ with 2 Equiv of Anhydrous NaL_{OEt}

A solution of NaL_{OEt} (305mg, 0.546mmol) in THF (6mL) was added dropwise to a slurry of $UI_3(THF)_4$ (248mg, 0.273mmol) in THF (6mL). An immediate color change from dark blue to dark brown was observed. The mixture was stirred at room temperature for two hours. The THF solvent was stripped off. The residue was triturated with hexane (6mL) and then was extracted with 8mL of toluene. The toluene solution was concentrated to 3mL. The resulted thick syrup was stored at -40°C for a few days. The resultant crystals were separated from the syrup and were washed with 2mL of hexane. In this way 100mg of green crystalline product was obtained in 38% yield. The product was characterized as a 2:1 of mixture of $U(L_{OEt})_2(OEt)I/U(L_{OEt})_2I_2$. ^1H NMR (toluene-d_8, 23°C, δ ppm): 200.72(s, H_2C, OEt, 21); 82.20(s, H_3C, OEt, 21); -5.84(s, Cp, L_{OEt}, 21); 3.4(s, H_3C, L_{OEt}, 21); 7.5(br, H_2C, L_{OEt}, 21); 17.95(s, Cp, 19); -1.5(s, H_3C, L_{OEt}, 19); 0.1, -0.5(br, br, H_2C, L_{OEt}, 19). ^{31}P NMR (toluene-d_8, 23°C, δ ppm): 141.2(s, 21); 163.7(s, 19). Anal. Calc. for $C_{53}H_{110}O_{28}P_9I_2Co_3U_{1.5}$: C, 28.14; H, 4.90; I, 11.22. Found: C, 28.79; H, 4.69; I, 12.15%.

$[U(L_{OEt})_2(THF)_2][BPh_4]_2$ (18)

A solution of NaL_{OEt} (389mg, 0.696mmol) in toluene (5mL) was added to a slurry of $UI_3(THF)_4$ (316mg, 0.348mmol) in toluene (6mL). Filtration, after stirring for six hours, gave a clear green solution. Two equiv of solid TlBPh$_4$ powder was directly added to the toluene solution giving an immediate precipitation of yellow TlI. The reaction mixture was stirred for two hours, filtered and the residue was extracted with THF (ca. 8mL). Cooling the THF solution at -40°C gave 125mg crystalline powder. Further

concentration and cooling the solution at -40°C gave a second and a third crop of microcrystalline powder 20mg and 50mg, respectively, for a total yield of 27%. ^{1}H NMR (THF-d_8, 23°C, δ ppm): 13.64(s, 10H, Cp); 0.22(tr, 36H, H_3C, L_{OEt}); 3.10, 2.77 (br, br, 12H, 12H, H_2C, L_{OEt}); 7.14, 6.69, 6.54 (m, tr, tr, 16H, 16H, 8H, BPh$_4^-$); 3.53, 1.73 (m, m, 8H, 8H, THF). ^{31}P NMR (THF-d_8, 23°C, δ ppm): 172.0. ^{11}B NMR (THF-d_8, 23°C, δ ppm): -6.11. Anal. Calc. for $C_{90}H_{126}O_{20}P_6Co_2B_2U$: C, 51.68; H, 6.07. Found: C, 51.49; H, 6.35%.

U(L_{OEt})$_2$I$_2$ (19)

A THF solution containing excess NaI was added to a solution of U(L_{OEt})$_2$Cl$_2$ (131mg, 9.49x10^{-5}mol) in THF (5mL). The mixture became cloudy immediately. After stirring for one hour at room temperature the solvent was stripped off and the residue was triturated with hexane and then was extracted with 5mL of toluene. Cooling the toluene solution at -40°C for days gave brick-like, olive crystalline product (46mg, 31% yield). ^{1}H NMR (C$_6$D$_6$, 23°C, δ ppm): 18.1(s, 10H, Cp); -1.50(s, 36H, H_3C, L_{OEt}); 0.1, -0.5(br, br, 12H, 12H, H_2C, L_{OEt}). ^{31}P NMR (C$_6$D$_6$, 23°C, δ ppm): 163.3(s). Anal. Calc. for $C_{34}H_{70}O_{18}P_6Co_2I_2U$: C, 26.14; H, 4.52. Found: C, 26.32; H, 4.64%.

U(L_{OEt})$_2$(OEt)$_2$ (20)

A slurry of NaOEt (16mg, 0.483mmol) in THF (4mL) was added to a solution of U(L_{OEt})$_2$Cl$_2$ (332mg, 0.241mmol) in THF (6mL). The color changed gradually from grass-green through olive to brown. The mixture was stirred for 2 hours, after inverse filtration and the solvent was removed under vacuum. The residue was dissolved in hexane (2mL) and the solution was cooled at -40°C to give 245mg brick-like brown crystals in 73% yield. ^{1}H NMR (toluene-d_8, 23°C, δ ppm): 49.78(s, 4H, H_2C, OEt,); 19.88(s, 6H, H_3C, OEt,); -4.86(s, 10H, Cp); 3.87(s, 36H, H_3C, L_{OEt}); 6.78, 6.16(br,

br, 12H, 12H, H_2C, L_{OEt}). ^{31}P NMR (C_6D_6, 23°C, δ ppm): 114.0(s). Anal. Calc. for $C_{38}H_{80}O_{20}P_6Co_2U$: C, 32.63; H, 5.76. Found: C, 32.68; H, 5.74%.

Reaction of UI$_3$(THF)$_4$ with 2 Equiv of Hydrated NaL$_{OEt}$

A solution of hydrated $NaL_{OEt}(H_2O)_{1.5}$ (358mg, 0.642mmol) in THF (6mL) was added dropwise to a slurry of UI$_3$(THF)$_4$ (291mg, 0.321mmol) in THF (6mL). An immediate color change from dark blue to light green was observed. The mixture was stirred for four hours. After the solvent THF was stripped to dryness, the residue was extracted with 8mL of toluene. The toluene solution was stored in drybox at room temperature for a few days giving light green crystals. Two batches of crystalline product (193mg) for an overall yield of 42% were obtained. The product was characterized as $[(L_{OEt})U(CpCo\{P(O)(OEt)_2\}_2\{P(=O)(OEt)(O)\})(H_2O)]_2I_2$ (22). ^{1}H NMR (CD_2Cl_2, 23°C, δ ppm): 8.90, 4.61 (s, s, 5H, 5H, Cp); 1.58, 1.10 (s, s, 9H, 9H, H_3C, terminal L_{OEt}); 7.02, 6.32, 5.50, 4.88, 4.40, 4.10, 2.08, -8.30, -14.80 (s, 3H, 4 H_2C, terminal L_{OEt}, 5 H_3C, bridging L_{OEt}); 20.80, 20.22, 18.00, 12.58, 9.82, 7.22, -11.72, -12.30, -17.90, -25.30 (br, 1H, 10 H_2C, bridging L_{OEt}). ^{31}P NMR (CD_2Cl_2, 23°C, δ ppm): 132.7(s, 3P, terminal L_{OEt}); 192.1, 169.2, 108.9(tr, tr, tr, 1P, 1P, 1P, bridging L_{OEt}). Anal. Calc. for $C_{32}H_{67}O_{19}P_6Co_2IU$: C, 26.98; H, 4.74; I, 8.91. Found: C, 29.47; H, 4.82; I, 11.60%.

5.4.3. X-ray Data Collection, Structure Solution and Refinement

X-ray quality crystals of compound 17 were obtained by cooling a very concentrated toluene solution at -40°C for days in the dry-box. In a similar way cooling THF solution at -40°C gave crystals of compound 18 suitable for X-ray analysis. Crystals of complex 22 were obtained readily by storing a THF solution at room temperature in the dry-box for a few days. Crystallographic data are summarized in Table 5.3.

Table 5.3 Crystallographic Data for Complexes 17, 18, and 22

complexes	17	18	22
mol formula	$C_{53}H_{110}O_{28}P_9Co_3I_2U_{1.5}$	$C_{90}H_{126}O_{20}P_6Co_2B_2U$	$C_{64}H_{134}O_{38}P_{12}Co_4I_2U_2$
formula weight	925.19	959.32	2848.94
space group	$P\bar{1}$	$C2/c$	$P2_1/n$
a,Å	14.659(5)	20.348(6)	13.572(3)
b,Å	14.641(7)	11.600(4)	21.789(1)
c,Å	26.471(9)	25.931(7)	18.901(2)
a,deg	75.60(3)	90	90
b,deg	87.38(3)	109.42(2)	94.16(1)
g,deg	75.56(3)	90	90
V,Å³	5328(4)	5772(3)	5574.7(14)
Z	2	4	2
diffractometer	P1	P1	Siemens P4/RA
radiation(λ,Å)	MoKα(0.7107) from graphite monochromater		
scan mode	ω-2θ	θ-2θ	θ-2θ
2θ limits(deg)	3.0-43.0	3.0-45.8	2.0-50.0
temp,°C	23	23	24
no. of unique data[a]	12174(9746>3σ)	3966(2136>3σ)	12616(7171>2σ)
no. of variables	843	304	550
R₁	0.063[a]	0.039[a]	0.0574[b]
R₂	0.070[a]	0.045[a]	
wR₂			0.1288[b]

[a](I>3σ(I)); [b](I>2σ(I)); $R_1=\sum||F_o|-|F_c||/\sum|F_o|$; $R_2=[\sum w_1(|F_o|-|F_c|)^2/\sum w_1F_o^2]^{1/2}$; $wR_2=[\sum w_2(F_o^2-F_c^2)^2/\sum w_2F_o^4]^{1/2}$

5.5. References

(1) Zhang, X. Ph. D. Thesis, University of Alberta, 1995.

(2) Klaui, W.; Dehnicke, K. *Chem. Ber.* **1978**, *111*, 451-468.

(3) Huheey, J. E. In *Inorganic Chemistry*; Third ed.Harper & Row, Publishers, New York: Cambridge, 1983; pp 384.

(4) Klaui, W. *Angew. Chem., Int. Ed. Engl.* **1990**, *29*, 627-637.

(5) Jesson, J. P.; Trofimenko, S.; Eaton, D. R. *J. Am. Chem. Soc.* **1967**, *89*, 3148.

(6) Klaui, W.; Lenders, B.; Hessner, B.; Evertz, K. *Organometallics* **1988**, *7*, 1357-1363.

(7) Banbery, H. J.; Hussain, W.; Evans, I. G.; Hamor, T. A.; Jones, C. J.; McCleverty, J. A.; Schulte, H.; Engles, B.; Klaui, W. *Polyhedron* **1990**, *9*, 2549-2551.

(8) Klaui, W. *Helv. Chim. Acta.* **1977**, *60*, 1296-1303.

(9) Baudry, D.; Ephritikhine, M.; Klaui, W.; Lance, M.; Nierlich, M.; Vinger, J. *Inorg. Chem.* **1991**, *30*, 2333-2336.

(10) Wedler, M.; Gilje, J. W.; Noltemeyer, M.; Edelmann, F. T. *J. Organomet. Chem.* **1991**, *411*, 271-280.

(11) Li, L.; Stevens, E. D.; Nolan, S. P. *Organometallics* **1992**, *11*, 3459-3462.

Chapter 6

A New Approach to Asymmetrical Hydrotris(pyrazolyl)borate:
Synthesis and Characterization of [HB(pz)$_2$(N-pyrrolidinyl)]$^-$
and Its Transition Metal Complexes M[HB(pz)$_2$(N-
pyrrolidinyl)]$_2$ (M=Co(II), Ni(II))

6.1. Introduction

The poly(pyrazolyl)borate ligands, H$_n$B(pz)$_{4-n}^-$ (n=0-2; pz=substituted pyrazole) have proven to be extremely versatile and useful for the preparation of a wide range of metal and metalloid complexes, as witnessed by the appearance of numerous comprehensive reviews on the subject.[1-3] The classical synthetic route to these ligands, developed by Trofimenko in 1966,[4] involves the reaction of pyrazole with an alkali metal borohydride, eq. 6.1. The method is simple and by using the appropriately substituted

$$MBH_4 \ + \ n \, pzH \xrightarrow{\ \Delta\ } M[H_{4-n}B(pz)_n] \ + \ n/2H_2 \qquad\qquad 6.1$$

$$n = 2\text{-}4$$
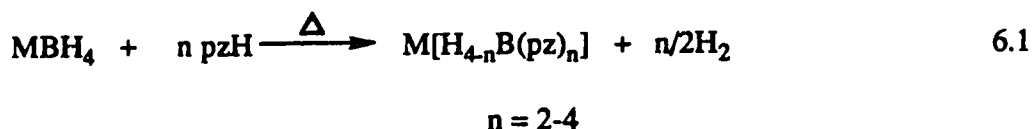
pyrazole it allows for the electronic and especially steric fine-tuning of the ligand system. Spectacular successes have been achieved in stabilizing highly reactive species by employing sterically hindered ligands such as Tp^{tBu,Me}.[5] However, the high temperatures required for the synthesis encourage intermolecular pyrazole exchange and hence pure hetero ligands, such as HB(pz)$_2$(pz')$^-$, or chiral HB(pz)(pz')(pz'')$^-$ ligands are not accessible via the classical synthesis.

In a very interesting recent development Tolman[6] has reported the synthesis of C$_3$-symmetric, chiral Tp^{R*} ligands, by attaching optically active substituents at the 3-position of the pyrazolyl ring. The preparation of metal complexes with these ligands has been developed also.[7] Agrifoglio and co-workers[8,9] explored the preparation of hetero

poly(pyrazolyl)borate ligands *via* the low temperature process depicted in Scheme 6.1.

Scheme 6.1

$$H_3BC_4H_4O \xrightarrow[-C_4H_4O]{+Hpz} BH_3(Hpz) \xrightarrow[-30^\circ C]{+I_2/-H_2} BH_2(Hpz)I$$

$$\xrightarrow[-30^\circ C]{+Hpz'} BH_2(Hpz)(Hpz')^+I^- \xrightarrow[-NaI, -2H_2]{+2NaH} NaBH_2(pz)(pz')$$
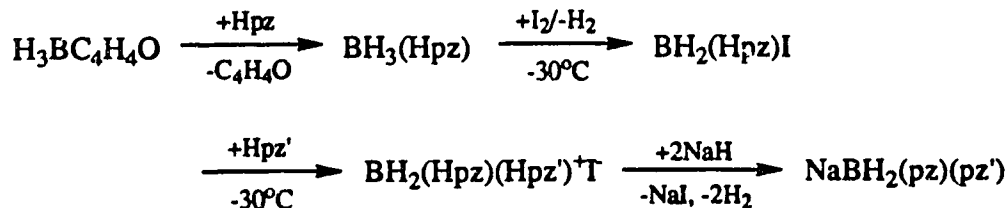
However, extension of the synthetic procedure to the preparation of $HB(pz)_2(pz')^-$ or $HB(pz)(pz')(pz'')^-$ has not yet appeared.

In this chapter we present our attempt toward hetero poly(pyrazolyl)borate ligands, the preparation of a new tripodal nitrogen donor ligand and the synthesis and characterization of its Co(II) and Ni(II) complexes.

6.2. Results and Discussion

6.2.1. Synthetic Strategy

The hydrotris(pyrazolyl)borate ligand, $HB(pz)_3^-$, can be viewed as the unstable hydrobis(pyrazolyl)borane species, $HB(pz)_2$, stabilized by the Lewis base, pyrazolide (pz)$^-$. Without Lewis bases, $HB(pz)_2$ dimerizes to form the stable pyrazobole, $[HB(pz)_2]_2$, because $HB(pz)_2$ is both a Lewis acid and a Lewis base. It occurred to us that by using the easily available pyrazobole as a starting material a synthesis of hetero ligands could in principle be developed. The strategy is shown in eq. 6.2. Lewis base promoted

$$[HB(pz)_2]_2 \xrightarrow{L} HB(pz)_2L \xrightarrow[-L]{+pz'^-} HB(pz)_2(pz')^- \qquad 6.2$$
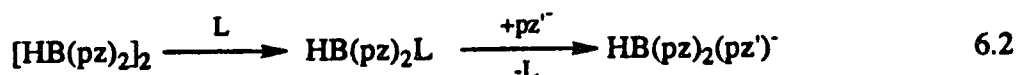
ring opening, followed by displacement of L from the adduct $HB(pz)_2L$ by a different pyrazolide should give the desired hetero ligand, $HB(pz)_2(pz')^-$. It is easy to see that

starting with mixed pyrazobole, [HB(pz)(pz')]₂, the chiral ligand, HB(pz)(pz')(pz")⁻,
should be obtained.

6.2.2. Ring Opening of Pyrazobole

Initially we hoped that the pyrazobole could be opened by pyrazolide itself. However, attempted ring opening with K(3,5-Me₂pz) was unsuccessful. Next a variety of neutral amines, such as NH₃, HNMe₂, NMe₃, NEt₃, N(ⁱPr)₃, pyrrolidine, and pyridine, were tried. Only with HNMe₂ and pyrrolidine did ring opening and formation of the amine adducts, HB(pz)₂(L) (L=HNMe₂ (23), N-prrolidinyl (24)), occur. On the basis of the apparent necessity of hydrogen on the amine nitrogen, we propose the following mechanism for the ring splitting reaction, scheme 6.2. Hydrogen bonding between the

Scheme 6.2
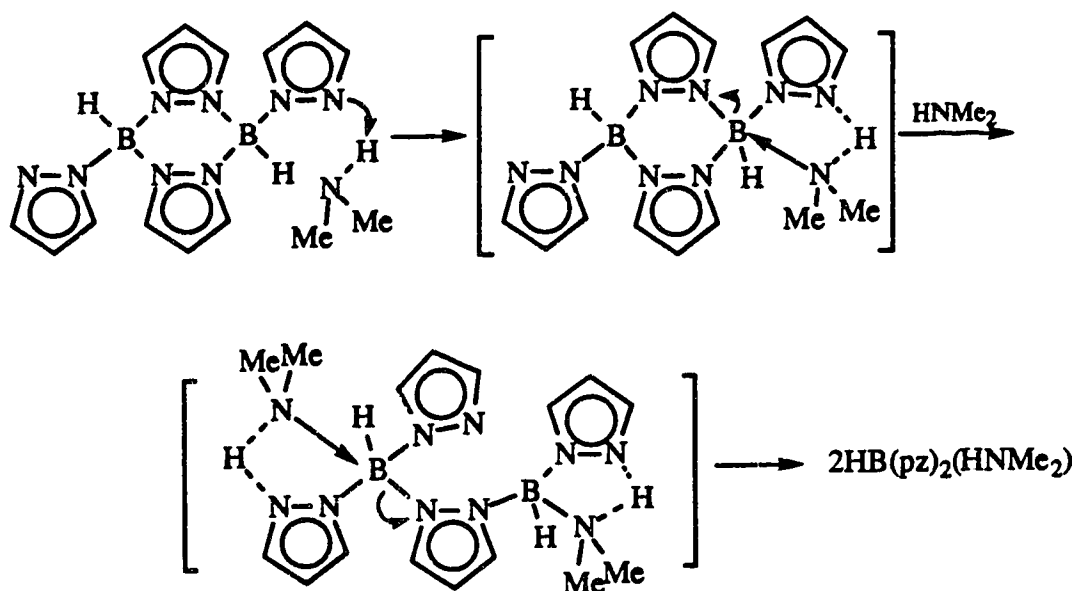
secondary amine and the terminal pyrazolyl group facilitates nucleophilic attack of the boron by the amine nitrogen and cleavage of the bridging B-N bond; the same process on the other boron leads to complete cleavage of the pyrazobole ring.

6.2.3. Reactions of the Amine Adducts with $(3,5\text{-Me}_2\text{pz})^-$

Unfortunately displacement of the amine by $(3,5\text{-Me}_2\text{pz})^-$ was not as su~~essful as we had hoped. Reaction of $HB(pz)_2(HNMe_2)$ with $(3,5\text{-Me}_2\text{pz})^-$ at 55°C did not give pure $HB(pz)_2(3,5\text{-Me}_2\text{pz})^-$. Instead, a 2:1 mixture of $HB(pz)_2(3,5\text{-Me}_2\text{pz})^-$ and $HB(pz)(3,5\text{-Me}_2\text{pz})_2^-$, as determined by ^1H NMR spectroscopy, was obtained. Thus, although the scrambling process has not been eliminated, its extent has been reduced as a result of our ability to reduce the reaction temperature from 190°C to 55°C.

The expected reaction is shown in eq. 6.3. However, a competing reaction is also

$$HB(pz)_2(HNMe_2) + (3,5\text{-Me}_2\text{pz})^- \longrightarrow HB(pz)_2(3,5\text{-Me}_2\text{pz})^- + HNMe_2 \qquad 6.3$$

possible (Scheme 6.3). Niedenzu et al.[10,11] reported that at ambient temperature, the N-bonded proton in $B(pz)_3(HNMe_2)$ is labile, and exchanges between the amine and pyrazolyl nitrogens; only at low temperatures does the proton bind to the nitrogen of the dimethylamine. Based on this observation, and assuming a labile proton in the present case also, we can visualize the formation of an intermediate which leads to the formation of $HB(pz)(3,5\text{-Me}_2\text{pz})(HNMe_2)$, and eventually to the scrambled product, $HB(pz)(3,5\text{-Me}_2\text{pz})_2^-$ (Scheme 6.3). It is clear that H^+ is the catalyst for the scrambling reaction. Since

Scheme 6.3
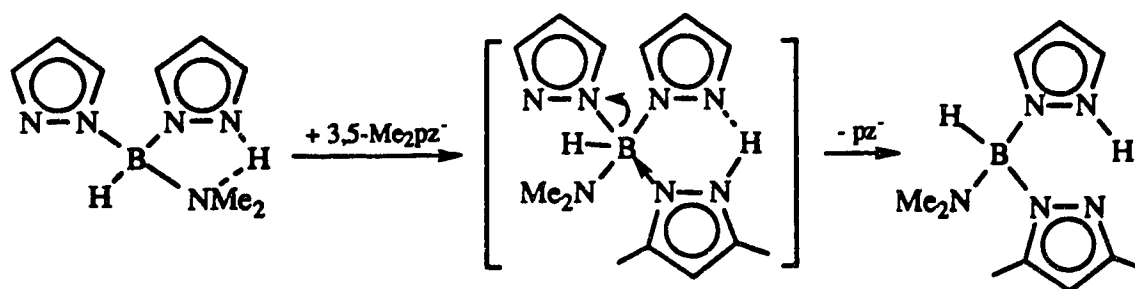
the successfully synthesized adducts all contain a labile H^+, the scrambling reaction can hardly be eliminated. It is possible that if $HB(pz)_2(NMe_3)$, instead of $HB(pz)_2(HNMe_2)$, could be obtained the scrambling reaction may be completely eliminated.

Attempts to replace the pyrrolidinyl group by (3,5-Me$_2$pz)⁻ at room temperature failed. When the reaction temperature was raised to 100°C, the displacement did occur, but the main peaks in the M.S. spectrum were 175, HB(pz)(3,5-Me$_2$pz) and 203, HB(pz)(3,5-Me$_2$pz)$_2$.

6.2.4. Preparation of MHB(pz)$_2$(N-pyrrolidinyl)(THF)$_n$ (M=Li (25), Na (26))

Niedenzu and Trofimenko[11] have shown that B(pz)$_3$(HNMe$_2$) could be readily deprotonated to give [B(pz)$_3$(NMe$_2$)]⁻, a hetero pyrazolylborate ligand which behaved as a tridentate ligand with transition metal ions *via* two pyrazolyl and amine nitrogens; that is, η^3-(pz)B(pz)$_2$(NMe$_2$)⁻, instead of η^3-(NMe$_2$)B(pz)$_3$⁻. With the availability of HB(pz)$_2$(HNR$_2$) (HNMe$_2$ and pyrrolidine) it was of interest to investigate whether these adducts could give similar anionic tripodal ligands. The pyrrolidine adduct was used since it is the more stable of the two. Just like B(pz)$_3$(HNMe$_2$), the HB(pz)$_2$(N-pyrrolidine) adduct could be readily deprotonated with Li^{t}Bu or NaH in THF to give the new hetero pyrazolylborate ligand, MHB(pz)$_2$(N-pyrrolidinyl) (M=Li, Na), in good yield. When well formed crystals of the salts were isolated from the solution at room temperature, they readily lost lattice solvents and crystallinity. Thus the structure of the ligand could not be determined. The amount of retained solvents of crystallization was variable and resulted in erratic elemental analysis.

The ^{1}H NMR spectra of both salts are simple and display a single set of three signals for the pyrazolyl hydrogens (7.57, 7.01, and 5.90 ppm (25); 7.75, 7.73, and 6.11 ppm (26)) in the expected 1:1:1 ratio. The Na⁺ salt shows two broad signals for the α- and β-hydrogens of the pyrrolidinyl group at 2.08 and 1.22ppm. However, for the Li⁺ salt the α-hydrogens of the pyrrolidinyl group give rise to two resonances at 1.07 and 0.25 ppm, indicating a stronger interaction between Li⁺ and the pyrrolidinyl nitrogen which

locks the nitrogen in a rigid position and prevents B-N(pyrrolidinyl) rotation that would exchange the environments of the α-hydrogens, as seen in the case of the Na^+ salt.

6.2.5. Transition Metal Complexes of $HB(pz)_2(N$-pyrrolidinyl)*

Transition metal complexes were readily prepared by mixing the ligand with anhydrous $CoCl_2$ or $NiCl_2$ in THF in a 2:1 molar ratio. The reaction with $CoCl_2$ proceeded readily. However, with $NiCl_2$ the reaction was not quite complete even after overnight stirring. The reason for this is most probably due to the much lower solubility of $NiCl_2$ in THF. Analytically pure, crystalline products were obtained by cooling THF solutions at -40°C or by storing the solutions at room temperature for a few days; $Co[HB(pz)_2(N$-pyrrolidinyl)]_2$ (27) is pink and $Ni[HB(pz)_2(N$-pyrrolidinyl)]_2$ (28) is light blue. Just like the reaction of Tp with $CoCl_2$, attempts to prepare the mono-ligand complex, $Co[HB(pz)_2(N$-pyrrolidinyl)]Cl$, by using one equivalent of the ligand failed. Only $Co[HB(pz)_2(N$-pyrrolidinyl)]_2$ (27) could be isolated. This is most likely due to the fact that our ligand is even less bulky than Tp. The ease of formation of $Co[HB(pz)_2(N$-pyrrolidinyl)]_2$ (27) species and the instability of $Co[HB(pz)_2(N$-pyrrolidinyl)]Cl$ complex were in line with expectation .

An interesting observation was made in the $CoCl_2$ reaction. It was noticed that addition of a solution of $NaHB(pz)_2(N$-pyrrolidinyl) to a slurry of $CoCl_2$ in THF resulted in the gradual dissolution of $CoCl_2$, and formation of a very intense blue solution with a white precipitate of NaCl. The characteristic blue color indicated a tetrahedral coordination environment around the Co(II) metal center.[12] However, when the solution was either cooled at -40°C or stored at room temperature for days, only light pink crystals of compound 27 were obtained. This pink color is in accord with six coordinate Co(II). Redissolution of the pink crystals did not give back the intense blue color. A light pink solution was obtained suggesting that the transition between tetrahedral and octahedral coordination is not reversible.

The IR spectra of both compounds are almost superimposable and suggest similar coordination geometry about the metal centers. The characteristic B-H stretching frequencies appear at 2398 and 2400 cm⁻¹ for Co(II) and Ni(II) complexes, respectively. The color of the complexes, pink cobalt and light blue nickel, are typical for the respective six-coordinate metal centers[13] and are also similar to the analogous $M(Tp)_2$ complexes.[12] The optical spectra are also similar[14,15] and strongly suggest the presence of six-coordinate metal centers.

The principle visible absorption band of $Co[HB(pz)_2(N\text{-pyrrolidinyl})]_2$ (27) is at 493nm, compared to 459nm in $Co(Tp)_2$, however the former band is flanked by two shoulders at 525 and 456nm, respectively. The most significant difference between the three band spectrum of $Ni[HB(pz)_2(N\text{-pyrrolidinyl})]_2$ (28) and $Ni(Tp)_2$, besides the generally lower energy position of the bands, is their higher intensity in the pyrrolidinyl derivative. The difference can be accommodated by taking into account of the nature of the current ligand system. Being an A_2B type tridentate ligand the coordination geometry of the metal center is no longer octahedral, at best it is a tetragonaly distorted octahedron with maximum C_{2h} symmetry. Thus the splitting of the visible band is not unexpected, and higher intensity bands in the nickel complex is most likely due to a non centro-symmetric structure.

6.2.6. Molecular Structure of $M[HB(pz)_2(N\text{-pyrrolidinyl})]_2$ (M=Co,Ni)

To verify the structure of the complexes single crystal X-ray structural analyses were carried out. The molecular structures of compounds 27 and 28 are shown in Fig. 6.1 and 6.2. Selected bond lengths and angles are listed in Table 6.1. Crystals of both compounds contain well separated monomeric units. It is clear from the figures that in both complexes the ligands are tridentate and the metals are six-coordinate. The four pyrazolyl nitrogens occupy equatorial positions and the two pyrrolidinyl nitrogens are trans to each other, thus a tetragonally distorted octahedral geometry results.
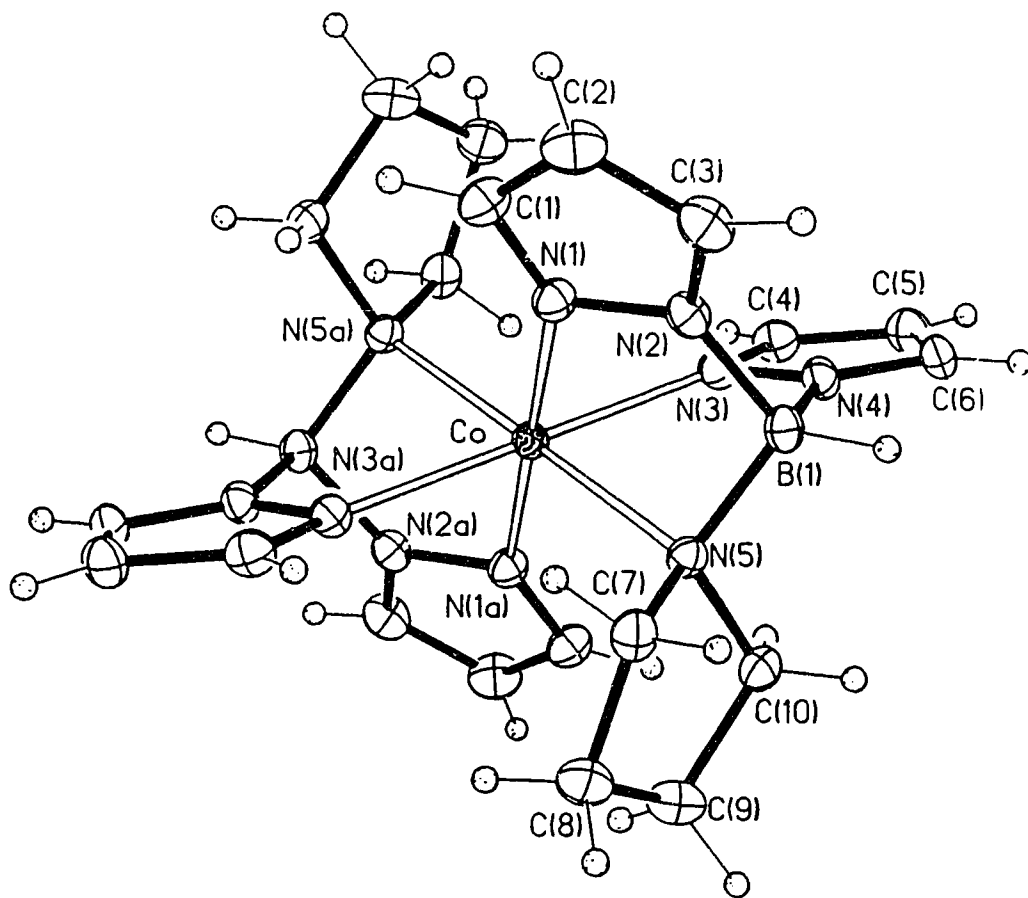
Fig. 6.1 Molecular Structure of Co[HB(pz)₂(*N*-pyrrolidinyl)]₂
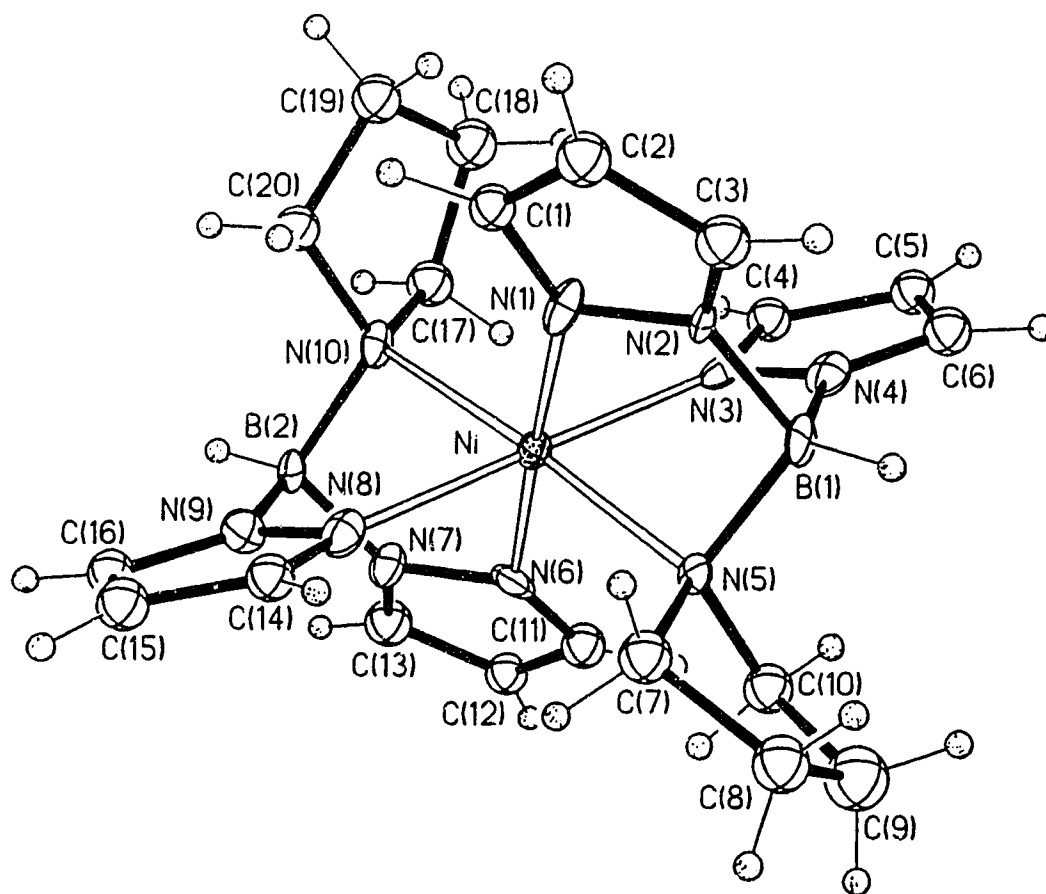
Fig. 6.2 Molecular Structure of Ni[HB(pz)2(*N*-pyrrolidinyl)]2

In the lattice of the Co compound there are two independent molecules with virtually identical parameters, and the cobalt atoms sit on points of inversion. The Ni comp x has no symmetry and accounts for the greater extinction coefficients seen in the visible spectrum. The four nitrogen atoms from the pyrazolyl rings are almost in a plane. The average $M-N_{pz}$ bond lengths (2.158(17)Å (27), 2.114(12)Å (28)) are slightly longer than those of $Co(Tp)_2$ and $Ni(Tp)_2$ (2.129(7)Å and 2.093(7)Å), respectively.[16,17] The average $M-N_{pyrrolidinyl}$ bond distances (2.262(15)Å, (27) and 2.206(35)Å, (28)) are significantly longer than the reported $M-N_{amide}$ bond lengths (1.928(5)Å, $Co(II)[N(SiMe_3)_2]_2(PPh_3)$; 1.88(1)Å $Ni(I)[N(SiMe_3)_2](PPh_3)_2$[18]; 1.916(9)Å, $Co_2[N(SiMe_3)_2]_4$[19]; 1.887(9)Å, $[Ni(II)(NPh_2)_3]^-$; 1.828(13)Å, $Ni_2[N(Ph)_2]_4$; 1.889(8)Å, $Co_2[N(Ph)_2]_4$[20]; 1.985(9)Å, $[Li(THF)_{4.5}][Co[N(SiMe_3)_2](OC^tBu_3)_2]$; 1.906(7)Å, $Li[Co[N(SiMe_3)_2](OC^tBu_3)_2]^{21}$. In fact the $M-N_{pyrrolidinyl}$ bond distances are even longer than the $M(II)-N_{pz}$ bond lengths (M=Co, Ni), a reflection of the rigidity of the ligand.

The angles between the $Co-N_{axial}$ bond and the two $Co-N_{eq}$ bonds for the same ligand are 77.2(1)°, 77.6(1)°, and the two $Co-N_{eq}$ bonds with the other ligand are 102.8(1)°, 102.4(1)°. Thus, the tilt angle of the axial ligand (12°) is larger than that in $Co(Tp)_2$ (5°). As a result of the shorter, one-bond B-pyrrolidinyl arm compared to the two-bond arm of the Tp ligand, the pyrrolidinyl nitrogen is pulled toward the Co metal center and the angle between the two $Co-N_{eq}$ bonds of the same ligand also become greater, 88.7(1)° than that of $Co(Tp)_2$ (85.3(3)°). The shorter Co···B distance in 27 is consistent with the this argument (2.87Å vs 3.20Å in $Co(Tp)_2$). The greater angular distortion and the different axial donor in 27 are responsible for the splitting of the visible band at 493nm.

The situation is quite similar in the Ni complex, the only difference is the orientation c he pyrrolidinyl rings. In the Co complex both envelope shaped pyrrolidinyl rings point in the same direction, $\alpha-CH_2$ moieties away from the metal center, whereas in the Ni compound the α-methylenes of one of the pyrrolidinyl rings point toward while the others

Table 6.1 Selected Bond Distances (Å) and Angles (°) for 27 and 28

	27		28
		Bond Distances	
Co-N1	2.145(2)	Ni-N1	2.12(1)
Co-N3	2.178(2)	Ni-N3	2.12(2)
Co-N1'	2.143(2)*	Ni-N6	2.12(1)
Co-N3'	2.167(2)*	Ni-N8	2.10(2)
Co-N$_{pz}$	2.16(2)^a	Ni-N$_{pz}$	2.11(1)^a
Co-N5	2.252(2)	Ni-N5	2.18(2)
Co-N5'	2.273(2)*	Ni-N10	2.23(2)
		Bond Angles (°)	
N1-Co-N3	88.7(1)	N1-Ni-N3	88.6(7)
N1-Co-N5	77.6(1)	N1-Ni-N5	79.5(6)
N3-Co-N5	77.2(1)	N3-Ni-N5	78.6(7)
N1A-Co-N3	91.3(1)	N1-Ni-N6	178.1(7)
N1A-Co-N5	102.4(1)	N3-Ni-N6	91.1(7)
N3A-Co-N5	102.8(1)	N5-Ni-N6	98.6(7)
N1-Co'-N3	89.4(1)*	N1-Ni-N8	89.7(7)
N1-Co'-N5	77.2(1)*	N3-Ni-N8	177.5(6)
N3-Co'-N5	76.6(1)*	N5-Ni-N8	99.3(7)
N1A-Co'-N3	90.6(1)*	N6-Ni-N8	90.6(7)
N1A-Co'-N5	102.8(1)*	N1-Ni-N10	103.5(6)
N3A-Co'-N5	103.4(1)*	N3-Ni-N10	103.4(7)
		N5-Ni-N10	176.3(6)
		N6-Ni-N10	78.4(7)
		N8-Ni-N10	78.7(8)

* The second independent molecule; ^{a} Averaged bond lengths

away from metal center. The result is loss of the center of inversion in the Ni complex, which is also reflected in the different Ni-N$_{pyrrolidinyl}$ distances, 2.23(2) and 2.18(2)Å.

6.3. Conclusions

The splitting of pyrazobole, [HB(pz)$_2$]$_2$, required secondary amines such as HNMe$_2$ and pyrrolidine and gave the adducts, HB(pz)$_2$HNMe$_2$ and HBpz$_2$(N-pyrrolidine). Although displacement of HNMe$_2$ from HB(pz)$_2$(HNMe$_2$) with (3,5-Me$_2$pz)$^-$ did not give pure HB(pz)$_2$(3,5-Me$_2$pz)$^-$, the scrambling of pyrazolyl groups has been reduced. The HB(pz)$_2$(N-pyrrolidine) adduct proved useful for the preparation of a hetero pyrazolylborate ligand by deprotonation with NaH or Li^{t}Bu. The ligand, HBpz$_2$(N-pyrrolidinyl)$^-$, was used in the preparation of Co(II) and Ni(II) complexes.

6.4. Experimental Section

6.4.1. Preparation of Starting Materials

Pyrrolidine, pyridine, and N(^{i}Pr)$_3$ were refluxed with CaH for 48 hours, this was followed by distillation and collection under a nitrogen atmosphere. Gaseous NH$_3$, HNMe$_2$, NMe$_3$, and NEt$_3$ were used directly from the cylinder. Anhydrous CoCl$_2$ and NiCl$_2$ were prepared according to the published literature[22]. [HBpz$_2$]$_2$ was prepared by pyrolysing HB(pz)$_3$$^-H^+$ at 90°C under vacuum.

6.4.2. General Conditions for the Reactions of [HB(pz)$_2$]$_2$ with Amines

The reactions were carried out in a Schlenk tube using the amine as the solvent. Gaseous amines were condensed directly into heavy-duty Schlenk tubes under vacuum and the mixture was stirred at the temperature required.

6.4.3. Synthetic Procedures

$HB(pz)_2(HNMe_2)$ (23)

A 100mL heavy-duty Schlenk tube was charged with pyrazobole (1.0g, 3.43mmol). Under vacuum, 20mL of $HNMe_2$ was condensed into the Schlenk tube and the mixture was heated at 90°C overnight. $HNMe_2$ was removed and the residue was washed with pentane. ^1H NMR ($CDCl_3$, 23°C, δ ppm): 7.60(d, 2H, 5-H-pz); 7.56(d, 2H, 3-H-pz); 6.20(t, 2H, 4-H-pz); 2.37(s, 1H, Me_2NH). M.S. (FAB, cleland): 192(M+H); 124(M-pz+H).

$HB(pz)_2(N$-pyrrolidine) (24)

Pyrazobole (1.80g, 6.17mmol) was dissolved in 30mL pyrrolidine. The solution was stirred at 100°C for four hours. The solvent pyrrolidine was stripped off and the glassy residue was washed with 20mL pentane, and dried under vacuum. This way 1.88g of white powder was obtained in 70% yield. ^1H NMR ($CDCl_3$, 23°C, δ ppm) 7.59(s, 2H, 5-H-pz); 7.53(d, 2H, 3-H-pz); 6.17(t, 2H, 4-H-pz); 3.02, 2.84(m, m, 2H, 2H, α-H-pyrrolidine); 1.86(m, 4H, β-H-pyrrolidine). M.S. (FAB, m-nitrobenzyl alcohol): 218(M+H); 150(M-pz+H).

$LiHB(pz)_2(N$-pyrrolidinyl) (25)

To a slurry of 24 (0.932g, 4.30mmol) in 80mL of pentane, Li^tBu solution (2.53mL, 1.7M) was added dropwise at -78°C. After stirring for two hours at -78°C, the mixture was allowed to warm to room temperature during two hours. Inverse filtration, followed by removal of solvent gave a white solid which was transferred to the drybox. THF was added to a slurry of the solid in 20mL of pentane until a clear solution was obtained. Cooling the solution at -40°C gave 0.59g of colorless, crystalline product. Concentration and cooling the filtrate at -40°C gave a second crop of crystalline product, 0.05g. Total yield is 63%. At room temperature the crystals, once seperated from

solution, quickly lost their shine and cystallinity and crumbled to a white powder; evidence of ready loss of lattice solvent. ^{1}H NMR (C_6D_6, 23°C, δ ppm): 7.57(d, 2H, 5-H-pz); 7.01(s, 2H, 3-H-pz); 5.90(t, 2H, 4-H-pz); 1.07, 0.25(br, 2H, 2H, α-H-pyrrolidine); 1.86(br, 4H, β-H-pyrrolidine).

NaHB(pz)$_2$(N-pyrrolidinyl)(THF) (26)

A THF solution of 24 (1.95g, 8.99mmol) was added to a slurry of excess NaH in THF. The mixture was stirred for 5 hours at room temperature and filtration gave a clear solution. The solvent was stripped off and the so formed white solid was transferred in the drybox. THF was added to the slurry of the solid in about 15mL pentane until a clear solution was obtained. Cooling the solution at -40°C for days gave brick-like crystals (1.06g). Concentration and cooling the filtrate at -40°C gave a second crop of crystalline product (0.33g). Total yield is 65%. At room temperature the coordinated THF is readily lost. ^{1}H NMR (toluene-d$_8$, 23°C, δ ppm): 7.75, 7.73(s, s, 2H, 2H, 3,5-H-pz); 6.11(t, 2H, 4-H-pz); 2.08(br, 4H, β-H-pyrrolidine); 1.22(br, 4H, α-H-pyrrolidine); 3.32(m, 4H, β-H-THF); 1.34(m, 4H, α-H-THF). ^{11}B NMR (THF-d$_8$, 23°C, δ ppm): -9.05

Co[HB(pz)$_2$(N-pyrrolidinyl)]$_2$ (27)

A solution of NaHB(pz)$_2$(N-pyrrolidinyl) (264mg, 1.11mmol) was added to a slurry of CoCl$_2$ (72mg, 0.555mmol) in 5mL of THF. The mixture was stirred for 2 hours. The precipitate was separated by centrifugation. The solvent was stripped off, and the residue was washed with hexane (4mL) and redissolved in THF. Cooling the THF solution at -40°C gave pink crystalline product (103mg) in 40% yield. IR (KBr, cm^{-1}): v(C-H) 2960 s, 2834 s; v(B-H) 2398 s; 1501 s, 1395 s, 1308 s, 1207 s, 1119 s, 1047 s, 975 m, 881 m, 755 s, 716 m, 626 m. UV-visible (CH$_2$Cl$_2$, nm): 456 sh (13.3), 493 (15.7), 525 sh (11.6), 589 (4.8), 1023 (5.7). M.S. (E.I. 70ev, 200°C) M/Z 491(M$^+$)

420(M$^+$-pyrrolidinyl); 351(M$^+$-pyrrolidinyl-pz). E.A. calc. C, 48.92; H, 6.16; N, 28.52, Found: C, 48.91; H, 6.39; N, 28.52.

Ni[HB(pz)$_2$(*N*-pyrrolidinyl)]$_2$ (28)

To a slurry of NiCl$_2$ (276mg, 2.13mmol) in 8mL of THF was added a solution of LiHB(pz)$_2$(*N*-pyrrolidinyl) (590mg, 4.26mmol). The mixture was stirred overnight and the color of the slurry changed from yellow to grey. Inverse filtration gave a very light blue solution. By cooling the solution at -40°C light blue microcrystalline powder (55mg) was obtained. Further concentration and cooling of the solution at -40°C gave a second crop microcrystalline powder (154mg). The combined yield is 20%. IR (KBr, cm^{-1}): v(C-H) 2963 s, 2830 s; v(B-H) 2400 s; 1501 s, 1397 s, 1309 s, 1209 s, 1118 s, 1047 s, 976 m, 881 m, 751 s, 719 m, 624 m. UV-visible (CH$_2$Cl$_2$, nm): 360 (30.6), 557 (12.6), 628 sh (10.9), 798 sh (10.0), 950 (13.8). M.S. (E.I. 70ev, 180°C) M/Z 490(M$^+$-1); 421(M$^+$-pz-H). E.A. calc. C, 48.94; H, 6.16; N, 28.54, Found: C, 48.91; H, 6.47; N, 28.32.

6.4.4. X-ray Data Collection, Structure Solution and Refinement

Crystals suitable for diffraction were obtained by storing THF solutions of both compounds at room temperature for days in the dry-box. Their parameters and other crystallographic data are summarized in Table 6.2.

Table 6.2 Crystallographic Data for Complexes **27** and **28**

compounds	**27**	**28**
	(a) Crystal Parameters	
formula	$C_{20}H_{30}B_2N_{10}Co$	$C_{20}H_{30}B_2N_{10}Ni$
formula weight	491.1	490.9
crystal system	triclinic	monoclinic
space group	$P\bar{1}$ (No. 2)	$P2_1$ (No. 4)
a, Å	9.603(3)	8.317(11)
b, Å	9.740(3)	13.451(19)
c, Å	12.783(5)	12.230(11)
α, deg	93.99(3)	---
β, deg	100.08(3)	93.83(1)
γ, deg	95.29(2)	---
V, Å³	1167.7(6)	1141.9(26)
Z	2	2
cryst dimens, mm	0.12x0.26x0.30	0.26x0.26x0.54
crystal color	pink	lavender
D(calc), g cm³	1.397	1.428
μ(MoKα), cm⁻¹	7.7	8.81
temperature, K	233	234
	(b) Data Collection	
diffractometer	Siemens P4	
monochromator	graphite	
radiation	$MoK_\alpha(\lambda=0.71073Å)$	
2θ scan range, deg	4.0 - 55.0	4.0 - 50.0
data collected (h,k,l)	±12, ±12, +16	±9,+15, +12
rflns. collected	5624	2209
indpt. rflns.	5380	2091
indpt. obsvd. rflns $F_0 \geq ns(F_0)$ (n=4)	4082	1494
std. rflns.	3	3
var. in stds., %	<1	<1
	(c) Refinement	
R(F), %	3.46	8.15
R(wF), %	3.20	10.62
D(r), eÅ-3	0.28	0.95
N_o/N_v	9.7	7.5
GOF	1.49	1.67

6.5. References

(1) Niedenzu, K.; Trofimenko, S. *Top. Curr. Chem.* **1986**, *131*, 1-37.

(2) Trofimenko, S. *Prog. Inorg. Chem.* **1986**, *34*, 115-209.

(3) Trofimenko, S. *Chem. Rev.* **1993**, *93*, 943-980.

(4) Trofimenko, S. *J. Am. Chem. Soc.* **1966**, *88*, 1842.

(5) (a) Hasinoff, L.; Takats, J.; Zhang, X.; Bond, A. H.; Rogers, R. D. *J. Am. Chem. Soc.* **1994**, *116*, 8833-8834; (b) Kitajima, N.; Tolman, W. B. *Prog. Inorg. Chem.* **1995**, in press.

(6) LeCloux, D. D.; Tokar, C. J.; Osawa, M.; Houser, R. P.; Keyes, M. C.; Tolman, W. B. *Organometallics* **1994**, *13*, 2855-2866.

(7) LeCloux, D. D.; Keyes, M. C.; Osawa, M.; Reynolds, V.; Tolman, W. B. *Inorg. Chem.* **1994**, *33*, 6361-6368.

(8) Agrifoglio, G. *Inorg. Chim. Acta* **1992**, *197*, 159-162.

(9) Frauendorfer, E.; Agrifoglio, G. *Inorg. Chem.* **1982**, *21*, 4122.

(10) Niedenzu, K.; Seeling, S. S.; Weber, W. *Z. Anorg. Allg. Chem.* **1981**, *483*, 51.

(11) Niedenzu, K.; Trofimenko, S. *Inorg. Chem.* **1985**, *24*, 4222-4223.

(12) Trofimenko, S. *J. Am. Chem. Soc.* **1967**, *89*, 3170.

(13) Lever, A. B. P. *Inorganic Electronic Spectroscopy*; Elsevier Publishing Company: Amsterdam/London/New York, 1968, pp 318, 333.

(14) Jesson, J. P. *J. Chem. Phys.* **1966**, *45*, 1049.

(15) Jesson, J. P.; Trofimenko, S.; Eaton, D. R. *J. Am. Chem. Soc.* **1967**, *89*, 3148.

(16) Churchill, M. R.; Gold, K.; Maw, C. E. J. *Inorg. Chem.* **1970**, *9*, 1597.

(17) Bandoli, G.; Clemente, D. A.; Paolucci, G.; Doretti, L. *Cryst. Struct. Commun.* **1979**, *8*, 965.

(18) Bradley, D. C.; Hursthouse, M. B.; Smallwood, R. J.; Welch, A. J. *J. Chem. Soc., Chem. Commun.* **1972**, 872-873.

(19) Murray, B. D.; Power, P. P. *Inorg. Chem.* **1984**, *23*, 4584-4588.

(20) Hope, H.; Olmstead, M. M.; Murray, B. D.; Power, P. P. *J. Am. Chem. Soc.* **1985**, *107*, 712-713.

(21) Olmstead, M. M.; Power, P. P.; Sigel, G. *Inorg. Chem.* **1986**, *25*, 1027-1033.

(22) Pray, A. R. *Inorganic Syntheses* **1990**, *28*, 321.

Chapter 7

Conclusions

The main efforts of this thesis work were devoted to the synthesis of U(III) hydrotris(3,5-dimethylpyrazolyl)borate complexes. The investigation was initiated by the preparation of $U(Tp^{Me2})_nI_{3-n}(THF)_m$ (n=1, m=2; n=2, m=0) with a structurally well-defined precursor, $UI_3(T?$ ... then focused on the derivative chemistry of $U(Tp^{Me2})I_2(THF)_2$. ... of $UI_3(THF)_4$ with the Klaui ligand, $Na[(\eta^5-Cp)Co\{P(=O)(C^{F?})\}_2]$ studied in the hope of synthesizing analogues of the U(III) hydrotris(pyrazolyl)borate complexes and comparing their structures and reactivities. Although the hydrotris(pyrazolyl)borate ligands are very versatile ligands,[1,2] the synthesis of hetero $HB(pz)_2(pz')^-$ and chiral $HB(pz)(pz')(pz'')^-$ ligands is still to be achieved. An approach toward such ligands was explored.

Straightforward metathesis between $UI_3(THF)_4$ and KTp^{Me2} afforded the complexes $U(Tp^{Me2})I_2(THF)_2$ and $U(Tp^{Me2})_2I$ in good yields. $U(Tp^{Me2})_2Br$ was prepared in a similar fashion. The compound $U(Tp^{Me2})_2I$ underwent ready iodide abstraction with $TlBPh_4$ and gave the cationic compound, $[U(Tp^{Me2})_2THF]BPh_4$. All four compounds have been fully characterized. X-ray structural analyses revealed that the mode of coordination of the hydrotris(pyrazolyl)borate ligand, Tp^{Me2}, depends on the nature of the ancillary ligands on the U(III) metal center.

The reactions of $U(Tp^{Me2})I_2(THF)_2$ with $NaN(SiMe_3)_2$ and $KCH(SiMe_3)_2$ in 1:1 and 1:2 molar ratio gave $U(Tp^{Me2})[N(SiMe_3)_2]_2$ (5), $U(Tp^{Me2})[N(SiMe_3)_2]I$ (7), and $U(Tp^{Me2})[CH(SiMe_3)_2]_2(THF)$ (6); the mixed amido/hydrocarbyl derivative, $U(Tp^{Me2})[N(SiMe_3)_2][CH(SiMe_3)_2]_2$ (8), was also successfully prepared. The complexes 5, 6, and 8 have been fully characterized and the X-ray analysis has demonstrated that the coordination congestion is in the outer coordination sphere rather than in the inner

coordination sphere. In solution, the complexes are fluxional; the slower rearrangement of 8 compared to 5 can be rationalized by the site preference of the hydrocarbyl for the apical position of the trigonal bipyramidal coordination geometry. Complexes 5 and 6 are thermally unstable in solution and the decomposition processes are solvent dependent. Complex 5 decomposes more rapidly in donor solvents, such as DME, than in hydrocarbons; $U(Tp^{Me2})[N(SiMe_3)_2](3,5-Me_2pz)$ and $U[N(SiMe_3)_2]_2(3,5-Me_2pz)_2$ were obtained from the decomposition in DME and hexane, respectively. In both cases B-N bond cleavage of the Tp^{Me2} ligand dominates the thermal processes. The formation of a U(IV) complex in hexane was unexpected. Although $U(Tp^{Me2})[CH(SiMe_3)_2]_2(THF)$ reacts readily with H_2 and CO, the nature of the formed products could not be elucidated.

The reactions of $U(Tp^{Me2})I_2(THF)_2$ with alkoxides and aryloxides were not clean and were accompanied by oxidation of U(III); only the U(IV) complexes, $U(IV)(Tp^{Me2})(O^tBu)_3$, $U(Tp^{Me2})(OC_6H_2Me_3-2,4,6)_3$,[5] and $U(Tp^{Me2})(OC_6H_3{}^iPr_2-2,6)_3THF$, could be isolated. The redox complication could be eliminated by using the chelating ligands, dpm⁻, $^tBuCO_2{}^-$, and $H_2B(pz)_2{}^-$. Although the dpm⁻ ligand displaced the Tp^{Me2} moiety as well and gave $U(dpm)_3$, with the latter two ligands U(III) complexes, $U(Tp^{Me2})(O_2C^tBu)_2$ and $U(Tp^{Me2})[H_2B(pz)_2]_2$, were isolated.

Oxidation of U(III) also complicated the reactions of $UI_3(THF)_4$ with Kläui ligand, L_{OEt}. Thus Kläui analogues of the $U(Tp^{Me2})_nI_{3-n}$ complexes could not be prepared.

To expand the scope of the versatile hydrotris(pyrazolyl)borate ligands, the addition of hetero (HB(pz)_2(pz')⁻) and chiral (HB(pz)(pz')(pz")⁻) ligands to the arsenal of the synthetic chemist would be welcome and very desirable. An attempt to prepare hetero hydrotris(pyrazolyl)borate ligand, HB(pz)_2(pz')⁻, was made *via* ring splitting of pyrazobole, [HB(pz)_2]_2, with secondary amines such as $HNMe_2$ and pyrrolidine, followed by displacement of the amine from $HB(pz)_2$(amine) with (3,5-Me_2pz)⁻. Although the

approach was not completely successful, it has led to the preparation of the hetero poly(pyrazolyl)borate ligand, $HB(pz)_2(N\text{-pyrrolidinyl})^-$. The transition metal complexes of the ligand, $M[HB(pz)_2(N\text{-pyrrolidinyl})]_2$ (M=Co(II) and Ni(II)), were also prepared and characterized.

Future work should be directed toward the reactivity study on the amido and hydrocarbyl complexes. Preliminary results have already demonstrated high reactivity of these complexes, especially in hydrogenolysis and carbonylation reactions. It would be highly desirable to discover the appropriate experimental conditions, and ancillary ligands to isolate the primary product of these reactions and to compare their structures, properties and reactivities to the related U(III) pentamethylcyclopentadienyl complexes.[6]

7.1. References

(1) Trofimenko, S. *Acc. Chem. Res.* **1971**, *4*, 17-22.

(2) Trofimenko, S. *Chem. Rev.* **1972**, *72*, 497-509.

(3) Trofimenko, S. *Prog. Inorg. Chem.* **1986**, *34*, 115-209.

(4) Trofimenko, S. *Chem. Rev.* **1993**, *93*, 943-980.

(5) Marques, N.; Marcalo, J.; Pires de Matos, A.; Bagnall, K. W. *Inorg. Chim. Acta* **1987**, *134*, 309.

(6) Fagan, P. J.; Manriquez, J. M.; Marks, T. J.; Day, C. S.; Vollmer, S. H.; Day, V. W. *Organometallics* **1982**, *1*, 170-180.